An Investigation of Active Tonal Spectrum Control as Applied to the Modern Trumpet

by

Peter B. Pickett

Thesis submitted to the Faculty of the

Virginia Polytechnic Institute and State University

in partial fulfillment of the requirements for the degree of

MASTER OF SCIENCE

IN

MECHANICAL ENGINEERING

Dr. William R. Saunders, Chair

Dr. Allen Bachelder

Dr. A. A. Beex

Dr. Ricardo Burdisso

June 8, 1998

Blacksburg, VA, USA

Keywords: Trumpet, Active Noise Control, Spectrum Shaping, Adaptive Control

An Investigation of Active Tonal Spectrum Control as Applied to the Modern Trumpet

by
Peter B. Pickett
Dr. William R. Saunders, Chair
Department of Mechanical Engineering

Abstract

Techniques are available today to attenuate the output sound of the trumpet. All of these techniques involve using passive mutes. Due to the limitations in the sound one can obtain with passive mutes, another solution, using active noise control, is proposed to predictably attenuate the output sound of the trumpet. With the new system, it is theorized any desired output sound can be obtained.

Within this thesis a model of the trumpet physics is derived and an investigation of the implementation of two analog feedback controllers and two digital LMS controllers is performed. The model of the trumpet mechanics is studied to understand the trumpet system before applying the control systems. Analysis is performed on the type and the location of the acoustic control actuator and the error sensor to be used. With the chosen actuator and sensor, the two types of controllers are designed and realized. The farfield spectrum of the trumpet's response to a single note is analyzed for each controller and the resulting attenuations compared. The model of the trumpet system is then used to demonstrate the coupling of the trumpet and the player and to show the effects of the controllers on the behavior of the player's embouchure.

With the inclusion of the controllers in the trumpet system, the farfield spectrum was successfully attenuated at two harmonics of the tone passed through the trumpet. Testing was not performed with an actual trumpet player due to the high sound pressure levels (160 dB SPL) required from the control actuator. From a derived model of the control actuator, specifications for an acoustic driver capable of delivering the high sound pressure level were calculated. Design and fabrication of the proposed actuator will be completed during future work.

Acknowledgements

Throughout the extent of my undergraduate and graduate career spent at Virginia Tech during the last seven years, many people have contributed to my advancement as a human being, to my intellectual abilities, and to my musical abilities. All of these people at one point or another noticed some characteristic I had not and helped me to bring it to the forefront and use it to the best of my ability.

Before I even arrived in Blacksburg, I was constantly encouraged and guided by my parents. Without them, I would have not have seen even the faintest of lights at the end of the tunnel. At some points in my college career I had to trust them in their vision for the future and hope that it was the right direction for me and each time it was. Nobody could have done this better than them and I will always be indebted to them.

To Meg Saunders who patiently waited and encouraged me during the last half of my Masters program, who constantly reminded me that it was all worth it and to continue working on into the night. Without her, I would not have been able to complete this work as I have. May she know that her undying support will always be appreciated.

During first week here at Virginia Tech in 1991, I accidentally met Dr. Allen Bachelder, who from that point on encouraged me to play my trumpet more and continually practice to become a better player and musician. At that point, I became terminally addicted to playing, starting my journey to reaching the all-encompassing, ethereal attainment of music.

During my constant wandering between the disciplines of engineering and music, I met Dr. Will Saunders, whose foresight saw my constant desire to tie together the two disciplines. With his patience, reassurance, and forethought I was able to carry out my research, successfully complete my thesis, at times explore totally unrelated topics for seemingly no reason, and to continue my full time music career. Nobody else would have allowed me to be so free and to have so much freedom in my attainment of knowledge and experience.

Other people who have attributed to my success here at Virginia Tech include Mike Vaudrey who despite the hour of day or whatever he was doing at the time stopped and answered my questions and for without whom this thesis would have not been possible. Also, many thanks go to Dan Clatterbuck and Chris Fannin, my officemates, who would always listen to my gripes about experiment failures, computer crashes, and other unanswerable questions.

Professors who have lent their expertise throughout my studies include Dr. Beex, Dr. Ricardo Burdisso, and Dr. Harry Robertshaw, without whom I would not have obtained the knowledge to complete this work.

And to all my friends in Blacksburg, without you, I could not have enjoyed the total experience of this town and its many venues for music and the arts.

Table of Contents

Figure List

Symbols

A, **B**, **C**, **D**	nodes on the simplified lip model
A, *B*, *C*, *D*	complex amplitudes of forward and backward traveling waves
Bl	speaker electromechanical coupling constant
b	width of the lip
C	arbitrary damping constant on lips
$C_{speaker}$	speaker cone suspension damping
c	speed of sound
d	the length of the lip
F_{closed}	extra forced added when the upper and lower lips come in contact.
f_{lip}	resonate frequency of the player's embouchure
f_o	fundamental frequency
G	control actuator-to-error transfer function
H	controller transfer function
i, *j*	defined as the $\sqrt{-1}$
J	digital controller-to-error transfer function approximation
k	wave number
k_{lip}	lip stiffness
$k_{speaker}$	speaker cone suspension stiffness
l	axial length of a particular horn
m	lip mass
m	exponential horn flare constant
m_{out}	microphone output voltage
$m_{speaker}$	mass of speaker cone
$p_{Bernoulli}$	Bernoulli pressure on the bottom lip surface
p_{cont}	control pressure
p_{lip}	internal, reflected pressure applied to the external lip surface
P_o	static pressure provided by player to the internal lip surface

p	pressure present in mouthpiece cup
R	radius of infinitely baffled piston
$R_{speaker}$	speaker coil resistance
S_1	cross sectional area of throat of a particular horn
S_2	cross sectional area of mouth of a particular horn
S_{lip}	area of the lip opening
t	time
U	total volume velocity
U_{acoust}	acoustic volume velocity
U_{lip}	volume velocity generated by embouchure movement
V_{in}	voltage applied to speaker coil
z_{a1}	throat impedance of a particular horn
z_{a2}	mouth impedance of a particular horn
Δt	discrete time step length
Δx	distance over which air expansion occurs after lip opening
ρ	density of air
ζ	position of lip tip relative to the origin
ζ_{equi}	equilibrium position of lip tip

Chapter 1. Introduction

1.1. Introduction

Each musical wind instrument has particular mechanical and acoustic dynamics that give the instrument its characteristic sound. At times during a performance or practice, the player and/or listener would like this sound to be different than what it is. A listener may desire the sound of the particular instrument to be quieter, so either the player must make a conscious effort to reduce the volume of sound or a passive mute is employed. Passive mutes already exist that modify an instrument's sounds. With today's available passive mutes, the player doesn't have complete control over what type of sound he/she produces. The player is left to contend with the dynamic response of the mute and the instrument.

A new methodology for modifying the sound of a trumpet, an active noise control (ANC) system, is posed in this thesis. An active noise control system generates additional noise, causing either destructive or constructive interference within the system acoustics. With an ANC system employed, it is theorized that any wind instrument's system dynamics can be modified to change the particular instrument's response so as to produce any desired sound, whether it is characteristic to the instrument or not. In this research, an ANC system was investigated that would have the ability to modify in real time the dynamics of a musical wind instrument.

Since all wind instruments, including brass and woodwind families, are acoustic resonating devices, an ANC system of this type could theoretically be applied to any of them. The brass instruments, unlike the woodwind instruments, already have many passive mutes available, including straight mutes, cup mutes, practice mutes, and many more. With the proposed ANC control system, the effects of any of these mutes, as well as many other sounds, could be simulated with the flip of a switch from the player instead of having to physically switch mutes. Due to the author's familiarity with the trumpet, it was the instrument chosen for this thesis.

1.2. Motivation and Applications

A goal of each musician is to have absolute control over the unique sound generated by his/her instrument. Many years of practice, quality of instrument, and good mental concepts all contribute to the development of a desirable and personal sound. However, in many situations, the player is called upon to produce drastically different sounds. This is where passive mutes, as mentioned before, and the proposed ANC system could be employed.

Many musical applications exist for a device that could change the trumpet sound to a variety of other sounds in real time. These include use in:

1) muted portions of musical passages
2) historically correct performances
3) a trumpet-based synthesizer
4) improving intonation

Throughout many passages in symphonic, chamber, and solo works, the trumpet is called upon to use a mute to obtain a sound desired by the composer. This requires the trumpet player to insert a mute, in some cases very quickly, to alter the sound making smooth transitions between muted sections difficult. With an ANC system, the trumpet player could simply press a button or flip a switch to obtain the new muted sound instantaneously.

The trumpet's characteristic sound has changed as the trumpet has matured through history. Depending on the type of music performed today, players may want to reproduce the tone color of the original instruments, giving a historically-correct performance. In order to accomplish this, the players either need to use historically-correct instruments or actively modify today's instruments with the new proposed ANC system to reproduce the historically-correct tone color.

Another use of the actively controlled tonal modification system would be as a real-time synthesizer, accessible by a trumpet player. Theoretically, the trumpet output spectrum could be controlled to produce almost any acoustic output desired. The player could choose

what instrument he/she would like to sound like and have the ANC system modify the output spectrum to obtain the desired sound.

Along with changing the overall tonal sound level of the trumpet, the ANC system could also change the frequency at which the trumpet system resonated. During a musical passage, a trumpet player may find that his/her trumpet plays certain notes out of tune. This is partly due to the incorrect placement of the resonances in conventional trumpets. By modifying the dynamics of the trumpet and moving these resonances dynamically with the ANC control system, the trumpet could be made to play more in tune.

1.3. Objectives

This thesis presents preliminary research towards the future application of the ANC system to the previously listed applications. The objectives for this thesis target only a small portion of the bigger picture. The objectives are to apply ANC to

1) demonstrate successful selective tonal attenuation and
2) maximize the control zone over which this attenuation occurs.

The first objective of the application of the ANC system is to demonstrate selective tonal attenuation of the trumpet output. The most absolute effect an ANC system could have on the output spectrum would be to attenuate all of the tones in the outgoing sound completely. Instead, by attenuating selective tones, most but not all of the energy in the trumpet output sound could be attenuated. This form of an electronic 'practice mute' is believed to be an excellent aid in practicing for two reasons. It would allow the player to practice anywhere without disturbing bystanders and unlike conventional passive practice mutes, it would not restrict the airflow through the instrument.

The second objective of the application of the ANC system is to obtain maximum global control. Regardless of where the listener is located, he/she will ideally perceive the same acoustic effect as if they were at another location. The easiest way to ensure this is by

placing a control actuator as close to the original disturbance source as possible. With the control actuator collocated exactly with the disturbance and an appropriate controller, only destructive interference occurs.

A system of this type has not been realized prior to this thesis. New, passive mutes are often introduced for attenuating the trumpet significantly, but never has an active tonal control system been proposed. The closest type of system to this is the Yamaha Silent Brass System. The Yamaha system consists of an excellent passive practice mute with an enclosed microphone that feeds into a reverb processor, an amplifier and to the player's headphones. In order to achieve the objectives of this thesis with the Yamaha system, the signal from the Yamaha Silent Brass System's enclosed microphone could be processed with some form of electronic filters and fed to an external amplifier and speaker to effect a global tonal change.

Though the overall sound would be changed by the Yamaha system, the player/trumpet interaction is disturbed by the flow restriction of the passive practice mute. The air-flow restriction causes the player to feel more blowing resistance while he/she is playing the trumpet. Even though the trumpet can still be played successfully, it is different than playing a trumpet with an unrestricted airflow. Extended practice on this flow-restricted system is believed to develop habits not necessarily beneficial to normal trumpet playing.

1.4. Overall ANC/Trumpet System

A schematic for the overall ANC trumpet system layout is shown in Figure 1.1. The input to the trumpet is the player and the output is the acoustic radiation to the listener from the trumpet. Within this system is a measurement device that detects the sound field, a control actuator that influences or acts on the trumpet acoustics, and some form of controller that takes the system measurements and generates a control signal to change the system accordingly. As mentioned previously, other wind instruments may be substituted for the trumpet.

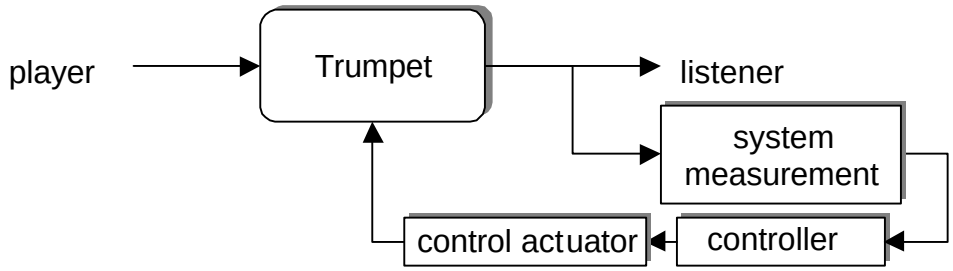

Figure 1.1 Overall trumpet system layout

Each specific component of this overall system is important to the attainment of the stated objectives. In order to apply ANC to the trumpet effectively, the interaction between the player and the trumpet was initially studied. From this understanding, the type and location of the control actuator and system measurement device was chosen.

The objectives are stated from a listener's point of view, but do not totally quantify the result of applying the ANC system to the trumpet. The effect of the ANC system is also studied from the player's point of view.

A discussion of each element in the overall trumpet schematic is presented in the following sections.

1.4.1. The Trumpet

The musical instrument controlled in this research was the trumpet. The trumpet system was mathematically modeled to better understand and explain the dynamics involved in the coupling together of the player's embouchure and the trumpet itself. The system only sounds like a trumpet to the listener and feels like a trumpet to the player when the natural frequencies of the player's embouchure and the trumpet coincide. This stable, coupled oscillation creates the characteristic trumpet output. If the coupling dynamics are haphazardly disturbed with a poor, disruptive controller, then the trumpet/player interaction is also disturbed, perhaps causing the player to feel uncomfortable and possibly making the trumpet system unplayable altogether. With the analytical trumpet model, the motion of the

lips and the pressure in the mouthpiece are observed during the controlled condition to observe the effects on the player.

1.4.2. Measurement and Actuation Components

The control system in this project consisted of an error sensor, control actuator, and controller. The selection of these components directly affects how well the control system performs. The two components forming the interface between the trumpet system and the control system, the control actuator and error sensor, are especially critical. If these components do not accurately and predictably reproduce and measure what is input to them, many difficulties arise in the prediction of performance and in the design of the controller.

The error sensor was located as close as possible to the originating disturbance, the player's embouchure. The error sensor was located on a pressure tap on the trumpet mouthpiece. Measurements of the pressures at this point in the trumpet bore were found to be approximately 160 dB (SPL)[*] while the trumpet was being played. Standard condenser microphone elements are not capable of measuring this amount of pressure and do not produce accurate representations of the pressure over time. Instead a B&K microphone was used that was capable of measuring high sound pressure levels and reproducing the trumpet throat pressure waveform with good fidelity.

In order to achieve global control, the control actuator is required to be located as close to the originating disturbance as possible. The input location of the control actuator was determined to be at the trumpet mouthpiece, near the player's buzzing embouchure. In order for the ANC system to achieve a high level of control, the control actuator must be able to match the overall level of the disturbance pressure. Therefore, the control actuator must be capable of introducing sound pressures of 160-180 dB (SPL) into the trumpet system. Selection of an appropriate driver becomes difficult with this high level of required sound pressure.

---

[*] *re 20 μPa. All (SPL) measurements are referenced to 20 μPa.*

The driver implemented for preliminary testing was only able to produce a maximum of 110 dB SPL without significant distortion. The speaker output limitation is due to the lack of attainable speaker cone deflection, the maximum power handling ability of the speaker coil and the strength of the speaker magnet. Therefore, a model of the speaker system was derived to model the performance of the current driver. From the model, a higher output speaker was theorized.

1.4.3. Quantification of Measurements

As each active control solution was applied to the system, measurements were needed to reliably compare control methods, control actuators, and other system changes. Unfortunately, the trumpet acoustic output alone can not be used as the final measurement. Due to the human components, the player and the listener, in the overall system, certain immeasurable qualities must also be taken into account. For example, how does the player feel when the active control system is activated? Does the control system change significantly how the trumpet feels to play? Does the new system output sound good or bad? These immeasurable evaluations are left to personal qualitative opinions.

Several marketability and artist-acceptance issues were also addressed. These included ease of use, size, weight, and most importantly, the range of effect that this system could bring to the trumpet. If the effect is minimal, there is minimal reason to use the currently developed system. If the effect is non-harmonic, i.e., creates a distorted sound or creates out-of-tune sounds, there would be no mainstream usage as a standard mute system. If the effect is harmonic, but the system is too bulky, heavy, or requires too much power to operate, then the system would not be accepted by the majority of musicians and passed off as a gadget or toy. Therefore, effort was made to examine the eventual usability of the current ANC system.

1.5. Summary of Findings

Analog feedback and digital LMS controllers were successfully used to modify the trumpet system output. The digital LMS controllers performed better than the feedback controllers due to their ability to adapt to the exact tonal frequencies present. The amount of control attenuation at a single tone with the feedback controller ranged from 10 to 15 dB versus 20 to 25 dB of attenuation obtained with the digital LMS controllers. Though the analog feedback controllers are much less expensive to implement, they are only effective at the specific design frequencies. Thus, they will only work for a single trumpet note exactly in tune limiting their usefulness in a performance situation with a real player. The digital LMS adaptive controllers have the ability to adapt to changing trumpet intonation, so they will still achieve good attenuation even when the player is slightly out of tune.

The quality, or timbre, of trumpet output sound with the application of the two controllers was similar. The second feedback controller designed and implemented reduced the fundamental and the first harmonic of the trumpet output spectrum 10 and 15 dB respectively. With these first two tones reduced, a change in trumpet pitch was not perceived, but a change in timbre was noticed. The resulting trumpet output sound was thinner and brighter than the uncontrolled sound.

With the filtered-E digital LMS controller, the fundamental and second harmonic tones were reduced 23 dB and 19 dB respectively. The sound with the digital LMS controller implemented was again thinner than the uncontrolled sound but did not lead to significant loudness reductions due to nonlinear actuator response. While the control actuator was driven by the digital LMS controller, the actuator generated higher frequency tones not present in the controller signal.

The control actuator and error microphone utilized were found to be inadequate for high level control as would be required with a real trumpet player. The LMS controller demanded a very high sound pressure output from the control actuator. The acoustic output from the control actuator was very distorted. Though successful control was obtained at two frequencies, significant distortion caused additional sound to be produced at higher

harmonic frequencies. Therefore, a model of the control actuator was developed in order to estimate the characteristics of a driver capable of successfully producing the high pressure levels without significant harmonic distortion.

In order to observe the effect of the controllers on the embouchure movement of the player, a feedback control algorithm was applied to the model of the trumpet and player interaction. It was shown that with the controller activated, the amount of embouchure travel was reduced. If the embouchure travel is reduced too much, then the trumpet is believed to be uncomfortable and unplayable. Ideally, the trumpet player should not perceive any difference in how the trumpet feels. With the current choice of control actuator placement and controller selection, the amount of embouchure travel is reduced.

1.6. Presentation of Thesis

After this introductory chapter, a brief historical review of the trumpet is presented in *Chapter 2*. From this chapter, the reader will acquire a general understanding of how the early trumpet and its characteristic sound has developed into its present form.

Chapter 3 presents the derivation of the analytical trumpet model. This model predicts the physics of the trumpet/player interaction and demonstrates how the player interacts with the trumpet. With this model, changes in the trumpet construction and control algorithms were simulated to observe changes in embouchure movement.

Two analog feedback controllers and two digital LMS controllers are implemented in *Chapter 4*. Each control system required a control actuator and error sensor. Qualities of these components are discussed in relation to their performance in the specific control system. With each controller, the actual trumpet response is studied and qualitatively reviewed.

Due to the very high sound pressure levels present in the trumpet, a very high output control actuator was needed to effectively control the trumpet output with a real player. An

analytical model of the implemented control actuator is developed in *Chapter 4* to determine appropriate parameters for a successful, high-sound-pressure-level control actuator.

The final chapter summarizes the results of the application of each controller and the qualitative issues at hand with trying to actively affect the trumpet sound output. Future technical objectives are defined, along with discussions of the remaining obstacles that impede the practical implementation of the active tonal modification controllers for the modern trumpet. It is hoped that this preliminary study will lead to further development of the ANC system as applied to the trumpet as well as all modern wind instruments.

Chapter 2. Historical Development of the Trumpet

The modern trumpet has evolved to what it is today from thousands of years of development. Todays instrument is a reflection of advances in form, function, and technology. Throughout the historical development of the trumpet, the timbre, range, and usage have changed significantly. Despite all of the advancements in technology, the trumpet still is an imperfect and limited instrument. It is still limited in dynamic range, frequency range, tone color, and technical execution flexibility. The development of the present form of the trumpet is covered here and will help the reader understand how the sound of the trumpet has developed.

2.1. Early Trumpets

The earliest trumpet is considered only to be a megaphone, a not-so-finely proportioned tube that was a means of amplifying the user's vocal sounds of howls, roars, etc., to the rest of the world. To create even more frightening sounds, a lip-energized noise was used and the tube was found to amplify and project the lips' buzz. Though no one knows when this buzzing of the lips was discovered, one myth suggests the buzzing discovery was made accidentally by blowing on a spiral conch shell. To quote Canon Galphin: "It has been suggested that the method of raising the sound waves by the vibration of the lips was discovered by our forefather' preprandial requirements or postprandial satisfaction. One of the earliest forms of lip-voiced instrument is the spiral shell, found as the Cank or conch-trumpet in Asia and as the Bio in Europe. Now, in order to get at the fish concealed within it, it was necessary to break off the tip of the shell and either to push it or blow it out. With the final blast that heralded the meal the vibration of the lips was discovered."

The didgeridu of the Australian aborigines is a well-known example of a primitive trumpet-like instrument. This instrument was usually made out of a tree or branch that had the interior hollowed out by bugs and the bore generally conically shaped. Occasionally long sections of cane were used, giving a cylindrical shape. With either one, the player vibrates

the lips at the fundamental frequency of the instrument while humming another frequency. This instrument demonstrates the relative unimportance of the shape proportions in the early development of the trumpet, thus the sound was not a pure tone.

2.2. Musical Usage of Trumpets

2.2.1. Egyptian Origins

The earliest actual account of the musical use of a trumpet or horn was found in Mesopotamia (3000-4000 BC). Legend and recorded sources cite a Sumerian hero named Gilgamesh who constructed an instrument from a hollow branch of a tree and connected it to a larger section from another tree forming a stepped cylindrical bore, as described in a narrative of the hero's labors. This is related to the basic construction of a didgeridu, but with the added technical refinement of the Sumerians who had extensive artistic and technical skills as evidenced by the lavishly decorated horns mentioned often in the Cuneiform scripts.

From Egypt, there is extensive evidence of early trumpets. In the inventory of King Tushratta's presents given to Amenophis IV of Egypt (1400 BC), about forty instruments are mentioned. Included in these are ox-horns as well as straight trumpets sometimes made of gold. Uses of these early trumpets mainly included military duty, i.e. fear-invoking noisemakers. Though no trumpets have been excavated from the Mesopotamian archaeological sites, illustrations from the time suggest their existence.

Later in Egyptian history, during the New Kingdom (1580-1090 BC), the first truly cylindrical bore trumpet was discovered. The oldest specimen of the completely metal trumpet was discovered in the tomb of King Tut-ankh-amen. Paintings of this trumpet are prevalent in the art of the tombs as shown in Figure 2.1.

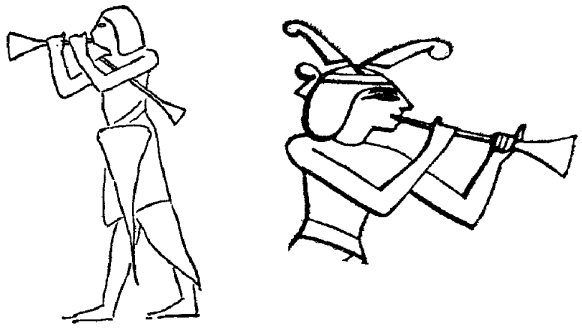

Figure 2.1 Ancient Egyptian trumpets from the new kingdom

This is also the first time the trumpet was used for a purpose other than war, the worshipping of Osiris. The instrument was sometimes attributed to the god himself, as suggested by Eustathios[*]. Clay models of horns and trumpets were also found among the votive objects during the later Greek period in Egypt attributed to Osiris.

These trumpets averaged only two feet in length so their fundamental pitch is approximately an octave above today's trumpet and their tone very bright. It is most probable these trumpets were used rhythmically and not for melody. With their small bore, they could only produce the first, second and maybe the third harmonics but the reader is reminded that this has been demonstrated with a modern embouchure unlike the one actually used. The small bore also gives the tone resembling "the braying of an ass.[†]" Played by a modern player (Dr. Hans Hickman), the tone could be described as the tooting of an English hunting horn. This suggested that the sound obtained in ancient times was produced by overblowing, forcing large amounts of air through the horn, and exciting a large number of higher harmonics, giving the bright, crass sound also suitable for war.

2.2.2. Greek Origins

[*] *Homer s commentator*

Plutarch

Despite the high artistic and technical abilities in Greek society, trumpets and music did not advance as much as the rest of Greek society. Only one form of the trumpet has been found recorded. The one specimen from the 5th century BC is preserved in the Museum of Fine Arts, Boston, Massachusetts. It is formed from thirteen sections of ivory fitted together with bronze rings and terminated with a bronze bell with a total length of 62 inches. With a totally cylindrical shape, the tone of the "Salphinx" was recorded by Aeschylos in 'Eurenides' as *diatoros* ('yelling'). The overall shape of the trumpet is straight, most likely related to the early Egyptian and Jewish trumpets.

Up until this point in time, the trumpet was generally a noisemaker and no discernment was made between any different shapes, forms, or purposes of the trumpet.

2.2.3. Roman Origins

At approximately the same time, the Romans developed trumpets much further than the Greeks and created no less than four distinct bronze instruments, each with a separate purpose. Each horn was used for a military duty as before. These four types were the *Tuba*, *Lituus*, *Cornu*, and the *Buccina*.

The infantry Tuba was similar to the Greek Salphinx, but generally shorter. The shape differed from the Salphinx in that the Tuba was a conical shape, starting at a diameter of about 0.4 inches and expanding to 1.1 inches at the root of the flaring bell. Since it was shorter, it played quite a bit higher and with the conical shape, had a more pleasing sound.

Figure 2.2 A Roman tuba and player

The cavalry Lituus was the first to define the ultimate modern day trumpet shape, the cylindro-conical form. The Etruscans, thought by the Greeks and Romans to have invented the trumpet, were great bronze workers and fashioned the cavalry Lituus out of bronze to be just like the original Lituus. The original Lituus was a reed stem connected to a cow horn for a bell and gave birth to the first true trumpet. The finest example of a Lituus was discovered at Cerveteri and is now in the Vatican Museum. It is about 63 inches long, making its fundamental pitch about a low G on a modern day trumpet. This new trumpet was observed to play the first octave harmonic and not the fundamental as the Tuba demonstrated. This characteristic is also identical to the modern day trumpet.

The third Roman trumpet was the Cornu. The Cornu was constructed of about 11 feet of tubing wrapped in a circular wrap 3 ½feet across braced with a highly ornamented wooden rod. The Cornu often depicted in Roman sculpture and art was used mainly in high-ranking military activities in the presence of the Commander-in-Chief where special fanfares were required. This horn can reproduce quite a few harmonics due to its long length, played by modern day players with modern mouthpieces. The actual use probably did not include more than the first 3 or 4 harmonics. From artwork, we see that the Roman players tended to play forcefully and with puffed cheeks (Figure 2.3).

Figure 2.3 Roman artwork depicting a short Cornu, played with puffed cheeks

In order to hold the cheeks under the great pressure, a *capistrum*, a leather headband, was used to support the cheeks. With the cheeks puffed and a capistrum in place, the selection of higher harmonics is difficult. The sound of the Cornu was described as 'horribilis', 'raucus', and 'rudis,' as well as 'mimax murmur,' a threatening rumble. A Cornu was discovered from c. 692 and is preserved at the British Museum. It includes the beginning of the modern day mouthpiece. It was shaped with a hemispherical cup with an overall diameter of 1¼ inches and about ½inch deep. The rim is turned in around its edge to provide a more comfortable surface to press the lips against.

Figure 2.4 Roman Cornu mouthpiece, c. 692

The fourth Roman horn, the Buccina, was a simple bugle horn used for announcing the four watches of the night in the camp and to sound reveille in the morning. The horn is sometimes confused with the Cornu in some texts and thus leads to some confusion, but nonetheless is truly one of the first trumpets. The Buccina was constructed from a natural ox-horn with the tip removed and may be played with or without a metal mouthpiece. The Buccina is refered to as the shepards' instrument by Virgil in the Aeneid. A usable specimen is also located in the British Museum: "when the cracks due to perished solder are stopped up, notes are quite easy to blow and by no means make an unmusical sound." But as with most early trumpets, the technique was not as the modern technique, but was overblown to

create utter terror as written in the second book of Polybius' *History*: "The tumult of the army of the Celts terrified the Romans, for there was amongst them an infinite number of horns and trumpets which … made a clamour so terrible and loud that every surrounding echo was awakened…." At this point in history, the trumpet still was only a fanfare and war instrument and was not developed as the lute, harp or other melodious and refined instruments.

2.3. Modern Trumpets

As time progressed the trumpet developed from a noisy, warlike instrument to a musical, solo instrument. In order for the natural trumpet to be useful, it needed to be able to play more notes. Since there were not any valve or tuning devices as of yet, the players still had to have control over their embouchures to choose which harmonic they were playing. To increase the number of playable harmonics, the trumpet was lengthened. This lengthened trumpet was curved around in an S shape and then folded to form a zigzag. These were still used in the field during military exercises.

With the publishing of Virdung's *Musica Getutscht* in 1511, we see the beginnings of a trumpet as a musical, artistic instrument, moving away from Military duty. He mentioned and included pictures of three different types of folded trumpets: *Thurmer Horn*, *Felt Trumpet*, and *Clareta*. The first two were still military type trumpets, consisting of the folded S shape as mentioned before, but the Clareta was constructed with a smaller bore and thinner material, both contributing to being able to play the higher harmonics.

The distinction between the military trumpet and the musical trumpet began to all but disappear during the 17th century. *Praetorius* called this new blended trumpet 'Trommet.' At this point, the higher harmonics were being cultivated and composers started to employ these. These new registers in the trumpet eventually influenced and made possible the high trumpet parts of Bach and Handel during the 18th century.

2.3.1. Trumpet Mute Origins

This purpose of this thesis was to explore and design a new "muting" system. It is a common misconception when a brass instrument is muted that the purpose of the mute is to reduce the volume of sound. The effect of a reduction in the volume of sound may be apparent, but this is due to a reshaping of the harmonic content of the resulting sound [Bate, 1978]. The mute reshapes the trumpet output spectrum to form different characteristic sounds.

Mutes, though thought to have been invented this century, have been known to exist since the 17th century, and were mainly used in the military. The first recorded piece of music known to call for a muted trumpet is Alessandro Scarlati's *Mitridate Eupatore* of 1707 [Dent, 1905]. Directions call for 'Due Trombe nell Orchestra alla Sordina,' meaning 'Two Trumpets in the Orchestra to the Mute.' The mute that was used was a piece of wood shaped to fix snuggly into the end of the trumpet bell with a hole bored through the middle.

Figure 2.5 Original wooden trumpet mutes

A craze of new mutes appeared in the 1920's in dance and jazz bands. Included were the cup mute, harmon mute, bucket mute, wah-wah mute and others. All of these mutes are passive mutes made of cardboard, felt, fiberglass, plastic, wood, and various metals. They

have attached to them corks that allow the player to wedge the mute into the trumpet bell. Depending on the mute, corks may seal up the trumpet bell only allowing sound to pass through the mute, or the corks may allow sound to escape around the mute. The corks and various mutes can be seen in Figure 2.6.

Figure 2.6 Pictures of common trumpet mutes

2.3.2. Valve Systems[*]

As the trumpet developed a more pleasing sound due to improving player ability and quality of the instruments, demand was placed on increasing the range and intermediate notes of the instrument. Early trumpets were fixed in length and therefore, could play notes only within their respective harmonic series. If the horn was long enough, then the harmonics that the player could control were close together in the range desirable for the music.

Since the length of the instrument controlled the pitch of the trumpet, sections of tubing were added to lengthen the effective length of the trumpet. These 'crooks' allowed the player to play with a different harmonic series. Unfortunately, these crooks could not be

[*] *For an extensive review of the history of valve inventions, refer to [Bate, 1978]*

changed quickly to allow the player a continuous chromatic scale within the range of the instrument.

An attempt to quickly change the pitch of the trumpet was attempted with a technique called 'stopping,' attributed to Hampel of Dresden, c. 1750. In order to implement this technique, the trumpet needed to be constructed so that the player could insert his/her hand into the bell section and provide enough resistance to change the pitch. This type of trumpet, called a 'Trompette Demilune' in France was a wrapped up trumpet pitched in F. As the hand is inserted and the amount of muffling is increased, the pitch decreases. This technique is still used today with French horns; the player's hand is still inserted in the bell to control fine changes in pitch and timbre. Unfortunately, when the hand was inserted far enough to reduce the pitch a half step (100 cents) or even a whole step (200 cents), the characteristic of the sound changed from the recognizable, bright trumpet sound to a muffled, softer sound. If the player compensates for this quieter sound by blowing harder, the resulting sound became harsh and rough. For this reason, the stopping of the trumpet was not adopted for filling in missing notes in the harmonic series. As Bates describes:

> "Taking these various points into consideration I think we must conclude that although the close-coiled trumpet of the Baroque period could be hand-stopped, the technique was probably used more to correct relative intonation than to supply entirely missing notes, and in any case it could not be carried as far as early Renaissance polyphonic music required."

Another attempt to chromaticize the trumpet came about with the German *Zugtrompete* or Slide-trumpet. Bach made use of this Tromba-da-tirasi in pieces that required more than just a natural trumpet in D, including parts that contained notes in the third octave. Since the Zugtrompete included a section that extended and contracted, the bore must have been cylindrical. This cylindrical section thus formed the majority of the instrument, giving the Zugtrompete the same bright sound as the traditional natural trumpets. With this invention, some of the missing notes of the chromatic scale could be filled in without sacrificing the clear trumpet sound, such as stopping would.

Figure 2.7 Zugtrompete with slide fully extended

Attempts to fully chromaticize the trumpet resulted in the keyed trumpet, attributed to Riedl, 1796, and played by Anton Weidinger in 1801. Both Haydn and Hummel wrote concertos for solo keyed trumpet to show off its new abilities. This trumpet was the first truly chromaticized trumpet capable of playing a full chromatic scale over a two-octave range. Since the keyed trumpet included significant open ports at times for certain notes, the tone was not consistent across the entire range of the instrument, but certainly better than that for a stopped trumpet. The length of the keyed trumpet was half the length of the traditional natural trumpets, thus the fundamental was one octave higher. Since the bore was still relatively cylindrical, the keyed trumpet retained the bright sound of the previous trumpets, but again suffered when more than one port was open.

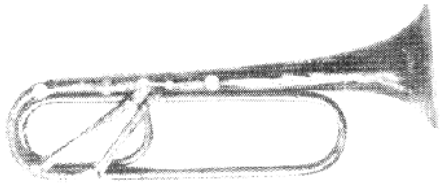

Figure 2.8 Keyed trumpet

This concept of keys was applied to the bugle with hopes of improving the tone quality. The only difference between the keyed trumpet and keyed bugle was the bore shape. The tone was better than for the keyed trumpet, but still had limits in tone quality with too many ports open. If the keys are all closed, then the tone is typically quite good due to the very conical shape of the bore, starting out at the mouthpiece with a diameter of 7/16" increasing to 1" in the middle of the horn, and finishing with 6" diameter bell. As Carse (p. 285) mentioned: "When the keys are raised, the quality and intonation seems to deteriorate more or less progressively, and the tone becomes rather husky."

Figure 2.9 Keyed bugle

The last large advancement of the trumpet evolved from the end of the 18th century to the middle 20th century. This advancement, the valve as we know it, allowed players to instantly include extra sections of tubing to their instruments. Charles Clagget made the first written record of this concept in 1788, though some argue of its true value*. Due to advancing technology, valves progressed from clunky, difficult to use, and leaky devices to today's refined and polished Périnet valve. Valves added to the flexibility of the trumpet, giving the player the ability to successfully change the effective length of the instrument very quickly. Valves also changed the sound of the trumpet throughout their development. Early valves by Schuster and Stölzel included sharp bends in the tubing, which affected the sound significantly. The sharper bends and discontinuities added acoustic reflections in the tubing, causing the tone and intonation to suffer†. Advancements were made to limit the sharpness of the bends within the valves and eventually evolved to today's valve, often taken for granted.

Due to physical valve limitations, even today's modern valves include some formidable bends, still affecting the tone somewhat. This can be demonstrated by replacing the valve section in a modern trumpet with a short piece of straight tubing and comparing the timbre of the modified horn with the original. This timbre change may or may not be desirable, depending on the player.

---

* *Bates mentions: There seems to be no doubt that most of Clagget s geese were swans and that he over-valued his invention, nevertheless his chromatic horn was undoubtedly constructed*

As mentioned by Italian Composer Spontini, Kapellmeister to the King of Prussia, 1826.

2.4. Summary

The trumpet, throughout its development and maturation, has become a very widespread and popular instrument in modern music despite some lulls in usage in its history. Its flexibility has grown and it has been applied to more and more musical venues from subtle orchestra enhancements to solo performances.

With the invention of the slide and later the valve, the ability to play a continuous chromatic scale came about and thrust the trumpet into the solo world. But with the valve some sacrifices had to be made acoustically due to the sharp turns and bends resulting in a change in timbre which is still part of the modern instrument as we know it.

The modern trumpet sound has evolved from the noisy and raucous sound of the original trumpets to the clear and bright sound of the first natural trumpets, and finally to the darker, fuller sounds of today's instrument. Along with the instrument itself developing through history, trumpet mutes also evolved. Further development of the instrument is pursued through this thesis investigation of integrating the trumpet with an ANC system. This system could bring together several centuries of trumpet sound development and trumpet mute development. Combining them with modern trumpet construction into one system will allow the player extended flexibility and control over his/her sound. By no means is this meant to be a final solution, only a system that will allow additional timbre flexibility.

Chapter 3. An Analytical Trumpet Model

In order to understand the process involved in the physical playing of a trumpet and to understand the dynamics that will eventually be controlled, a mathematical model needed to be developed. In order to accurately derive a mathematical model of the trumpet the actual physics involved in the generation of the trumpet sound are addressed. After these physics are determined, appropriate dynamic equations are applied to generate the mathematical model. A time domain simulation is created from these equations based on a model developed by Adachi Seiji [Seiji, 1995].

From this simulation, several characteristics of the trumpet/player system are observed. The coupling of the player and trumpet system is studied. Small changes in the trumpet system are shown to cause large changes in the intonation of the instrument. A quantity unable to be directly measured, the embouchure displacement, is also visualized. The model provides a basis for comparison of different trumpet systems and different controller systems.

3.1. Elements of the Trumpet/Player system

The trumpet itself can be simplified to be an acoustic duct with a circular cross section that varies in area along its length. Left out of this analysis are the subtle ways bends and turns in the tubing affect the sound pressure propagation. The trumpet acts as an acoustic filter that resonates at some frequencies and dampens others. The input to the acoustic filter is the player's vibrating (buzzing) lips and the output consists of pressure waves emanating from the bell. The player's lips are set into motion by the air pressure applied by the player's diaphragm. The first element modeled is the player's lips, or the embouchure.

3.1.1. The Embouchure

The player forms his/her lips into an embouchure by stretching the lips out so to create lip tension and pressing them closed. Initially the upper and bottom lips are touching, thus closing the air passageway. When the trumpet mouthpiece and trumpet are applied to the lips, an approximately airtight seal is formed. As the player increases the pressure from his/her respiratory system, air is forced against the inside of the player's lips and the lips are forced open. The air pressure escapes into the trumpet and the lips collapse back to an almost closed condition due to the loss of pressure. The air pressure difference builds up again between the player's mouth cavity and the trumpet system, and the lips are forced open again. This repeated opening and closing of the lips generates cyclical pressure waves that travel into and through the trumpet.

When the pressure waves reach the bell of the trumpet, some of the energy is released into the atmosphere and some is reflected back into the trumpet since the bell and the farfield are not exactly impedance matched. This is the case with acoustic waves traveling in any finite-length tube. The reflected pressure wave travels back through the trumpet and impinges on the player's lips applying a force opposite of the player-generated air pressure. If the player has tension on his/her embouchure that creates a particular natural vibrating frequency, at which the trumpet also resonates, the whole player/trumpet system will resonate at that frequency and the associated overtones or harmonics. This stable, self-sustained oscillation occurs only when the player's embouchure is tuned to one of the natural frequencies of the trumpet.

In order to simulate all the aspects of the player, each element must be modeled. The first element in the system is the player's respiratory system. This includes the diaphragm, the trachea, and the mouth cavity. The respiratory muscles generate a pressure on the lungs, which force air through the trachea to the lips and into the trumpet. The pressure that the player generates is approximately static for a given player and is between 2.0 and 5.0 kPa depending on the volume and pitch, as was measured with a U-tube manometer. The airflow from the lungs, through the trachea, to the lips is assumed laminar and not high speed. The player's respiratory system and cavities are assumed for this model not to have any acoustic resonances or interactions, but to only generate a static pressure on the internal

side of the player's embouchure. Any sound energy that enters the mouth cavity is assumed absorbed by the player and not reflected back into the system.

While in vibrating motion, the player's lips move in all directions. The lips are deformable structures that change as the note is being produced making the development of a detailed model difficult. To simplify the model, the lips are assumed to be a lumped mass and have only two degrees of freedom. The first degree of freedom is an extensional motion where the lips act as valve moving up and down in the plane of the lips. The second degree of freedom is a swinging motion where the lips are free to rotate inward and outward.

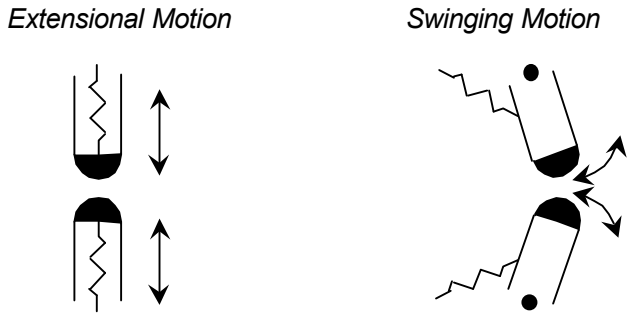

Figure 3.1 Simplified motions of the embouchure

The player, both before and during the production of a note adjusts the mass, stiffness, and damping of his/her embouchure indirectly. Depending on how tight the player chooses to pull his/her embouchure, there may be a little or a lot of lip mass vibrating in the mouthpiece. By choosing a mass, stiffness and damping of the lip system, a precise resonance of the lips can be specified in the model. When the player picks a resonance frequency that the trumpet supports, a well developed, self-sustaining oscillation occurs.

By combining the two types of motion, a two-degree-of-freedom model is produced. A side view of the upper lip of the embouchure model is shown Figure 3.2. The lip is assumed to be a parallelogram **ABCD** that extends into the page a distance b. The length of the lip is defined as the distance **AD** or **BC** represented as d.

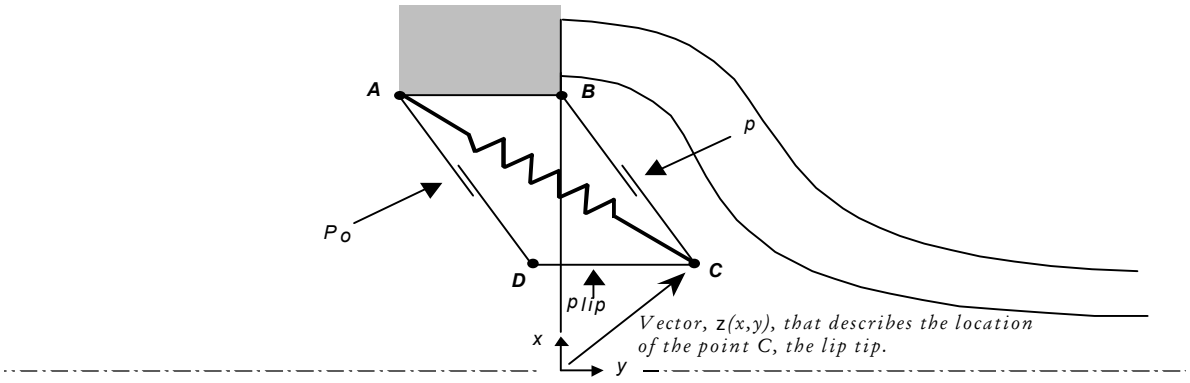

Figure 3.2 Embouchure model schematic, upper lip

The upper and bottom lips are assumed to be symmetrically shaped and also to move symmetrically. The center of the coordinate system is placed at the center of the trumpet mouthpiece rim. The forces on the embouchure include:

- P_o the static pressure applied perpendicularly to the inside lip surface by the player
- p the pressure resulting from the reflected pressure waves applied perpendicularly to the outside lip surface
- p_{lip} the Bernoulli pressure caused by air flow between the upper and lower lips.

The mass of the lip, m, is assumed to be a lumped mass equidistant from the points **A**, **B**, **C**, and **D** at all times. The vector $\mathbf{z}(x,y,t)$ fully describes the location of the lip at time t.

The stiffness of the lip system is assumed to be equal in both the x and y directions. The spring constant is equal in both the x and y directions, so the true mechanical schematic is shown in Figure 3.3.

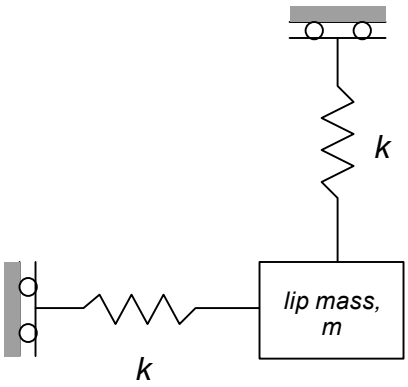

Figure 3.3 Simplified lip schematic

The simplified schematic shows how the two stiffnesses affect the system. The two single degree-of-freedom systems are not directly mechanically coupled since their motions are always orthogonal. The force from the player's respiratory system is applied to both of the systems throughout the simulation. If the inside lip surface is vertical, i.e. the lip surface **AD** is parallel to the *y*-axis, the player-applied air pressure acts perpendicularly to the lip surface and will only affect the horizontal system. The lip tip will be forced out to the right and lip surface **AD** will no longer be parallel to the *y*-axis. The player-applied air pressure will now affect both single degree-of-freedom systems since the air pressure acts perpendicularly to the lip surface **AD**.

The three forces on the lip system can be represented as follows. The first force is an internal lip force, the spring restoring force acting on the lip relative to the lip equilibrium resting position, z_{equi}.

$$-\frac{1}{2}k(z - z_{equi}) \tag{3.1}$$

The second force is an external force, the pressure differential force generated by the blowing pressure and the reflected pressure from the trumpet acting on the lip surfaces **AD**

and **BC**. The $\perp$ operator indicates a vector perpendicular to the argument but with the same magnitude. This is shown vectorially in equation (3.2).

$$b(p_o - p)(\mathbf{z} - \mathbf{z}_{joint})^{\perp} \tag{3.2}$$

The third force is also an external force, the Bernoulli pressure, caused by the air flow between the lips. It acts perpendicularly against the bottom lip surface. The vector $\hat{e}_y$ is the unit vector in the y direction.

$$bdp_{lip}\hat{e}_y \tag{3.3}$$

The damping in the lip system is represented as:

$$-\frac{1}{2}\frac{\sqrt{mk}}{C}\frac{d\mathbf{z}}{dt} \tag{3.4}$$

The value C is an arbitrary number to vary the amount of damping in the system depending on whether the lips are closed ($C=0.5$) or open ($C=3.0$). This will be addressed later.

Combining these forces together by applying Newton's 2nd law to the forced two degree of freedom system results in a second order, two-dimensional dynamic equation for the embouchure.

$$\frac{1}{2}m\frac{d^2\mathbf{z}}{dt^2} = -\frac{1}{2}\frac{\sqrt{mk}}{C}\frac{d\mathbf{z}}{dt} - \frac{1}{2}k(\mathbf{z} - \mathbf{z}_{equi}) + b(p_o - p)(\mathbf{z} - \mathbf{z}_{joint})^{\perp} + bdp_{lip}\hat{e}_y \tag{3.5}$$

The term on the left-hand side represents the inertia (mass and acceleration) of the lip system and the terms on the right-hand side represent the forces on the system. The ½ factor is present in the inertia term since the mass is located half way between the tip and rotational joint at all times, reducing the inertia by half.

Since $\mathbf{z}(x,y,t)$ is a two dimensional vector, equation (3.5) can be split into its respective x and y components to create two orthogonal second order equations:

$$\begin{aligned}\frac{1}{2}m\frac{d^2\mathbf{z}_x}{dt^2} &= -\frac{1}{2}\frac{\sqrt{mk}}{C}\frac{d\mathbf{z}_x}{dt} - \frac{1}{2}k(\mathbf{z}_x - \mathbf{z}_{equi_x}) + b(p_o - p)(-\mathbf{z}_y + \mathbf{z}_{joint_y}) \\ \frac{1}{2}m\frac{d^2\mathbf{z}_y}{dt^2} &= -\frac{1}{2}\frac{\sqrt{mk}}{C}\frac{d\mathbf{z}_y}{dt} - \frac{1}{2}k(\mathbf{z}_y - \mathbf{z}_{equi_y}) + b(p_o - p)(\mathbf{z}_x - \mathbf{z}_{joint_x}) + bdp_{lip}\end{aligned} \tag{3.6}$$

When the upper and lower lips are open, there is an opening for the air to pass through, S_{lip}. The area of the lip opening is used to calculate the acoustic volume velocity. When the lip tip, $\mathbf{C}$, is at position $\mathbf{z}(x,y)$, S_{lip} is defined as:

$$S_{lip} = \max(2b\mathbf{z}_y, 0) \tag{3.7}$$

This defines the area of the lip opening always to be non-negative since a negative lip opening area can not exist.

During the buzzing cycle, the top and bottom lips may come in contact with each other. In this case, an extra force, F_{closed} is added in the y direction to account for the additional force experienced when the upper and bottom lips touch and push against each other. This nonlinear condition is expressed with equation (3.8).

$$F_{closed} = \begin{cases} -3k\mathbf{z}_y\hat{e}_y & if\ S_{lip} = 0 \\ 0, & if\ S_{lip} > 0 \end{cases} \tag{3.8}$$

In addition, the damping is also increased while the lips are in contact due to the deformable nature of the lips. This is taken into account by decreasing the value of C. This can be described with equation (3.9).

$$C = \begin{cases} 0.5 & if\ S_{lip} = 0 \\ 3.0 & if\ S_{lip} > 0 \end{cases} \tag{3.9}$$

The total volume velocity generated by the lips system is a combination of the acoustic volume velocity from the moving airflow and by the air volume displaced by the lips moving in space while buzzing. The former is generated by the changing pressure gradient between the static pressure and the reflected pressure waves from the trumpet. The later, the volume velocity produced displacement of air by the lips, can be described by equation (3.10):

$$\begin{aligned} U_{lip} &= \left[b(\mathsf{z} - \mathsf{z}_{joint}) \times \frac{d\mathsf{z}}{dt} \right] \bullet \hat{e}_z \\ &= b\left[(\mathsf{z}_x - \mathsf{z}_{joint_x}) \frac{d\mathsf{z}_y}{dt} - (\mathsf{z}_y - \mathsf{z}_{joint_y}) \frac{d\mathsf{z}_x}{dt} \right] \end{aligned} \tag{3.10}$$

The mass and stiffness of the system, m and k define the vibrating frequency (f_{lip}) of the system. They are chosen by the player indirectly to select a specific frequency to play. This relationship between the mass and stiffness of the lips in the model and the frequency of vibration is expressed in equations (3.11) and (3.12) [Elliot and Bowsher, 1982a].

$$m = \frac{1.5}{(2\pi)^2 f_{lip}}\ kg \tag{3.11}$$

$$k = 1.5 f_{lip}\ \frac{N}{m} \tag{3.12}$$

In order to relate the pressures in the system, p_o, p_{lip}, and p, the conservation of momentum and the conservation of energy laws are used. The air-flow/lip system is broken into two parts, a contraction region, and an expansion region as shown in Figure 3.4.

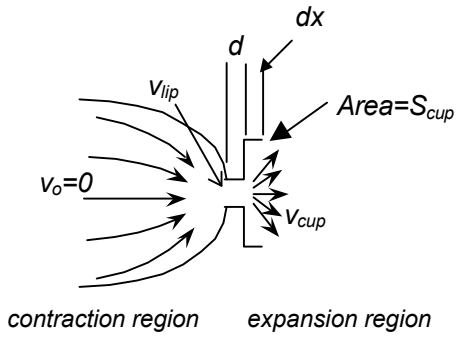

Figure 3.4 Flow model for embouchure

The contraction region represents the inside of the player's mouth, with the flow assumed laminar. The expansion region occurs right after the lip orifice, d, over the differential distance, Δx. The Reynolds number is relatively high (10^3) in the expansion region, so the flow is assumed a "jet," and cannot be assumed laminar.

Applying the conservation of energy law in the contraction region gives:

$$\dot{E} = \dot{E}_{ext} + \dot{W} \tag{3.13}$$

The first term on the left is the energy stored in the control volume. The first term on the right is the energy entering into the control volume and the second term is the work performed by the flow on the control volume. Assuming $v_o << v_{lip}$ and one-dimensional flow, the terms become:

$$\dot{E} = \frac{d}{dt}\int \frac{1}{2}\rho v^2 dVol = \rho U \int \frac{\partial}{\partial x} v dx \cong \rho U d \cdot \frac{d}{dt} v_{lip} \tag{3.14}$$

$$\dot{E}_{ext} = \frac{1}{2}\rho U (v_o^2 - v_{lip}^2) \cong \frac{-1}{2}\rho U v_{lip}^2 \tag{3.15}$$

$$\dot{W} = U (p_o - p_{lip}) \tag{3.16}$$

with

U = *the volume velocity flowing into the region.*

Substituting these expressions into the conservation of energy equation, (3.13), gives:

$$\rho U d \cdot \frac{d}{dt} v_{lip} = \frac{-1}{2} \rho U v_{lip}^2 + U(p_o - p_{lip}) \tag{3.17}$$

Solving equation (3.17) for p_o-p_{lip} results in the first of the desired pressure difference equations:

$$p_o - p_{lip} = \frac{1}{2} \rho \left(\frac{U_{acoust}}{S_{lip}} \right)^2 + \frac{\rho d}{S_{lip}} \frac{\partial U_{acoust}}{\partial t} \tag{3.18}$$

In order to arrive at the second pressure difference, p_{lip}-p, the conservation of momentum is applied in the expansion region. The conservation of energy cannot be applied as easily since the pressure expansion is sudden. The sudden expansion causes vortex shedding resulting in the fluid, air in this case, to lose energy in the form of heat, which is not easily accounted for mathematically. Applying the conservation of momentum instead within the region gives:

$$\dot{M} = \dot{M}_{ext} + F \tag{3.19}$$

The first term on the left is the momentum retained in the region. The first term on the right side is the momentum entering the region and the second term is the force along the axis of flow. These terms can be written as:

$$\dot{M} = \frac{d}{dt}\int \rho v dV = \rho \int \frac{dU}{dt} dx \cong \rho \Delta x \frac{d}{dt} U \tag{3.20}$$

$$\dot{M}_{ext} = \rho U(v_{lip} - v_{cup}) \tag{3.21}$$

In order to find the force, F, exactly, the pressure distribution on the lip needs to be determined. This would involve solving the Navier-Stokes equation for the lip system. In order to avoid this, the average pressure on the lips is introduced, resulting in a simpler expression for the force, F, on the lip system.

$$\hat{p} = average\ pressure(between\ p_{lip}\ and\ p)$$
$$F = \hat{p}(S_{cup} - S_{lip}) + p_{lip} S_{lip} - p_{cup} S_{cup} \tag{3.22}$$

Substituting this back into the conservation of momentum equation, (3.19), results in:

$$\rho \Delta x \frac{d}{dt} U = \rho U(v_{lip} - v_{cup}) + \hat{p}(S_{cup} - S_{lip}) + p_{lip} S_{lip} - p_{cup} S_{cup} \tag{3.23}$$

Simplifying this equation:

$$\hat{p} - p_{cup} - \gamma(\hat{p} - p_{lip}) = -\rho v_{lip}^2 \gamma(1-\gamma) + \rho \Delta x \frac{d}{dt} v_{cup} \tag{3.24}$$

with:

$$\gamma = \frac{S_{lip}}{S_{cup}} \tag{3.25}$$

The average lip pressure is still not known, but through the application of the conservation of energy law to the same region and observing how much energy is actually lost due to heat, we find that the average lip pressure is much closer to p_{lip} than p [Adachi, 1995]. Therefore,

to simplify the system, the average lip pressure is set equal to p_{lip}. Substituting into equation (3.24) and simplifying gives the desired second pressure relation:

$$p_{lip} - p = -\rho U_{acoust}^2 \left(\frac{1}{S_{cup} S_{lip}} - \frac{1}{S_{cup}^2} \right) \tag{3.26}$$

The last equation in the system gives an expression for the mouthpiece pressure. The output pressure can be represented as the input pressure plus the pressures that have propagated to the end of the trumpet and return back to the embouchure. In the time domain this gives a pressure convolution integral.

$$p(t) = Z_{cup} U(t) + \int_0^\infty r(s) \left(Z_{cup} U(t-s) + p(t-s) \right) ds \tag{3.27}$$

The reflection function, $r(t)$, defines how the pressure waves are reflected from the end of the trumpet after being introduced into the system at the mouthpiece, an impulse response function. In the frequency domain, it can be also be interpreted as the frequency response of the trumpet acoustic system. Z_{in} and Z_{cup} are the acoustic impedances of the trumpet and mouthpiece cup respectively. These will be derived and discussed in the next section.

The derivation of equation (3.27) and it's principles can be found in [Schumacher, 1981].

The definition of acoustic impedance, Z, is:

$$Z = \frac{P}{U} \tag{3.28}$$

with:

P=*acoustic pressure*

U=*acoustic volume velocity*

3.1.2. Trumpet Component Sections

The next segment in the sound generating system is the trumpet itself. The trumpet is simply a tube with a variable cross sectional area along its length. This variable cross section determines the frequency placement of the resonances and the tone quality/color of a particular trumpet. The resonances of the trumpet need to be aligned with the harmonic series in order for the horn to play "in tune." A skilled player can make the trumpet resonate at almost any frequency regardless of where the resonances of the trumpet lie, but the trumpet system will respond more easily and with better tone at the actual resonances of the trumpet. The intonation is primarily affected by the internal shape during the first two-thirds of the length of the trumpet.

The last third of the trumpet consists of the initial bell flare and bell mouth. This section strongly influences the tone color. Although there is great debate in the industry about whether the bell material affects the tone color and playing response, this model presented here assumes there is no significant structural acoustic interaction at any point in the trumpet system. This assumption is supported by some early experiments [Knauss and Yeager, 1941]. The initial experiment involved exciting the walls of a cornet bell electromagnetically and measuring the acoustic output as compared to the normal playing of the cornet. Results showed there to be no significant acoustic output from the vibration of the bell material. To verify this observation putty was applied to the inside of the bell of a cornet, completely damping it, and taking measurements of the farfield acoustic spectrum. The results again showed no difference in perceived tone color from that of an untreated cornet.

The section that the bell is attached to is the valve section. The valve section is primarily cylindrical in shape and lets the player vary the length of the entire horn easily and quickly by pressing down any combination of the three valves. These valves redirect the airflow through different lengths of tubing, changing the effective length of the acoustic system. Though the shape of the tubing in the valve section is cylindrical, significant turns and bends in the tubing occur. The acoustic effect of these bends is not included in the model.

The next section is the tuning slide. This section is also primarily cylindrical and allows the player to adjust the overall fundamental length of the horn so that the 2nd harmonic (sounding Bb), is in tune relative to the chosen standard.

The trumpet's leadpipe, attached to the tuning slide, is conically shaped. It functions to couple the mouthpiece backbore to the tuning slide. The backbore of the mouthpiece is a short (<3 inches), conical section at which the smallest cross-section is found. It connects to the mouthpiece cup.

The last element in the trumpet system is the mouthpiece cup. The shape of the mouthpiece cup is very important to the quality and tonal shape of the final sound of the trumpet. This is due to quick transitions in cross sectional area that occur in the mouthpiece. These quick transitions can cause more and larger shedding vortices to occur, setting into effect higher frequency components, and can result in a very bright sound. The mouthpiece also has a great influence on the intonation of the trumpet due to its impedance matching function. If the throat of the mouthpiece is too large or too small, significant intonation problems arise. Each section can be seen in Figure 3.5 and Figure 3.6.

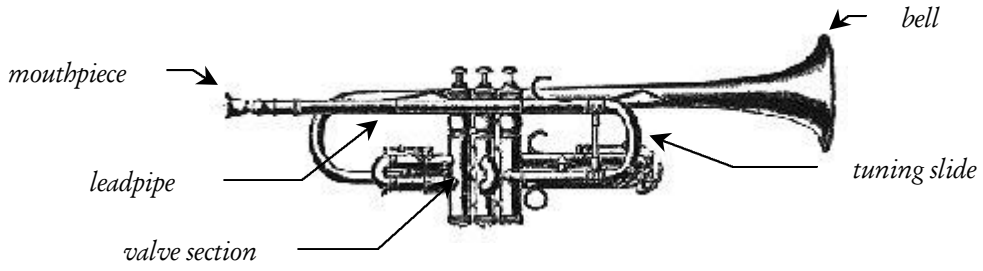

Figure 3.5 Schematic of trumpet

Figure 3.6 Schematic of trumpet mouthpiece

3.1.3. Determination of the Reflection Function, r(t)

The reflection function is a representation of how the trumpet responds to an impulse input. The reflection function can be used to study the instrument's transient response as well as the steady state response. The time domain model uses the reflection to establish how pressure inputs to the trumpet behave while in the trumpet.

In the frequency domain, the reflection function is defined as:

$$\hat{r}(f) = \frac{Z_{in}(f) - Z_{cup}}{Z_{in}(f) + Z_{cup}} \tag{3.29}$$

with:

$Z_{in}(f)$ = *the frequency-dependent input impedance of the trumpet.*

Z_{cup} = *the input impedance of the player*

Equation (3.29) is based on several assumptions. There is an impedance difference between the player and the trumpet, Z_{cup} and Z_{in}. Input pressure waves from the player are injected directly at the boundary between the player and trumpet towards the trumpet. The energy is partially transmitted into the trumpet and some is reflected back immediately, due to the impedance difference between the trumpet and the player. The energy that is reflected back from the boundary is assumed to completely dissipate, no longer affecting the system. The

dissipation is modeled as an infinitely long tube with a constant impedance, Z_{cup}, assuming plane wave propagation:

$$Z_{cup} = \frac{\rho c}{S_{cup}} \tag{3.30}$$

Schematically, the system is an infinite tube with a diameter equal to that of the mouthpiece cup, with impedance Z_{cup} attached directly to the mouthpiece.

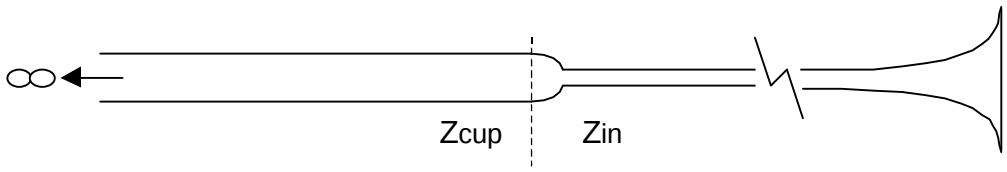

Figure 3.7 Schematic of reflection function assumption

Therefore, from basic acoustics, the reflection function is the ratio of the addition of and the difference of the two system impedances. If the impedances were identical, there would be no reflection and all of the incident energy from the player would be transmitted to the second medium (the trumpet) and the reflection function would be zero. The actual trumpet input impedance, Z_{in}, will be determined in *Section 3.1.4.*

In order to convert $r(f)$ to a time domain representation, an inverse FFT (IFFT) was applied to the frequency-based reflection function. Assuming the original frequency domain impedance data was of high resolution and was of high frequency, effects of numerical acausality are insignificant.

3.1.4. Determination of the Trumpet Input Impedance, Z_{in}

The acoustic impedance at a particular point in the system is defined as:

$$Z(x,y,z,t) = \frac{P(x,y,z,t)}{U(x,y,z,t)} \tag{3.31}$$

where P is the pressure and U is the acoustic volume velocity at the particular point. The impedance is the resistance that an acoustic wave 'feels' when it impinges on the particular point. The input impedance of the trumpet is the resistance to acoustic input to the trumpet system.

At the bell or mouth of the trumpet the output radiation impedance is assumed to be the same as an infinitely baffled piston of the same size as the mouth of the horn [Olson, 1967]. This is reaffirmed by the fact that the directionality of the bell is very similar to the infinitely baffled piston.

The infinite baffled piston impedance is determined analytically by using *Bessel* and *Stuve*[*] functions:

$$Z_{piston} = \frac{\rho c}{S_2}\left[\left(1 - \frac{BesselJ_1(2kR)}{2kR}\right) + \left(j\frac{Struve(2kR)}{2kR}\right)\right] \tag{3.32}$$

The acoustic radiation impedance is thus:

[*] *See Appendix B for an explanation of the Struve function*

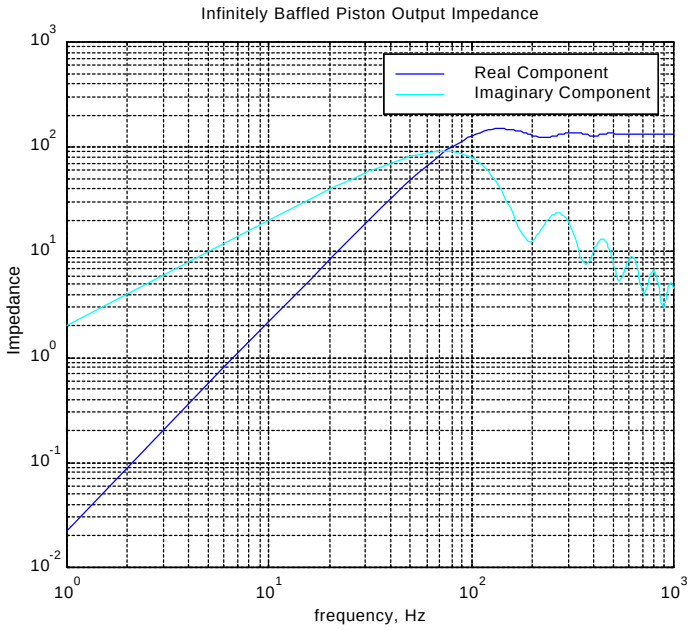

Figure 3.8 Radiation impedance of infinitely baffled piston

One approach to finding Z_{in} is to divide the horn into a few simple shapes such as cylindrical tubes, cones, and exponential horns and solve for the total input impedance. The solutions to the wave equation for plane waves in these types of tubes with varying cross sections has been previously completed [Olson, 1967]. The wave equation could ideally be solved for any variable cross sectional area, but may prove to be difficult, if not impossible with some horn shapes. The solutions to the cylindrical, conical and exponential shaped horns are listed below for convenience.

The input impedance, z_{a1}, in terms of the output impedance, z_{a2}, for a finite cylindrical tube assuming no wave propagation attenuation is:

$$z_{a_1} = \frac{\rho c}{S_1}\left[\frac{z_{a_2} S_2 \cos(kl) + j\rho c \sin(kl)}{j z_{a_2} S_2 \sin(kl) + \rho c \cos(kl)}\right] \tag{3.33}$$

Assuming $z_{a2} = Z_{piston}$, the resulting input impedance, z_{a1} is:

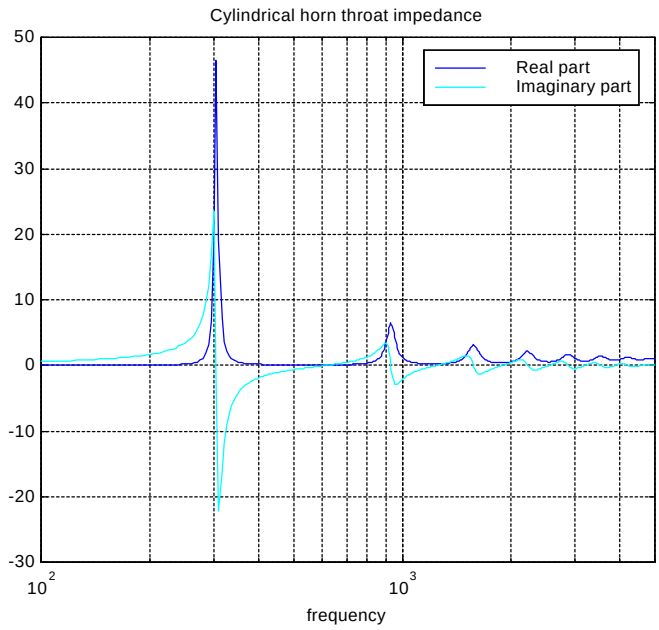

Figure 3.9 Finite cylindrical tube input impedance assuming an infinite baffled piston impedance as the mouth impedance

Similarly for a finite cone horn:

$$z_{a_1} = \frac{\rho c}{S_1}\left[\frac{jz_{a_2}\dfrac{\sin(k(l-\theta_2))}{\sin(k\theta_2)} + \dfrac{\rho c}{S_2}\sin(kl)}{z_{a_2}\dfrac{\sin(k(l+\theta_1-\theta_2))}{\sin(k\theta_1)\sin(k\theta_2)} - \dfrac{j\rho c}{S_2}\dfrac{\sin(k(l+\theta_1))}{\sin(k\theta_1)}}\right] \tag{3.34}$$

Assuming $z_{a2} = Z_{piston}$, the resulting input impedance, z_{a1} is:

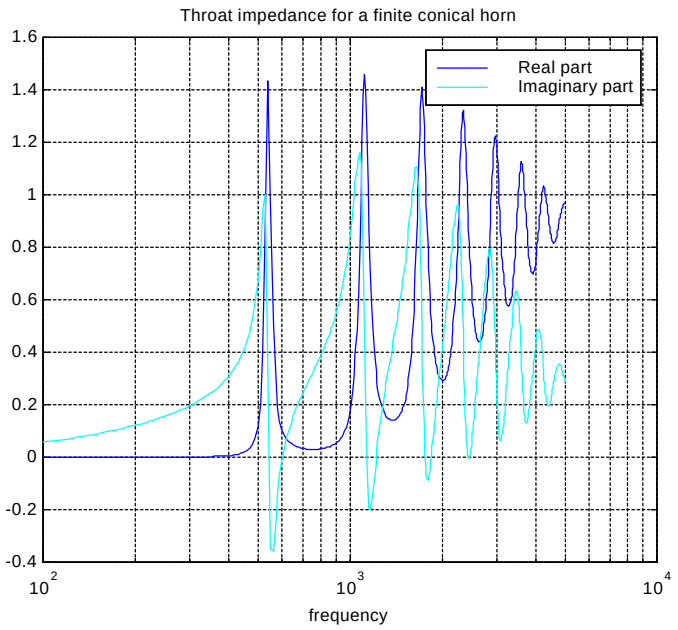

Figure 3.10 Finite conical horn input impedance assuming an infinite baffled piston impedance as the mouth impedance

And for a finite exponential horn with a flare constant, m:

$$
\begin{aligned}
z_{a_1} &= \frac{\rho c}{S_1}\left[\frac{S_2 z_{a_2}\cos(bl+\theta)+j\rho c\sin(bl)}{jS_2 z_{a_2}\sin(bl)+\rho c\cos(bl-\theta)}\right] \\
a &= m/2 \\
b &= \frac{1}{2}\sqrt{4k^2-m^2} \\
\theta &= \tan^{-1}\left(\frac{a}{b}\right)
\end{aligned}
\tag{3.35}
$$

Assuming $z_{a2}=Z_{piston}$, the resulting input impedance, z_{a1} is:

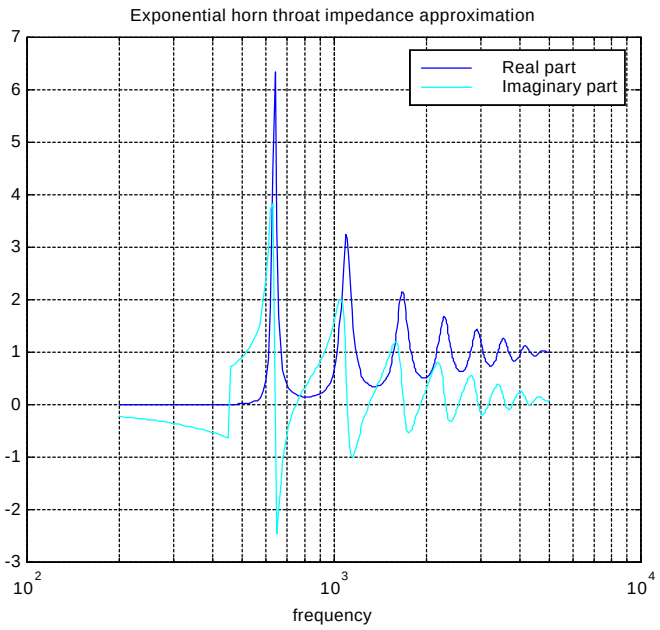

Figure 3.11 Finite exponential horn input impedance assuming an infinite baffled piston impedance as the mouth impedance

If a trumpet model is constructed of several of the above-mentioned basic shapes, placed end to end, a crude approximation can be made of the shape of the trumpet.

The throat impedance of one horn section is used as the mouth impedance of the next section back. By working backward through the horn to the mouthpiece, an approximation of the trumpet input impedance, Z_{in}, is calculated.

Unfortunately, the trumpet, mainly the bell, is not shaped like any of the simple shapes described above. The input impedance, Z_{in}, found from the first method doesn't reflect the real input impedance of a trumpet very accurately. Use of this method results in a very out-of-tune trumpet model (relative intonation is discussed in *Section 3.1.5*). The crude shape approximation and input impedance from this method are shown in Figure (3.12) and Figure (3.13) respectively.

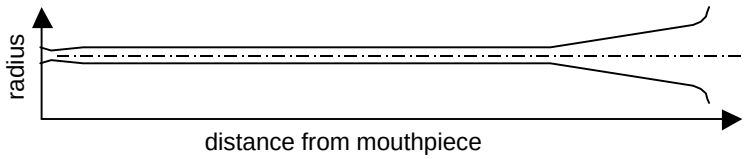

Figure 3.12 Crude shape approximation of trumpet

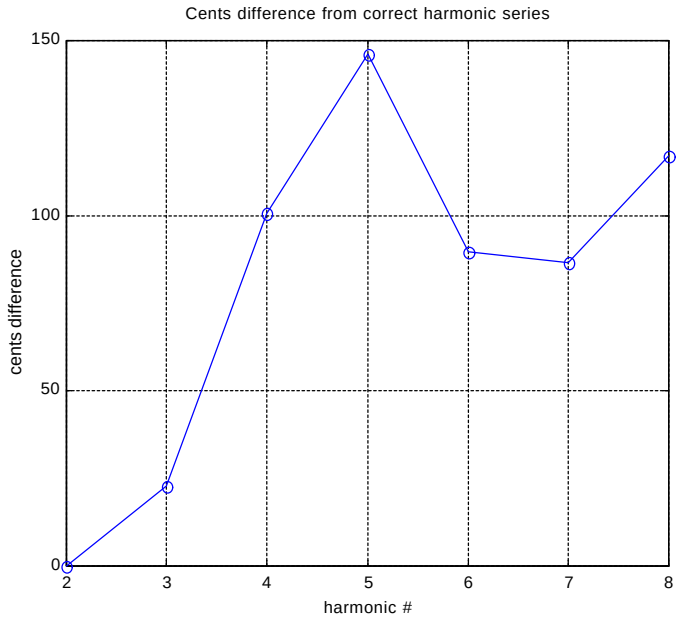

Figure 3.13 Crude impedance model intonation

A second method that is used to calculate the exact input impedance for the trumpet involves determining a mathematical equation for the shape of the trumpet. This equation can be substituted into the general, one-dimensional wave equation and analytically solved for the exact input impedance. Unfortunately, this does not lend itself to a simple or convenient solution.

A third method, similar to the first, was developed and can be used for any arbitrary horn shape. It involves breaking the trumpet up into only conical sections, each section being very short, <1". This method is analogous to approximating a curve with many short line segments. The impedance is then calculated backwards through the trumpet as before and an input impedance is determined which is shown to be fairly accurate. To demonstrate that

the discrete mathematical model for the trumpet returned valid results, several test cases were used for comparison.

Since the analytical exponential horn solution was already derived and an exact equation for the throat impedance available, a discrete element model was constructed of the same horn shape and the resulting input impedances compared. As can be seen from the throat impedance plots in Figure (3.14), the results are close to identical by choosing a minimum number of sections for the discrete element model.

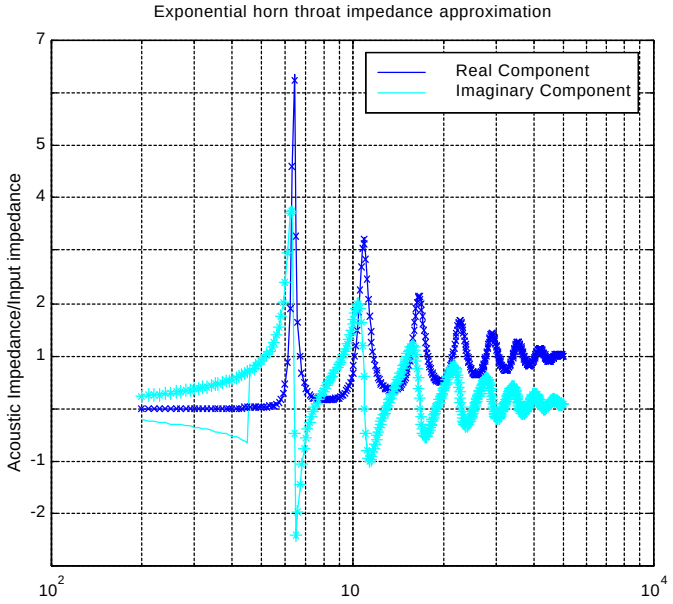

Figure 3.14 Exact exponential horn solution compared to discrete element horn approximation

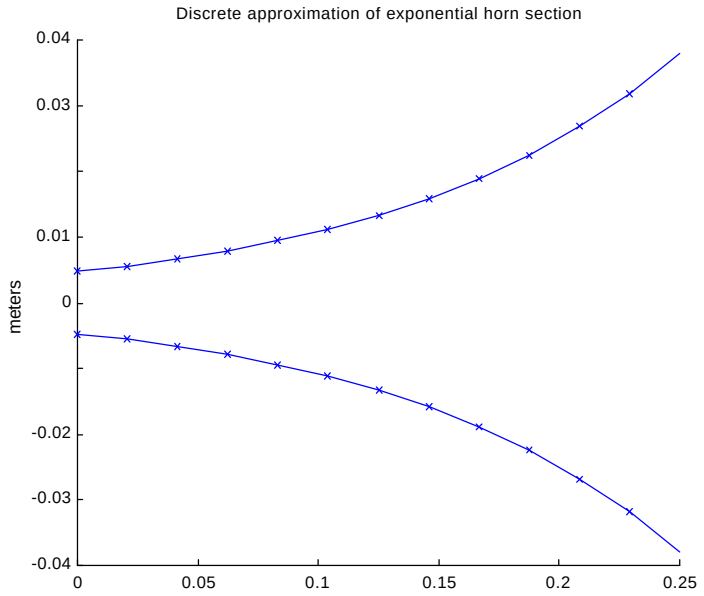

Figure 3.15 Comparison of analytical solution and discrete element model using twelve sections

Similarly, the discrete element model also works for a cylindrical shape. Matlab code to implement this technique is listed in Appendix A.

Since the discrete element model is shown to approximate the basic shapes and their impedances correctly, measurements of an actual trumpet were performed on a Yamaha 6810Zs Bb trumpet. This trumpet is known by the author to play in tune and produces a warm, full tone. Measurements of the outside diameter of the trumpet were taken approximately every 1" along the length of the horn, from the bell to the mouthpiece. The wall thickness was assumed constant and each measurement was corrected for this. Any inside diameter measurements that could be taken were since these would be fundamentally more accurate. At the mouthpiece, inside measurements were taken at closer intervals since the cross section changes rapidly at this point and is critical to achieving an accurate acoustic impedance model.

A discrete conical horn section approximated the acoustic element between each of these measurements. All of the discrete sections were mathematically attached end to end and the impedance calculated at the throat of the overall trumpet assuming the output impedance is

equal to an infinitely baffled piston as stated before. This impedance was then assumed to be the input impedance, Z_{in}, of this particular trumpet.

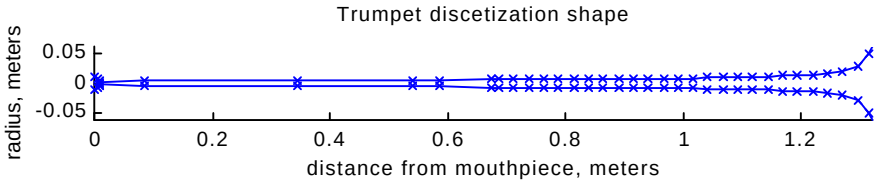

Figure 3.16 Discretized trumpet shape from Yamaha 6810Zs Bb trumpet

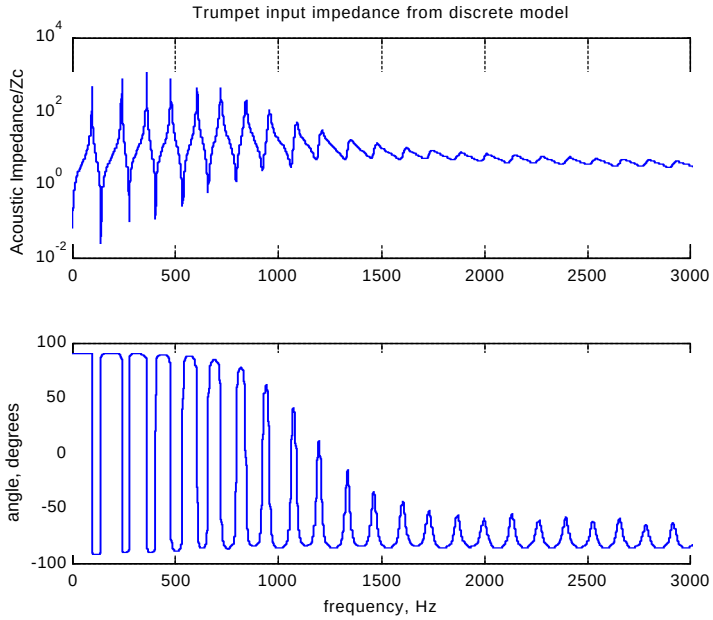

Figure 3.17 Calculated trumpet input impedance

The intonation of this trumpet input impedance is discussed in the next section.

3.1.5. Trumpet Intonation and the Harmonic Series

The intonations of the resonances of this trumpet model were checked against the standard harmonic series with which the trumpet should be aligned. The harmonic series is a set of overtones that correspond to specific musical intervals (Figure 3.18).

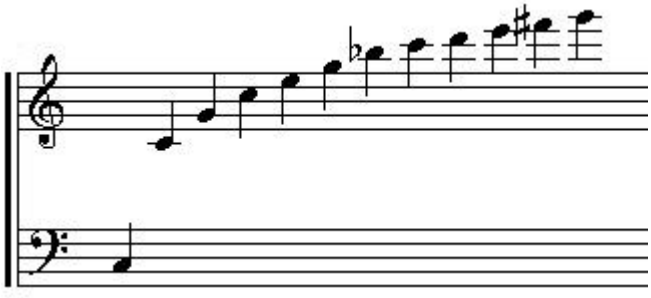

Figure 3.18 Standard trumpet harmonic series based on the fundamental C

These overtones occur on traditional trumpets and are what players have been used to since the advent of musical trumpets. The placement of the overtones is dependent on the shape construction of the trumpet as mentioned before. Changing the dimensions of the trumpet model will demonstrate this. Most modern trumpets as they stand play fairly well in tune.

By looking closely at the first eight harmonics or the bottom two octaves of normal playing usage, we see that the frequency of each peak in the input impedance is relatively in tune with the harmonic series (Figure 3.19). The lowest frequency peak in Figure 3.17 usually is flat (lower frequency than expected) and thus is not included in the harmonic series. This is the true fundamental resonance of the trumpet, but in practice is very rarely used due to its poor intonation. On larger brass instruments, French horns, trombones, baritones, and tubas, the true fundamental is closer in tune and is often used in practice.

The frequency difference between a resonant trumpet frequency (f_1) and the true harmonic series (f_2) frequency are represented in cents (¢). There are 100 cents between semi-tones (i.e. C and C#). Equal temperament tuning is based on log(2) semi-tone frequency ratios. Since there are 12 notes contained in an octave, there are 1200 cents in an octave.

$$cents = \frac{1200}{\log(2)} \log\left(\frac{f_1}{f_2}\right) \tag{3.36}$$

The intonation of the accurate approximation of the trumpet input impedance in the previous section is:

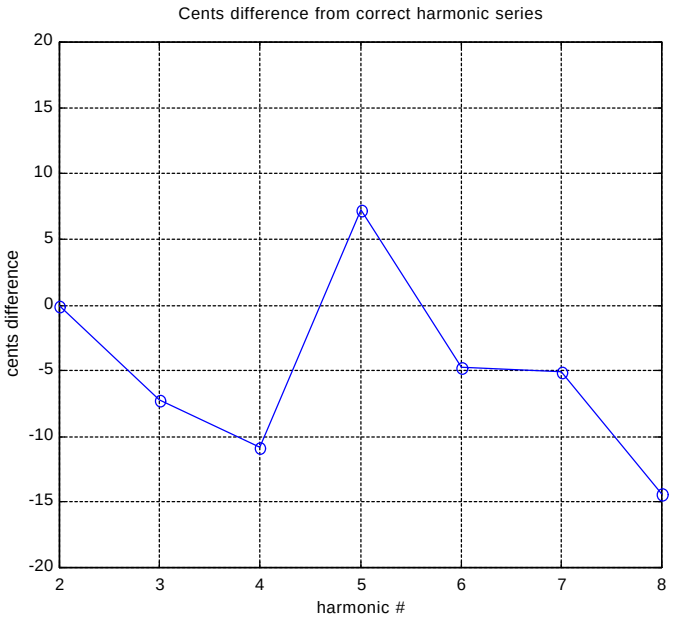

Figure 3.19 Correct intonation from the discrete element model

The relative intonation is much improved from the crudely shaped trumpet. The maximum amount the accurate model varies from the true harmonic series is –15 cents. The eighth harmonic frequency is f=232*4=928 Hz. With a variation of –15 cents, the sounding frequency will be 920 Hz.

This impedance model can also illustrate the effect of each section of the trumpet on the harmonic placement in the harmonic series. If only the cylindrical section of a trumpet is taken and stretched out to the full trumpet length, so that the fundamental remains the same as the trumpet, the resulting resonances are significantly sharper (higher in frequency) than the correct harmonic series. This can be seen in Figure (3.20) as curve A. Adding the bell

lowers the trumpet resonances significantly (curve B). Similarly, adding only a lead pipe and mouthpiece to the cylindrical tubing also lowers the series (curve C). But only with the addition of the bell, the lead pipe, and the mouthpiece does the harmonic series of the horn approach correct intonation.

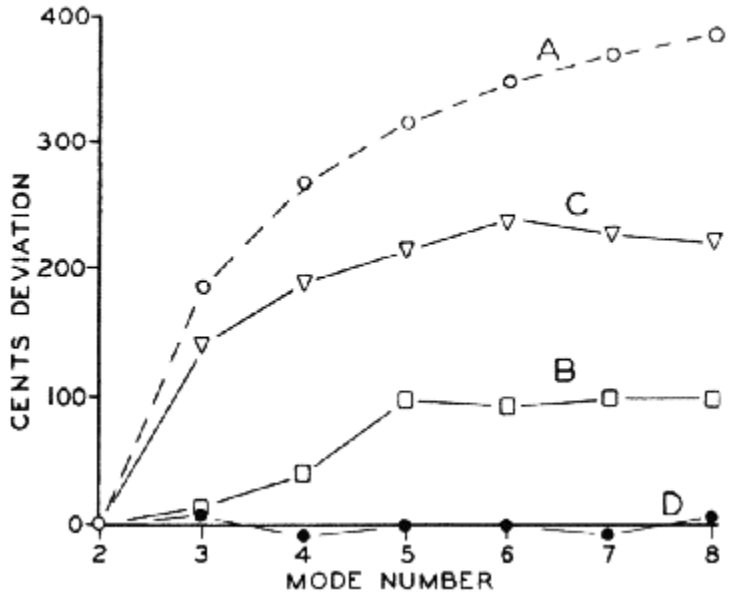

Figure 3.20 Intonation purposes of each general trumpet section [Backus, 1976]

The trumpet is very sensitive to dimensional changes. If the leadpipe is made to flare too quickly, the intonation may vary from a small amount to a large amount across the harmonics. For this example, the leadpipe was flared 0.010" more during the first 10 inches from the mouthpiece. The difference in intonation of the harmonics is shown in Figure (3.20). The 4th and 7th harmonics are more in tune than the original but the 3rd harmonic is significantly more out of tune.

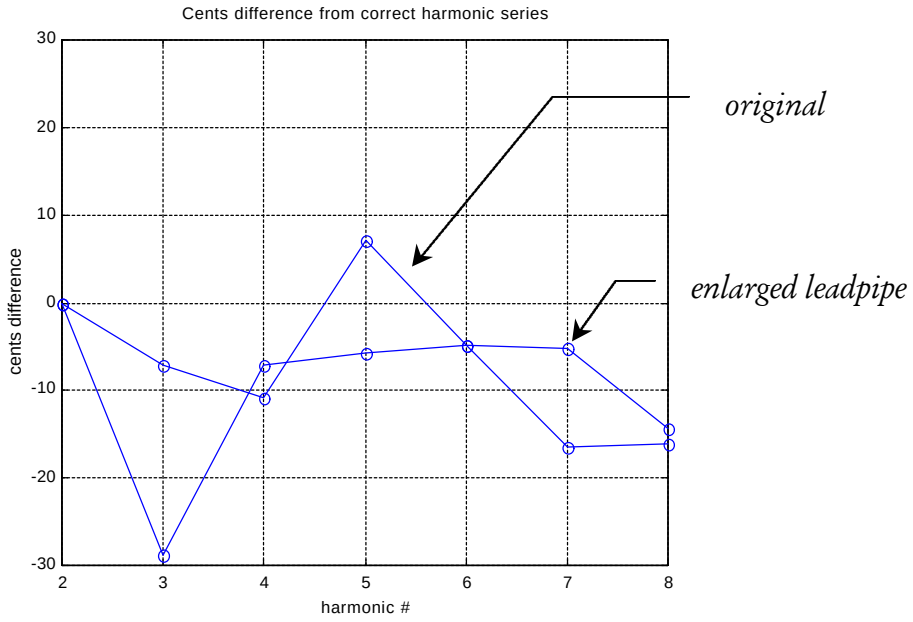

Figure 3.21 Intonation variability with shape perturbation

3.2. Discretizing the Simulation

With the representation of the dynamics in the trumpet model, a simulation will be performed. A time domain simulation was chosen to allow for flexibility in observing transient effects. In order to execute a time domain simulation, the equations in the model must be discretized. A truncated Taylor series is used to derive finite-difference approximations for the first and second derivatives in the equations.

The Taylor series expansion for an arbitrary function *f(t)* is:

$$f(t+\Delta t) = f(t) + f'(t)\Delta t + \frac{f''(t)}{2!}\Delta t^2 + \ldots \tag{3.37}$$

Truncating the Taylor series expansion after two terms results in:

$$f(t+\Delta t) \cong f(t) + f'(t)\Delta t \tag{3.38}$$

Solving for $f(t)$:

$$f'(t) \cong \frac{f(t+\Delta t) - f(t)}{\Delta t} \tag{3.39}$$

Equation (3.39) is the *forward-difference approximation* of the first derivative. Replacing Δt with $-\Delta t$ results in the *backward-difference approximation*:

$$f'(t) \cong \frac{f(t) - f(t-\Delta t)}{\Delta t} \tag{3.40}$$

By retaining one more term in the Taylor series expansion, a *central-difference approximation* can be obtained for the second derivative, $f''(t)$:

$$f''(t) \cong \frac{f(t+\Delta t) - 2f(t) + f(t-\Delta t)}{\Delta t^2} \tag{3.41}$$

Keeping the time step, Δt, relatively small, the error accumulated in the equations will be insignificant. Substituting the forward-difference approximation for the first derivative and the central-difference approximation for the second derivative into the second order differential equation and solving for $f(t+\Delta t)$, a discrete equation is made. The discrete equation relates the function value at time $t+\Delta t$ in terms of the function value at times t and $t-\Delta t$. Thus, a discrete time domain simulation can be performed, stepping at intervals of Δt.

The dynamic lip equation, equation (3.5) and the lip volume velocity, equation (3.10) are both discretized with the Taylor Series approximations. The last equation in the simulation, equation (3.27), involves a convolution integral, which must be evaluated at discrete time values instead of over infinite, continuous time. At this point in the simulation, variables that are still unknown at time $t+\Delta t$ are p and U_{acoust}. Equations (3.26) and (3.27) are solved simultaneously to calculate these last two variables.

For Matlab code implementing this simulation, refer to Appendix A.

3.3. Performing the Simulation

The simulation was performed for three cases. Each case consisted of simulating a specific resonant frequency of the trumpet's: *C* (232 Hz), *g* (348 Hz), and *c* (464 Hz). The mouthpiece pressure output of the model, *p*, was compared to actual measured mouthpiece cup pressure of the three notes to validate the model.

Several variables are held constant throughout the simulation. They are set before the simulation begins. They include:

c	speed of sound
ρ	average air density
S_{cup}	area of mouthpiece entryway
f_{lip}	the frequency of lip vibration
ζ_{equi}	equilibrium lip position
P_o	the player's blowing pressure.

In reality, some of these variables could change such as the player's blowing pressure, P_o. For example, during a crescendo, the player would increase the blowing pressure over time. For these simulation runs, these variables were held constant.

The lip position was initially set to the equilibrium position, ζ_{equi}, to simulate the player being at rest before playing a note.

The step size, Δt, was set to 1/8000 of a second. A step size of 1/32000 second was also used and the transient and steady state results did not change significantly, therefore, 1/8000 of a second was determined to be adequate. The simulation was performed for 1000 steps,

equaling $^{1}/_{8}$ second of simulation time. This allowed all transients to diminish and a steady state oscillation to develop.

The results of the simulation approximately match that of measurements of actual mouthpiece pressure (Figure 3.22 - Figure 3.24). Several reasons exist that explain the differences between the model and actual measured pressures. The input impedance included in the model was based on a set of non-exact trumpet bore measurements and therefore, does not represent the exact trumpet shape involved in the actual mouthpiece pressure measurements. Second, the model assumes there are plane waves in the mouthpiece cup at the plane of entrance. Since the player's lips actually extend into the mouthpiece and since the actual pressure measurements were not performed exactly at the plane of entrance, the pressure calculated from the model will deviate from the measured pressure.

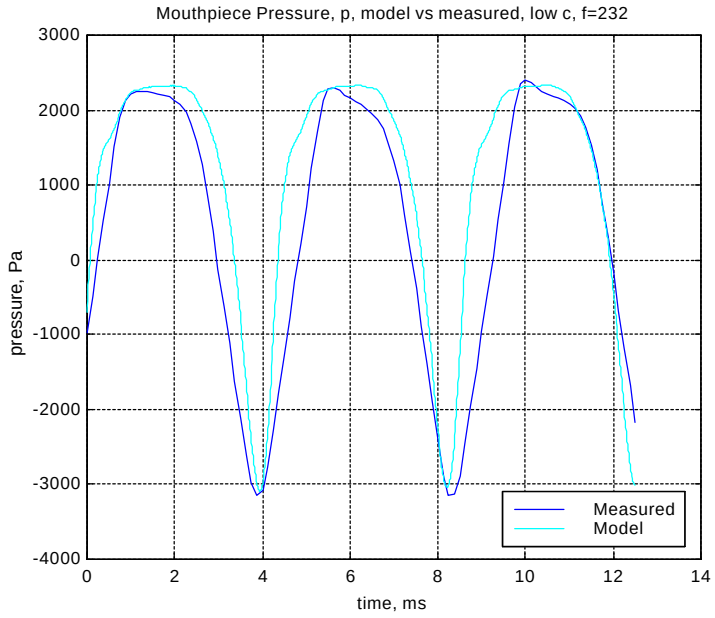

Figure 3.22 Simulated mouthpiece pressure, low c, f_o=232 Hz

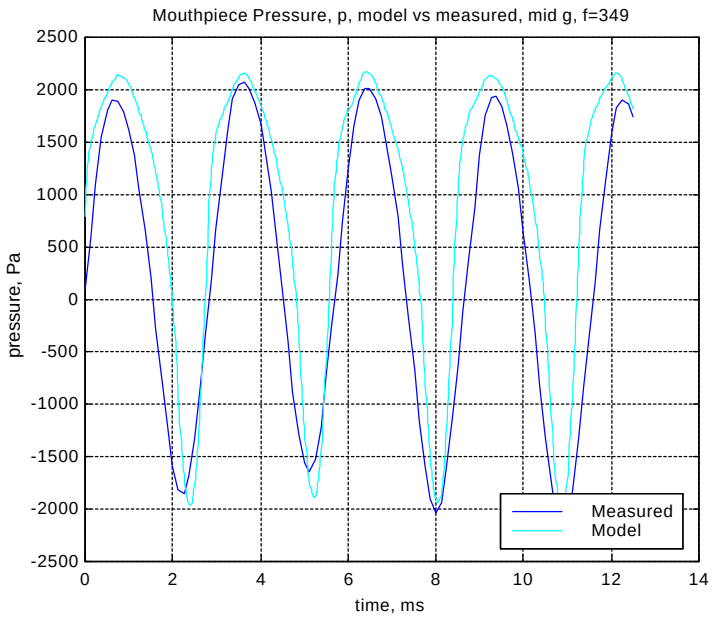

Figure 3.23 Simulated mouthpiece pressure, g, f_o=349 Hz

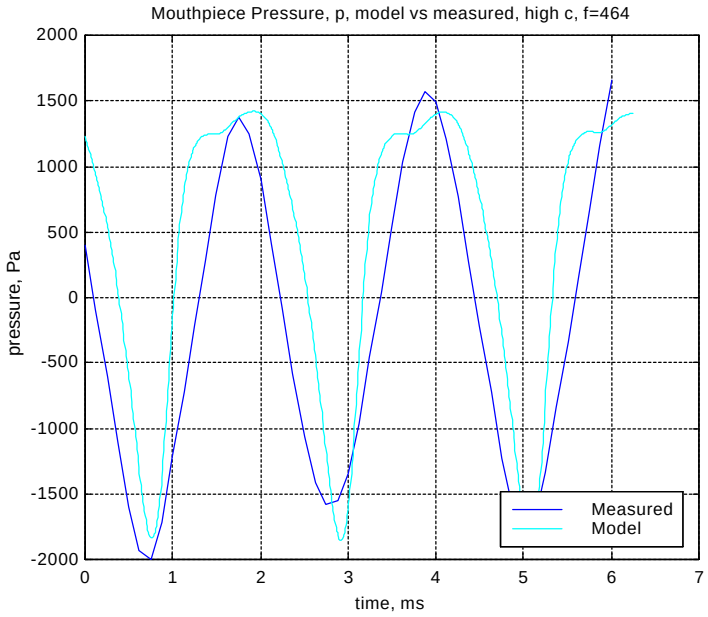

Figure 3.24 Simulated mouthpiece pressure, c, f_o=464 Hz

By plotting $z(x,y,t)$, we can observe the characteristics of how the player's lips displace while playing a particular note (Figure 3.25). From this, analysis can be performed on what effect a change in trumpet bore shape, or how a particular type of active noise control algorithm will affect the lip movement of the player. This effect is very important in how the player feels as he/she plays the controlled trumpet system. If the implemented control system starts to disrupt the movement of the player's lips, or even to the point of not allowing the player's lips to move at all, then the ANC system may be found to work too well and cause the player to feel uncomfortable. With too much change to the trumpet bore shape or with a particular method of control applied to the trumpet, the trumpet may play poorly or cease to be playable at all.

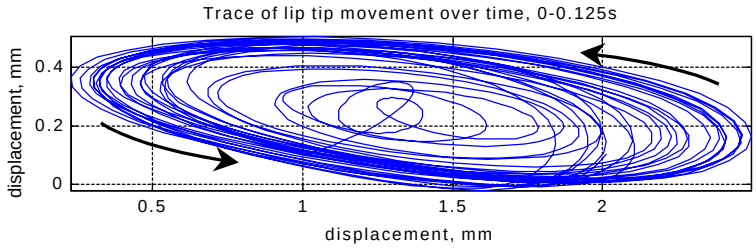

Figure 3.25 Lip tip movement over time

Ideally, the pressure input from the control actuator will only propagate towards the output of the trumpet and thus, only affecting the acoustic output and not propagating back towards the player's embouchure, but this was not the case. This is due to the chosen placement of the control actuator, which will be discussed in *Chapter 4*.

3.4. Other Uses of the Trumpet Model

The model that was developed is used for several design problems including active noise control analysis. Effects of various system changes on the mouthpiece pressure and the player's embouchure movement can be analyzed. Modeling different trumpet bore shapes can be used to optimize various aspects of the trumpet such as intonation and tone quality. Each trumpet bore shape can be virtually tested and the resulting input impedance, pressure

output, and embouchure travel response could be studied to determine whether one bore shape is better than another. Since the 'player' in the model does not change over time like a real person, the model could be used to test proposed changes over long periods of time.

3.5. Future Trumpet Model Work

Though the model incorporated numerous aspects of the trumpet system, there are many left to include in order to create an all-encompassing model. These aspects include but are not limited to bore tubing thickness, bore tubing material, bends in the tubing, structural-acoustic interaction, internal flow characteristics, temperature differences in the trumpet material and variable internal air properties. Incorporating these aspects into the model would result in an even more accurate acoustic output and could be used to show how even finer changes in the trumpet construction would affect the player's response to the trumpet and the acoustic output.

Currently the trumpet dynamics are included in the model of the input impedance and eventually in the calculated reflection function. In order to observe in more detail how small discontinuities affect pressure wave propagation in the trumpet bore a finite element pressure model could be developed. This model would break the trumpet system up into small finite pressure elements, each modeled as a cylindrical tube. As the player injected pressure waves into the system, the pressure waves would propagate through each finite element over time. Very subtle reflections could be observed as well as other aspects of the trumpet could be analyzed.

A finite element pressure solution would allow study of the pressure anywhere along the trumpet bore, showing reflections, losses, etc. This extension of the model would also accurately model the placement of the control actuator to the system. As will be seen in *Chapter 4*, the control actuator addition in the model applies the control pressure directly to the cup of the mouthpiece. In actual implementation, the control pressure was applied 2 inches further down the mouthpiece backbore. Changes such as these would contribute to a more accurate and detailed model.

Chapter 4. Application of ANC to the Trumpet System

Two forms of active noise control were applied to the trumpet system to attenuate and shape the tonal structure of the trumpet sound. The two methods of active control were analog feedback control and digital LMS adaptive feedforward spatial control. Both methods were successful in attenuating the first two tones present in the farfield trumpet sound.

The two objectives for the ANC application were maximizing the attenuation the of trumpet sound output and maximizing the zone of control (global control). In addition to analyzing the perception of the listener, analysis of the player also was performed. The influence of the control on the player affects the comfort level of the player, thus the playability of the combined ANC/trumpet system. This analysis was performed using the model developed in *Chapter 3*.

The two control methods that were applied to the trumpet system differ in their control algorithm implementation, but both require an error sensor and control actuator. The decision of what to use and where to put these two components depends heavily on what criteria are used and the goals that are sought. The selection and placement of these components are discussed in the following sections.

4.1. The Trumpet System

The uncontrolled farfield sound spectrum of the trumpet for a written second line 'G^4' (f_o=352 Hz) is shown in Figure 4.1. Farfield sound pressure measurements were taken approximately 1 bell diameter (5-6 inches) from the bell mouth. This has been found to be a good representation of the farfield perceived sound [Benade, 1976].

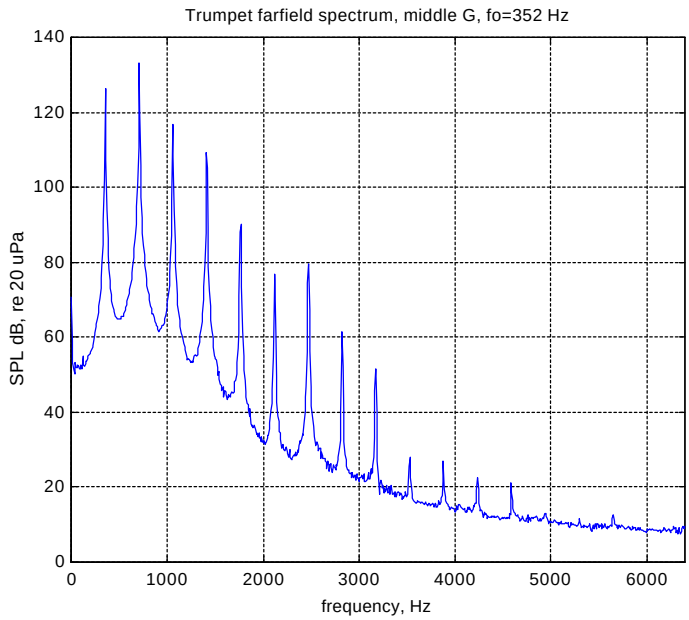

Figure 4.1 Trumpet farfield sound spectrum, f_o=352 Hz

The farfield spectrum is what the ANC system affects and also what the listener perceives. Reducing or reshaping this spectrum can realize different effects and is an objective of this system. For example, when the trumpet player inserts a straight mute, the farfield spectrum becomes:

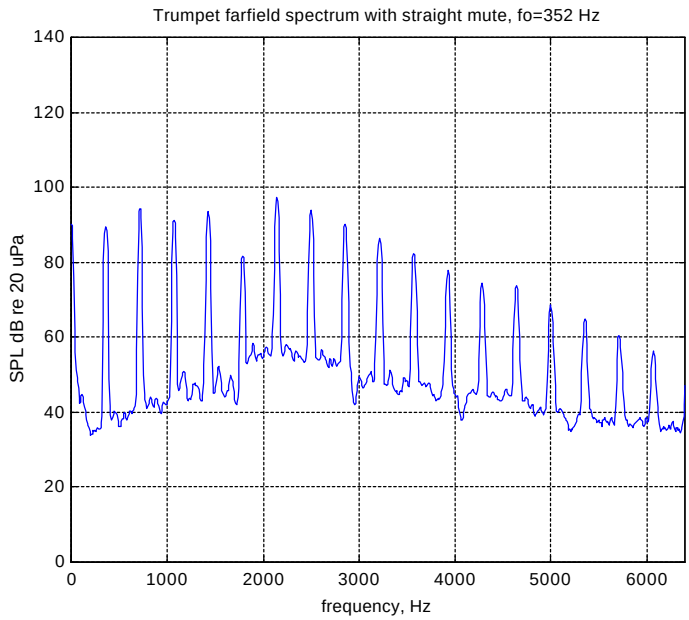

Figure 4.2 Trumpet farfield sound spectrum with straight mute, f_o=352 Hz

By creating this spectrum using only the trumpet and the ANC system, the user could easily switch the ANC system on or off as needed, without having to insert and remove a mute.

The spectrum content and shape shown are unique to the trumpet. Other instruments have different spectrums, content and shape. By changing the trumpet farfield sound spectrum to be similar to another type of instrument, almost any musical instrument sound could be simulated. Since the trumpet sound includes all harmonics of the fundamental frequency, a clarinet sound (Figure 4.3) could be synthesized by attenuating most of the even harmonics and reshaping the resulting sound spectrum, a form of subtractive synthesis.

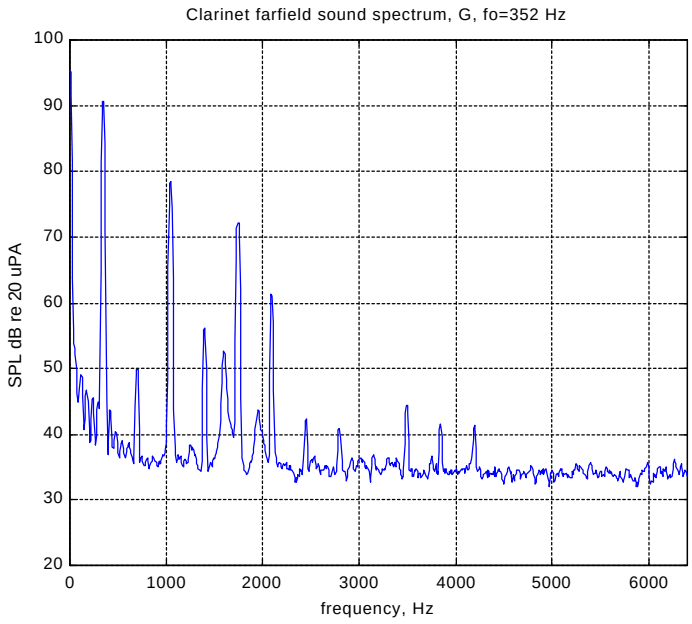

Figure 4.3 Clarinet farfield sound spectrum, f_0=352 Hz

Using this technique, almost any harmonic instrument could be synthesized from the original trumpet spectrum giving a trumpet player with the ANC system a very accessible form of a real-time synthesizer.

4.2. Type and Placement of Control Actuator

Before a specific type of controller can be designed and implemented, a control actuator and location must to be chosen. The effectiveness of the control system on the farfield trumpet sound is directly related to the control actuator type and placement. If the control actuator lacks ability to influence the system due to its type or from its location, the final system output will not change and the listener will not perceive a difference.

The effect that the control actuator has on the player is also important. If the control actuator is too heavy or bulky, then the suitability of the system will be low or not acceptable. The feeling experienced by the player from the control actuator while playing the trumpet-controller system is also very important. If the control actuator administers too

much authority, then it may cancel out the player's vibrating lips or disturb them significantly, making the entire system unplayable. This effect was investigated using the mathematical trumpet model presented in *Chapter 3* and will be discussed in *Section 4.9*.

4.2.1. Control Actuator at the Bell

The first, and perhaps obvious choice for the control actuator location is at the bell or the actual output of the trumpet system similar to the placement of a conventional mute. Since the trumpet sound is coming from the bell, ideally the control actuator output should also emanate from the bell. This can be approximately realized by placing a speaker directly at the bell opening as shown in Figure 4.4.

Figure 4.4 Control actuator suspended at trumpet bell opening

This control actuator placement has several problems and thus was not used. In order to easily achieve true global acoustic control, the control actuator is required to be located at the exact point of the disturbance. When the control actuator is located at the bell mouth, the trumpet sound is effectively coming from a different location than the control sound. This can be seen in the directivity plots in Figure 4.5.

The original directivity and sound of the trumpet are no longer present with the control actuator mounted on the direct acoustic axis of the trumpet bell. With the tonal control

system off, the player would expect the sound of the trumpet to be unimpeded and natural sounding, but instead, the sound is muffled due to the control actuator physically impeding the sound. In order to overcome this disadvantage, an acoustic/electronic feed through would have to be employed to effectively pass the sound through the control actuator blockage.

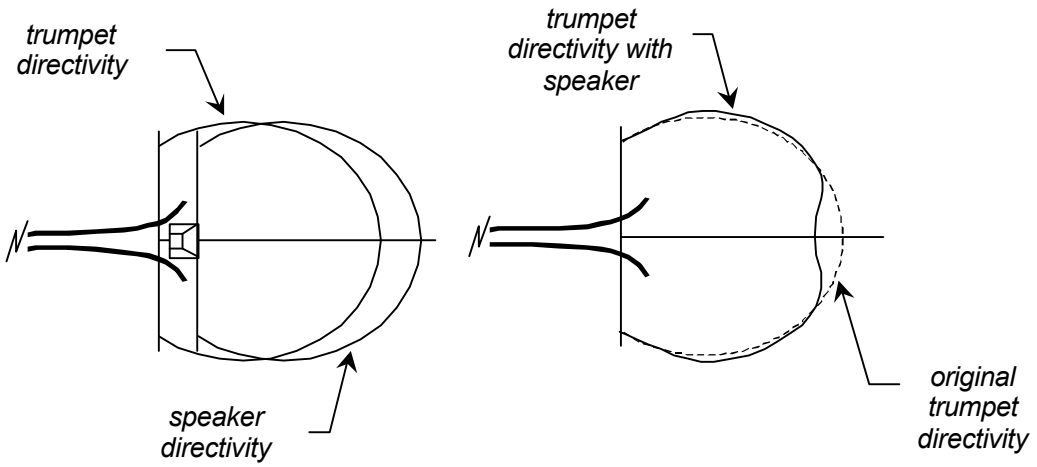

Figure 4.5 Collocation difficulty and directivity influence with control actuator at trumpet bell opening

Another disadvantage of this control actuator location is the uncomfortable weight experienced by the player. Since sound pressure levels at the bell opening are in the 130 dB (SPL), 200-3000 Hz range as seen in the trumpet spectrum in Figure 4.1, a control actuator would need to produce comparable sound pressure levels to achieve any perceptible control. A speaker capable of this sound pressure level is likely be fairly heavy and also bulky, not lending itself to a suitable solution.

An advantage of this control actuator placement is the ability to avoid feedback from the control actuator to the error sensor. Since the control actuator radiates out into the farfield and not back into the system, the error sensor, if located within the trumpet, would not sense any appreciable output levels from the control actuator, preventing any undesirable feedback dynamics from occurring.

Another advantage to this placement of the control actuator is that the player does not feel any physical effect of the control actuator. Only the farfield field pressure waves are affected and not the pressure waves in the interior of the trumpet system and in the player's mouthpiece. Therefore, the player will only hear a difference, not feel one.

4.2.2. Control Actuator at the Bell Crook

Another possible location of the control actuator is at the bell crook (Figure 4.6). With the control actuator upstream from the actual output of the system, the control actuator output would have a short time and space to blend with the disturbance sound and would output from the same location, the bell, giving effective collocation and resulting in good global control.

Figure 4.6 Possible driver location at bell crook

An obvious disadvantage of this system is that the player's trumpet would have to be heavily modified with the control actuator permanently or semi-permanently installed. Modification of the trumpet is desired to be at an absolute minimum due to cost, marketability, ease of installation, and player acceptance.

A control actuator in this location would still require a fairly large driver in order to generate the required sound pressure levels needed to effect perceivable control at the bell output. The bell however does help with matching the control actuator impedance effectively to the farfield, increasing the control actuator efficiency slightly.

4.2.3. Control Actuator at the Mouthpiece

Since modification of the player's trumpet is not desirable, but collocation is, the most inexpensive and effective solution is to locate the control actuator at the trumpet mouthpiece. The mouthpiece is an easily modified, detachable part, and is generally inexpensive as compared to the trumpet itself.

With the control actuator located far upstream from the trumpet output, the disturbance will ideally be eliminated before it ever reaches the bell and output to the farfield. At this point, the ANC problem becomes very similar to an acoustic duct noise control problem found in many HVAC systems. There is an upstream disturbance and a midstream control actuator with the goal of attenuating the downstream acoustic output. The basic system is shown in Figure 4.7. The noise source in the trumpet system is the player's vibrating lips. If this "noise" is attenuated midstream, it is believed that the output from the trumpet system into the farfield will also be attenuated.

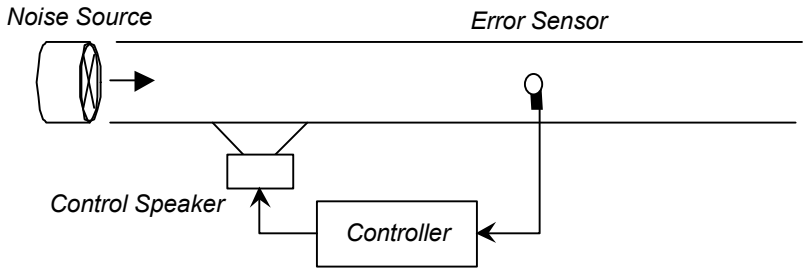

Figure 4.7 Basic active feedback system schematic

The type of control actuator, error sensor, and controller used for the trumpet experiments will be addressed in the following sections.

4.2.4. Type of Control Actuator

One of the most important characteristics of the control actuator in this application is the ability to produce high sound pressure levels on the order of 130 dB (SPL) at the output of the trumpet system. Initially a speaker was chosen to radiate from the bell (*Section 4.2.1*), simulating the trumpet output. A speaker that would not be obtrusive (2-3" diameter, with minimal depth) tends to have trouble producing enough sound pressure to have any perceivable effect on the farfield sound.

Since the control actuator location was chosen to be near to the beginning of the trumpet tubing, near the disturbance *(Section 4.2.3*), the control actuator would have to drive into a small opening into the inside bore of the trumpet. A normal speaker driver is not designed for this high-impedance application, so a horn compression driver was chosen. An adapter was made that connected the compression driver output to the control input of the mouthpiece. Since this driver is designed for a high-impedance load, it interfaced better with the trumpet system than a conventional speaker.

Initial tests demonstrated that the chosen control actuator location worked well in controlling low level disturbances, 80-90 dB (SPL). Unfortunately, high sound pressure level tests showed this driver to be deficient for good control and a source of non-linear, high-level distortion. This will be addressed with an analytical speaker model presented in *Section 4.8*.

4.3. Type and Placement of Error Sensor

With the control actuator located at the mouthpiece of the trumpet, anywhere the error sensor is placed, the control actuator signal will be present there in addition to the disturbance. This can cause problems in designing a controller due to the feedback path from the control actuator to the error microphone. The design of the analog feedback controller takes this feedback path into account.

For this system, possible error sensors/locations include:

- An accelerometer anywhere on the trumpet
- An external farfield microphone
- An external nearfield microphone
- An internal nearfield microphone

An accelerometer would be beneficial due to its ability to reject environmental noise and other non-trumpet system sound. This would be desired in an ensemble or group situation where there may be several trumpets along with other instruments and only the one trumpet sound is desired to be controlled. Unfortunately, the impact vibration from the player operating the trumpet valves is also sensed by the accelerometer.

If an external nearfield or farfield microphone were used, placed 6-36 inches from the bell to measure system output, other environmental sounds would enter the control system. This would cause the controller to attempt to affect these other disturbances, thus reacting and creating sound instead of attenuating the single trumpet output.

The simplest and most inexpensive solution was found to be a microphone that sensed the internal pressure in the trumpet system exclusively. This was accomplished by connecting the microphone to a small pressure tap on the mouthpiece. This minimized system modifications and allowed application to as many different trumpets as possible. Also, since the microphone is significantly far up the bore from the bell, it only senses the player-produced sound and rejects environmental noise.

For the LMS feedforward tests (*Section 4.7*), another upstream pressure port was added to obtain a reference pressure signal. This port was sealed for all feedback controller tests. The final mouthpiece configuration used for this research is shown in Figure 4.8.

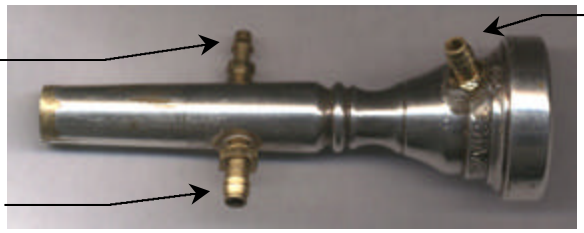

Figure 4.8 Fully modified trumpet mouthpiece

4.3.1. Microphone Selection

Initial tests showed that a real player's buzzing lips were overdriving the error microphone. Instead of the pressure waveform expected (Figure 3.22), a clipped version (max 130 dB (SPL)) was obtained (Figure 4.9). In order to attenuate and get a functional pressure signal from the microphone a small piece of masking tape was placed across the open end of the condenser microphone. Subsequent tests showed this to be inaccurate for capturing time sequences due to the phase lag due to the addition of the attenuation tape. This microphone/attenuation combination was still used for low level control system testing since it did not clip at low levels and the additional phase lag was accounted for in the system identification measurements. For all high level time waveform captures, a B&K type 4136 capable of measuring pressure levels of 180 dB (SPL) was used.

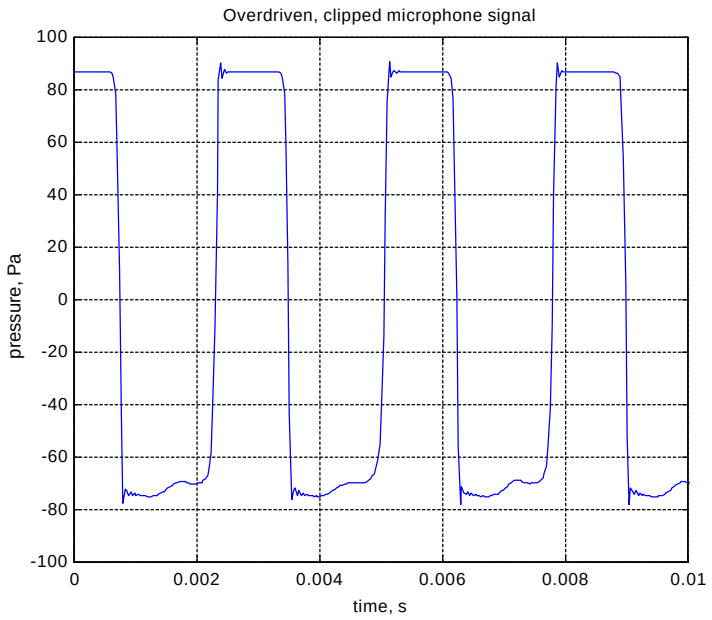

Figure 4.9 Clipped mouthpiece pressure waveform obtained from standard condenser microphone

4.4. Final System Details

With the modified mouthpiece, the control system could interface with the trumpet. The compression driver was attached through a high-impedance tube to one of the ports and the error microphone was attached to the other port.

4.4.1. High-Impedance Control Actuator Connection

A connecting tube with a high impedance was used to connect the control actuator to the port on the trumpet mouthpiece in order to prevent any acoustic system changes to the original trumpet (Figure 4.10). If the trumpet is played with the control actuator port open to free space, the pitch played by the player increases by a semi-tone (100 cents[*]) similar to the behavior of a woodwind tone hole. With the control actuator attached to the port with a low-impedance, flexible rubber tube, the trumpet still plays as though the port is open due to

[*] *For example, C to C# or Bb to B*

the large volume of the actuator and tube combination that acts as a zero pressure boundary at the mouthpiece port. The high impedance of the connecting tube causes the control actuator port on the mouthpiece to behave similarly to if it were completely closed.

The high-impedance tube was constructed with a small rubber tube with an inside diameter of 0.100". There is a round solid rubber section with an outside diameter of 0.050" inside the rubber tube. This resulted in the tube/insert combination having a significantly high impedance. This form of a high-impedance tube is similar to one used in musical instrument impedance measurements performed by [Backus, 1974]. Other forms of high-impedance tubes were tried including insulation filled tubes and very small diameter (<0.010" I.D.) tubes. These other solutions did not provide a high enough impedance to prevent any significant acoustic changes to the trumpet system.

A lengthy rubber high-impedance tube was initially employed to allow the player maximum freedom while using the ANC system. A drawback to having a lengthy, flexible tube connecting the control actuator to the trumpet system is the time delay incurred between the control actuator and the trumpet. This time delay makes the design of the feedback control very difficult due to the high phase lag incurred. The longer the connecting tube, the steeper the phase of the system rolls off, causing instabilities in the system due to phase crossovers. Ideally, the speaker membrane would be directly on the trumpet bore, implementing a zero time delay. A very short tube (0.25") was initially implemented to minimize the time delay but was found to be difficult to actually use, so a longer one (2.5") was developed and used for all tests. The difference in the phase lag between the short and long tube was not large enough to cause any major difficulties. Also, rubber tube wall losses contributed significant transmission loss from the speaker to the trumpet system when using the lengthy tube.

In actual realization, a flexible tube would have to be used to allow player freedom of movement, unless the driver was connected to the trumpet, in which a rigid tube could be designed and implemented.

Figure 4.10 High-impedance connecting tube showing tube insert

The control actuator was driven with a Dynaco Mark III tube amplifier. For amplifier details and performance, see *Appendix C*.

4.5. Repeatable System Testing

In order to assess the actual closed-loop response of the complete system, a human trumpet player could not be used due to variations in his/her pitch, volume, and tone over time. A repeatable, constant "player" was constructed by attaching a small speaker directly to the trumpet mouthpiece. Between the speaker and the mouthpiece, a sheet of stiff rubber was inserted. This membrane or barrier simulated the boundary condition of the player's lips, a closed end condition. The artificial player speaker was attached at all times during the tests. The control player is shown in Figure 4.11 along with the control actuator and error microphone.

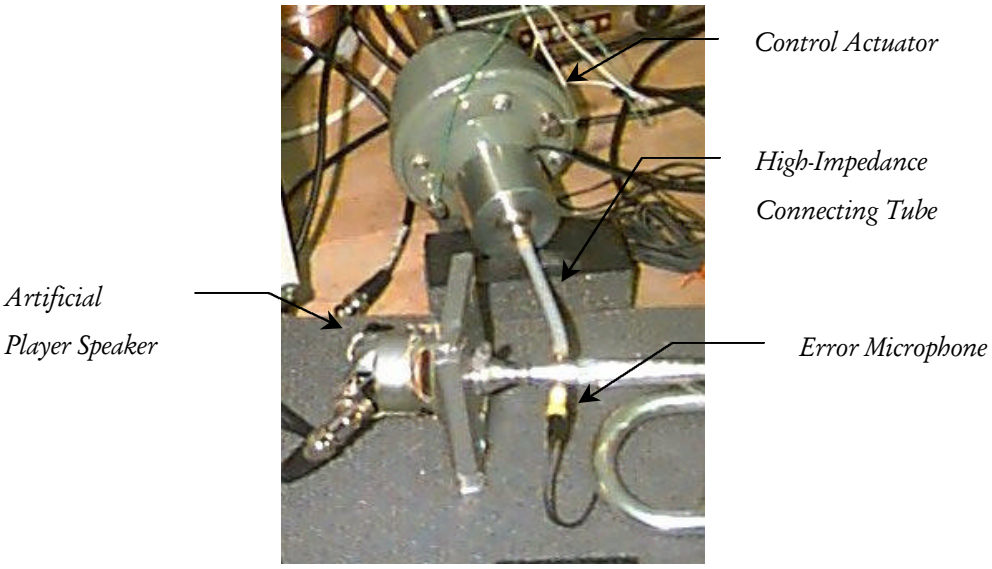

Figure 4.11 Control player speaker

Initially, the artificial player speaker was driven with random noise so the output of the trumpet and control system could be evaluated at all frequencies, not just the trumpet harmonic frequencies. In each case, the farfield spectrum was measured with and without the ANC system activated.

For qualitative tests, a recorded time sample of the pressure in the mouthpiece from the author producing the note 'G', f_o=352 Hz, was played back through the artificial player for all controller tests. With this true trumpet sound, a direct comparison could be made of the farfield sound quality and differences with and without the different controllers.

4.6. Feedback Controller Design

4.6.1. System Identification for Feedback Controller Design

A time domain model was derived earlier to illustrate how the actual system behaved and presented an idea of what type of input the controller would have to use. The feedback controller design was completed in the frequency domain and so was designed from actual measured system dynamics instead of the modeled time domain model dynamics. The

measured dynamics were a much better approximation of the system dynamics than the theoretical time domain model.

The block diagram of the entire feedback control system is shown in Figure 4.12. The microphone performs the pressure summation action in the system by measuring both pressure signals simultaneously from the control actuator and the disturbance (the player's lip vibrations). The transfer function ***G***, or the control-to-error transfer function was measured and used to design the feedback controller.

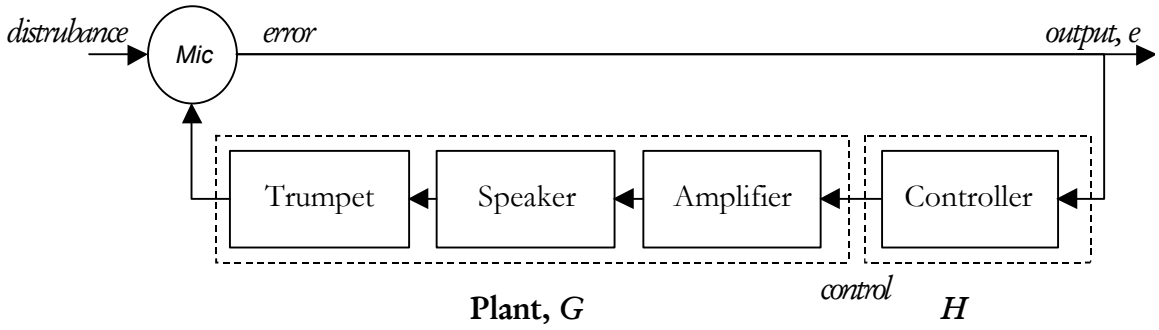

Figure 4.12 Block diagram of entire system

The speaker and the acoustic connector contributed the majority of the undesirable phase characteristics to the overall system transfer function. As seen in *Section 3.1.4*, the transfer function phase (input impedance phase) of the trumpet alone consistently oscillates between 90° and –90° (a minimum phase system), never reaching a negative feedback phase margin such as 180° or –180°. The speaker and acoustic connector add considerable phase lag (time delay) with increasing frequency making the complete system phase cross several phase crossovers. This time delay caused significant problems in achieving acceptable designs of the feedback controllers because of the increased phase lag.

The speaker's frequency response is not uniform or flat due to the speaker's design and the non-ideal acoustic loading. The particular driver used in this research was designed to connect to an exponential horn with a throat diameter of 1". In this case it was driving a very small tube (high-impedance) attached to a trumpet system with a throat size of

approximately 0.015". The measured transfer function of the speaker (input voltage to output pressure) is shown in Figure 4.13.

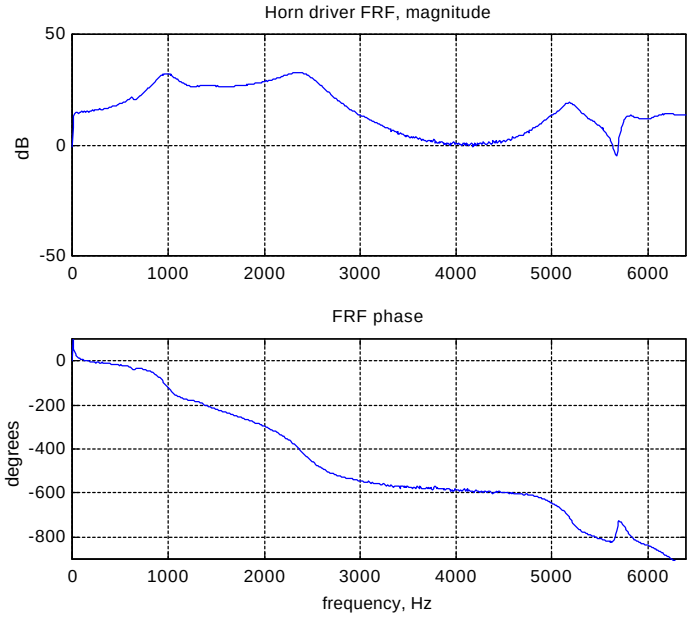

Figure 4.13 FRF of speaker (driven with Dynaco Amplifier)

4.6.2. Basic Feedback Theory

From the measured control-to-error transfer function, ***G***, a controller, ***H***, was designed using loop shaping methods. The open-loop transfer function, ***GH***, was designed to have greater than 0 dB of gain at particular frequencies so that when the loop was closed around the entire system, ***GH,*** with either negative or positive feedback, attenuation would occur in the closed-loop system at these frequencies. When the loop is closed, the system transfer function becomes:

$$Closed\ Loop\ Transfer\ Function = \frac{1}{1 \pm GH} \qquad (4.1)$$

$$+ \ if\ \ negative\ \ feedback$$

$$- \ if\ \ positive\ \ feedback$$

The measured open-loop plant transfer function, G, is shown in Figure 4.14.

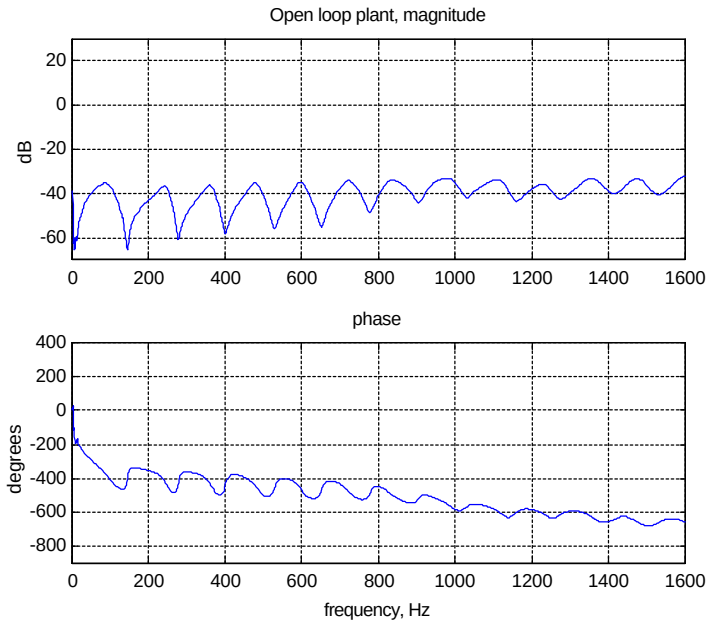

Figure 4.14 Open loop plant FRF, G

The transfer function magnitude of the plant is very low, averaging around –40dB, signifying quite a bit of loss from the control signal to the microphone. This is not due to the trumpet system itself being non-resonant or due to a poor acoustic driver, but rather the physical attenuation was that performed on the microphone to prevent it from being overdriven as described in *Section 4.4*. Also contributing to this low-level transfer function was the transmission loss in the high-impedance tube connecting the control actuator to the trumpet.

In order to obtain attenuation at a single frequency, the controller was designed as a pair of complex conjugate poles placed at the particular frequency to create a sharp resonance in the open loop transfer function, thus creating a notch in the closed-loop transfer function.

An additional 180° phase lag occurs due to this complex conjugate pole pair possibly making the system unstable (Figure 4.15). With the phase of the open loop system combined with the phase of the new controller (a complex conjugate pole pair), the phase now could cross one or more phase crossovers, the regions at which the system can become unstable. A

solution to this phase lag is to add a complex conjugate zero pair near the pole frequency. The complex conjugate zero pair causes a decrease in the open-loop gain and a 180° phase lead. If the complex conjugate zero pair is located at the same frequency as the conjugate pole pair, the zeros will cancel the effect of the poles resulting in no effect. With the complex conjugate zero pair, a +180° phase lead will occur at the zero location, ideally returning the phase back to where it was originally.

Care was taken to keep the phase of the open-loop system within the phase crossovers to insure a stable system. If the phase came within ~60° of a phase margin, then the system had the chance of becoming unstable in that frequency range if the gain of the system was near or greater than 0 dB. If a phase crossover did occur, the gain was designed to be well below 0 dB to prevent the system from becoming unstable.

When the open-loop system phase begins to approach the phase crossovers and the system loop is closed, 'spillover' results. Spillover occurs when the closed-loop system starts to amplify certain frequency bands. Ideally, spillover should be avoided, but in reality occurs because of the inability to avoid phase crossovers. Qualitative assessment of controller spillover will be discussed in more detail in *Section 4.6.5*.

4.6.3. Single Complex Conjugate Pole Pair Controller Design

An initial controller was built[*] implementing a single complex conjugate pole pair with a frequency of 352 Hz and a damping ratio ζ=0.01. A frequency of 352 Hz was chosen to attenuate the fundamental tone of the trumpet's middle line 'G.' All measurements and comparisons to the model were run using a middle line 'G.' The controller transfer function, $\boldsymbol{H}$, is shown in Figure 4.15.

[**] *Controllers were implemented with operational amplifiers. For schematics refer to Appendix D.*

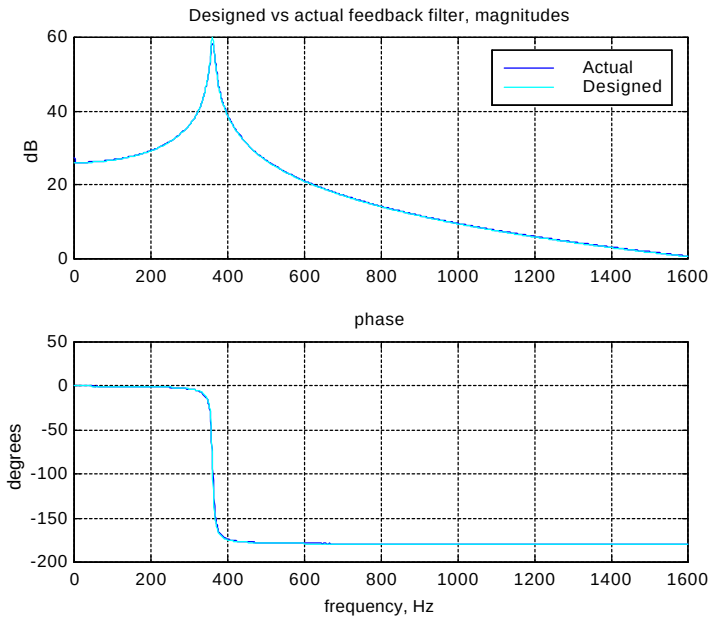

*Figure 4.15 Controller FRF, **H**, single complex conjugate pole pair, f=359 Hz, z=0.01*

When the single complex conjugate pole pair controller is applied to the system, the open loop system transfer function, ***GH***, becomes:

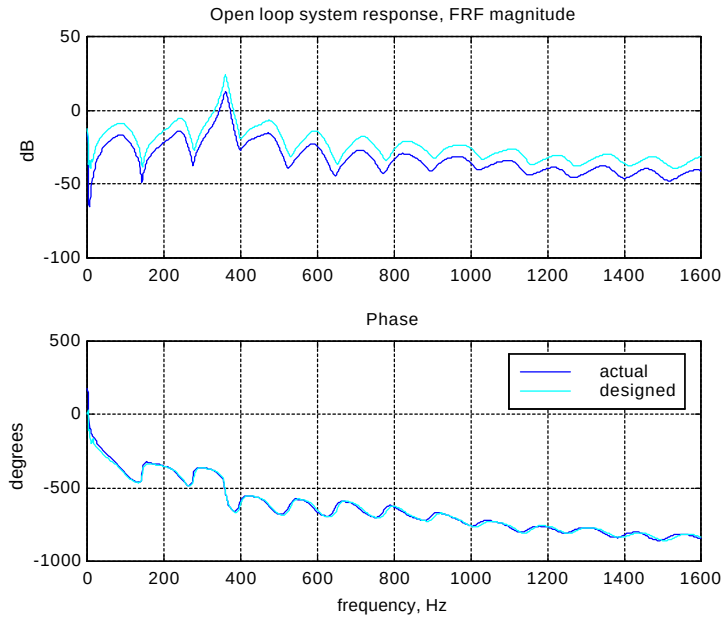

Figure 4.16 Full open loop system with single conjugate pole pair controller, predicted vs. actual

The additional 180° of phase lag can be seen at f=352 Hz as compared to Figure 4.14. The phase crossovers using positive feedback are 0°, ±360°, ±720°, etc. Since the phase stays within -360° to -720° when the magnitude of the system is greater than 0 dB, the system loop was closed using positive feedback to insure closed-loop stability. With the system loop closed with positive feedback, the predicted closed-loop transfer function that results is:

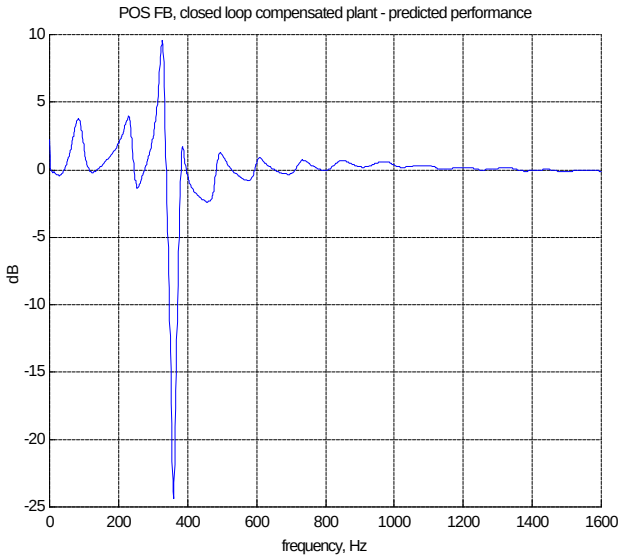

Figure 4.17 Single conjugate pole pair controller, closed-loop response

Theoretically, good attenuation occurs at 352 Hz, just as designed, but on either side of 352 Hz there is some amplification due to spillover. Referring to the open loop transfer function, ***GH***, in Figure 4.16, we see that just below 352 Hz the phase approaches within several degrees the phase margin crossover, -360°, while the magnitude is still greater than zero. At this point, the closed-loop transfer function ceases to attenuate the input and begins to amplify it.

Introducing random noise using the control player described in *Section 4.5*, the farfield trumpet spectrum with and without the single complex conjugate pole pair feedback controller was measured to be:

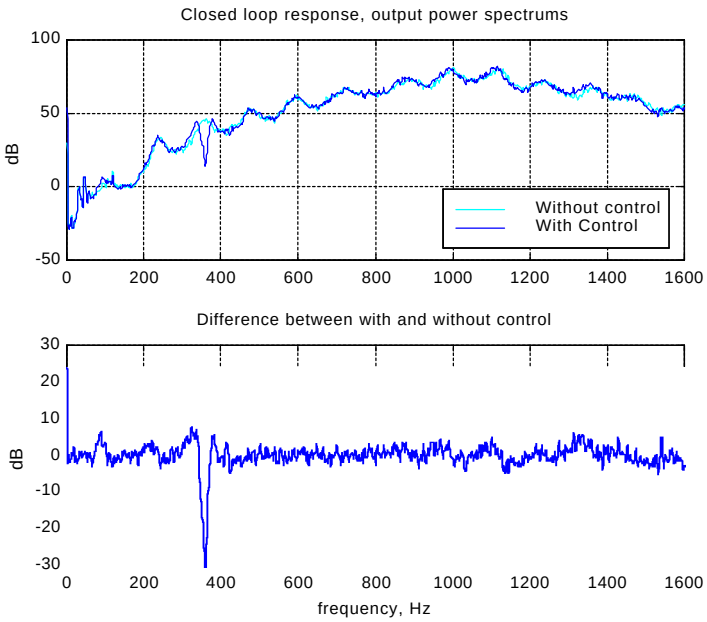

Figure 4.18 Farfield trumpet spectrum with and without controller activated with white noise input

One frequency band around 352 Hz is attenuated 26 dB and agrees with the predicted closed-loop response in Figure 4.17. Along with the one frequency notch, there is some spillover amplification apparent as well. The spillover illustrated in Figure 4.17 occurs in the measured output of the system just above and below 352 Hz.

In order to judge how this will actually sound, a time recording was made of the mouthpiece pressure while the author produced the note 'G', f_o=352 Hz. This mouthpiece pressure was reproduced with the artificial player speaker with and without the feedback controller activated (Figure 4.19).

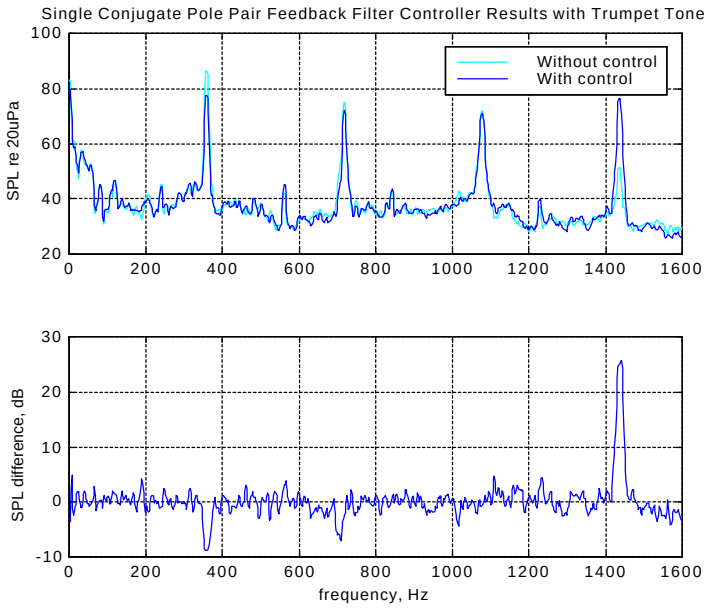

Figure 4.19 Farfield response with and without controller activated with trumpet sound input

Since the majority of the energy is in the single tone at 352 Hz and there is no significant acoustic energy in the near vicinity of the 352 Hz, only the 10 dB attenuation is apparent with the controller activated. The spillover is not distinguishable with the player input. With only a 10 dB reduction of the fundamental tone, there is only a slightly noticeable effect of the sound becoming thinner in the listener perceived sound.

This observation suggests the spillover predicted by the closed transfer function is unimportant and inconsequential. However, if the player were to play the pitch at a slightly lower frequency (flat), then the first tonal frequency would occur at the spillover frequency. The tonal would not be attenuated 10 dB but amplified 5-10 dB, having a completely opposite effect than desired. This disadvantage of the feedback controller will be discussed in *Section 4.6.5*.

4.6.4. Multiple Complex Conjugate Pole and Zero Pair Controller Design

In order to obtain a significantly perceptible change in the farfield output spectrum, more than a single tone needs to be significantly attenuated. To implement this in a controller design, two complex conjugate pole pairs were used to reduce the first two tones in the trumpet spectrum of G, f_0=352 Hz and f_1=704 Hz. In order to counteract phase crossover instabilities, another complex conjugate pole (f=560 Hz, ζ=0.04) was used along with two complex conjugate zero pairs (f=400 Hz, ζ=0.04 and f=590 Hz, ζ=0.02). The controller transfer function, $\boldsymbol{H}$, is:

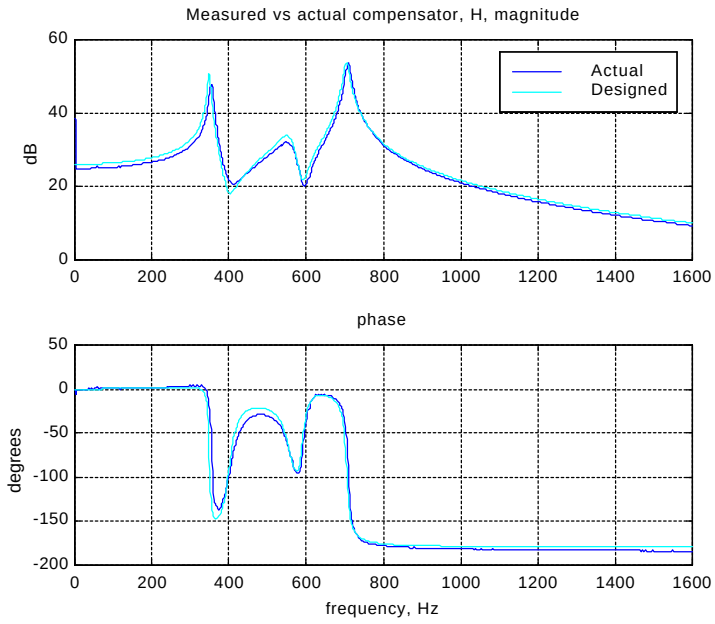

*Figure 4.20 Controller FRF, **H**, predicted vs. actual*

When the multiple complex conjugate pole/zero pair controller is applied to the open loop system the resulting open-loop transfer function, $\boldsymbol{GH}$, becomes:

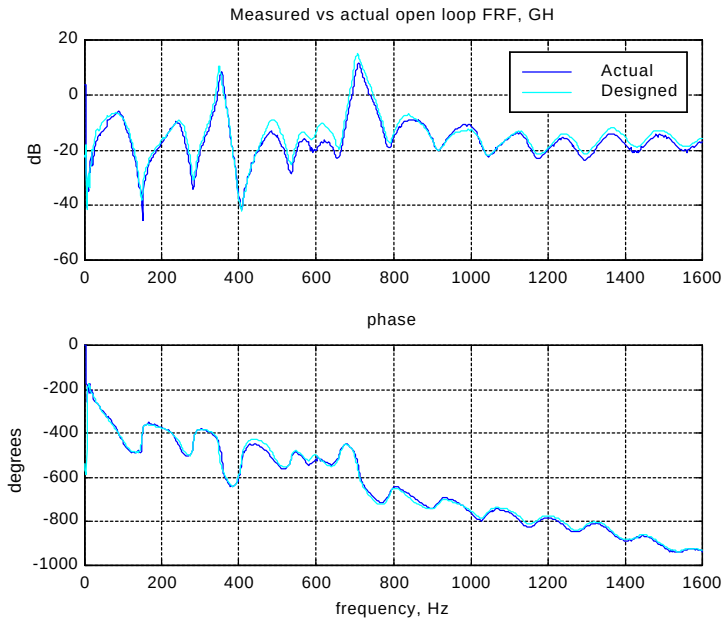

Figure 4.21 Full open loop system with multiple conjugate pole and zero pairs controller, predicted vs. actual

Again, since the phase of the system remains between –360° and -720° while the magnitude is greater than 0 dB, the system loop was closed with positive feedback. The predicted closed-loop performance based on the actual open loop plant using positive feedback is:

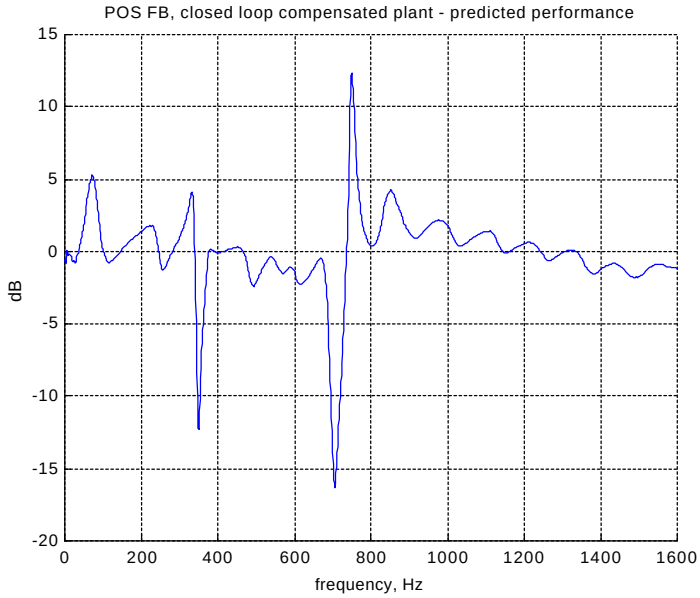

Figure 4.22 Predicted closed-loop response with a multiple conjugate pole/zero pair controller

Attenuation occurs as designed at 352 Hz and 704 Hz, and again, spillover occurs at other frequencies where the open-loop phase either came near or crossed the phase crossover points. In the design of the feedback controller, the amount of attenuation could have been increased, but at the expense of increasing the amount of spillover. Similarly, it is possible to decrease the degree of spillover at the expense of attenuation of the tone of interest.

To test the effectiveness of the multiple complex conjugate poles and zeros at all frequencies, the artificial player described in *Section 4.5* was driven with random noise. The resulting farfield trumpet spectrum was:

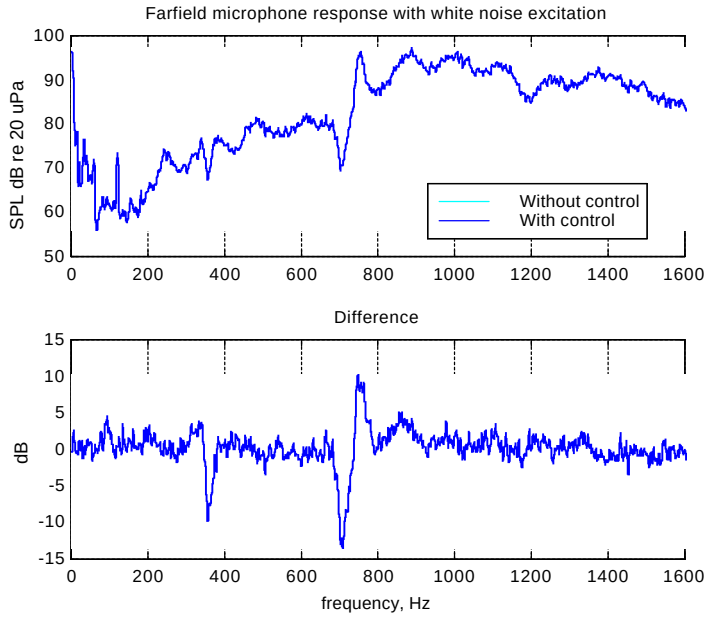

Figure 4.23 Farfield spectrum with multiple conjugate pole/zero pair controller

The two peaks at f=352 Hz and f=704 Hz are reduced approximately 10 dB and 14 dB respectively. This agrees with the predicted closed-loop response show in Figure 4.22. The predicted spillover is also apparent in the farfield trumpet spectrum at frequencies in the vicinity of 352 Hz and 704 Hz. The frequency bands where spillover occurs do not effect the output if the player of the trumpet/controller system plays exactly a G of 352 Hz. The majority of the energy is included in the trumpet tonals and not in the spillover frequency

regions. But again, if the player fails to keep this note exactly at f=352 Hz, then the controller will begin to amplify instead of attenuate the trumpet tonals.

In order to observe the qualitative difference the multiple pole/zero feedback has on the listener perceived sound, the same time pressure recording used with the single complex conjugate pole pair feedback filter was produced with the artificial player. The farfield spectrum was recorded with and without the multiple complex conjugate poles and zeros control system activated.

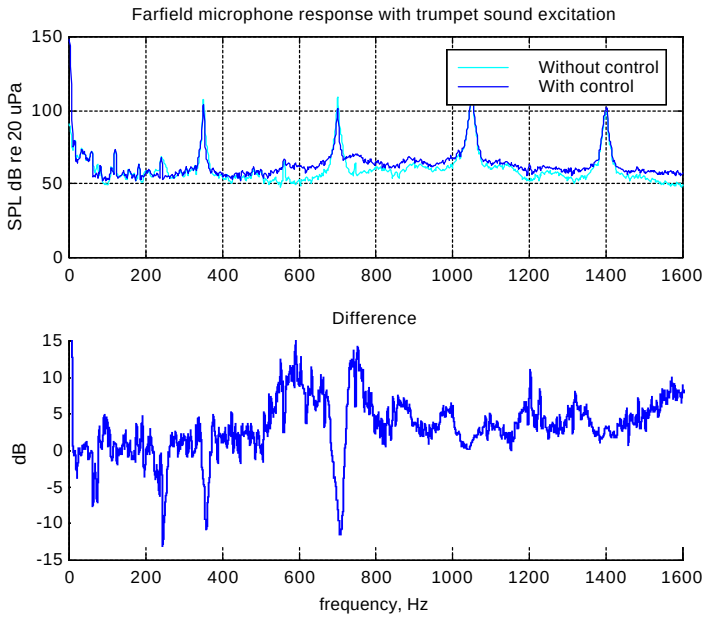

Figure 4.24 Farfield spectrum with multiple complex conjugate pole/zero pair controller with trumpet sound excitation

There are several frequency bands that are amplified in the resulting closed-loop system, similar to what was observed before in the single complex conjugate pole pair filter. However, the resulting amplification is insignificant since the energy in these frequency bands was initially very low.

This spillover amplification is acceptable as long as the player continues producing the same frequencies the feedback controller is attenuating. If the player begins to lower the frequency he/she is producing, the trumpet tonals will coincide with the frequency bands of amplification. At this point, the feedback controller will begin to have the opposite effect it

was designed for. The feedback controller will help to cause the player to generate a flat response by emphasizing the incorrectly played trumpet tonals.

4.6.5. Limitations of the Feedback Controller

This type of active noise control system has several limitations for the trumpet spectrum modification application even though it shows good attenuation where designed. One drawback is the system has the possibility of becoming unstable if the plant, G, changes. The analog feedback filter is not able to change its parameters after it has been designed and implemented. This could pose problems if the active noise control system is attached to a different trumpet that may have a slightly different FRF shape.

The spillover amplification that occurred in the closed-loop response was caused when the phase of the closed-loop system came into the vicinity of a phase crossover. Though the ANC/trumpet system did not become unstable, the spillover does cause an amplification in the trumpet farfield spectrum. As seen by the original trumpet FRF, the phase did not come near any phase crossovers, but with the addition of the control actuator and the high-impedance connecting tube, the phase lagged significantly across all frequencies. In order to minimize the majority of this phase lag, the distance between the control actuator output and the trumpet should be minimized.

A significant drawback to this type of controller as applied to the trumpet system is that it is only effective for a single trumpet note, in this case, a second line G, f_o=352 Hz. This is not practical for any performance or practice use. If several filters were built, each affecting a specific note, the player would be required to transport a large quantity of filters. The multiple-note system would also have to determine which note the user was playing, choose the appropriate controller, and implement it. Chances are the filters for all of the notes would not affect the sound similarly making for an erratic sounding system.

While the player is executing a particular passage, they are typically pressing the trumpet valves. When the trumpet valves are depressed, the trumpet system is altered. The

additional length of the trumpet now may cause the feedback controller in use to become unstable unless the controllers are very carefully designed.

By observing the predicted and actual closed-loop trumpet farfield spectrums, one notices the spillover does not occur at harmonic frequencies, but various other, almost random frequencies in relation to the original harmonics. In the first feedback controller example, the fundamental of the trumpet note, G, was attenuated ~25 dB, but just below that frequency, at 345 Hz, there is a 10 dB amplification. If the spectrum in Figure 4.1 is processed with this filter, the tone at 352 Hz is attenuated correctly as designed. If the player is exactly in tune and plays a second line G right at 352 Hz, the amplification is not a problem because the original tonal content at the spillover frequency, 345 Hz, is so low that a 10 dB amplification is not significant. However, if the player is incorrect in his/her note placement, then the significant tonal content will begin to coincide with the 10 dB amplification point and insignificant tonal content will occur at the –25 dB design point. At this point the filter will actually begin to help the player sound out-of-tune. This illustrates how sensitive a feedback controller is to changes in the trumpet system and player performance.

If in fact a feedback type of filter is desired, then an optimal controller design problem might be posed, maximizing the amount and bandwidth of attenuation and minimizing the amount of spillover. This would allow the player to be slightly off-pitch while the filter still returns the same effect. Unfortunately, separate filters would still be needed for each note on the trumpet.

For these reasons, an analog feedback control system still requires considerable research before it could provide a desirable real-world solution to this problem. A more advanced and potentially better solution would be to use digital LMS (Least Mean Square) adaptive control.

4.7. Digital LMS Controller

Since the trumpet system and the player do not remain constant during the duration of control, some form of adaptive control system was proposed to be a better solution. When the player's embouchure changed and the disturbance frequencies changed, the feedback controller did not change and thus the feedback control system failed to obtain significant attenuation if any. With the implementation of an adaptive control algorithm, the controller will change when the disturbance frequencies change, so attenuation of the output will still occur.

The digital LMS controller attempts to minimize the error, e_k, between an input signal, x_k and a desired signal, d_k, by adjusting the FIR filter weights, w_k (Figure 4.25) using a method of steepest descent to predict the next time-step filter weights. The LMS weight update equation is written as [Widrow and Stearns, 1987]:

$$w_{k+1} = w_k + 2\mu e_k x_k \tag{4.2}$$

This form of calculating the weights is used in the filtered-X method of digital LMS control and is reviewed briefly in the next section.

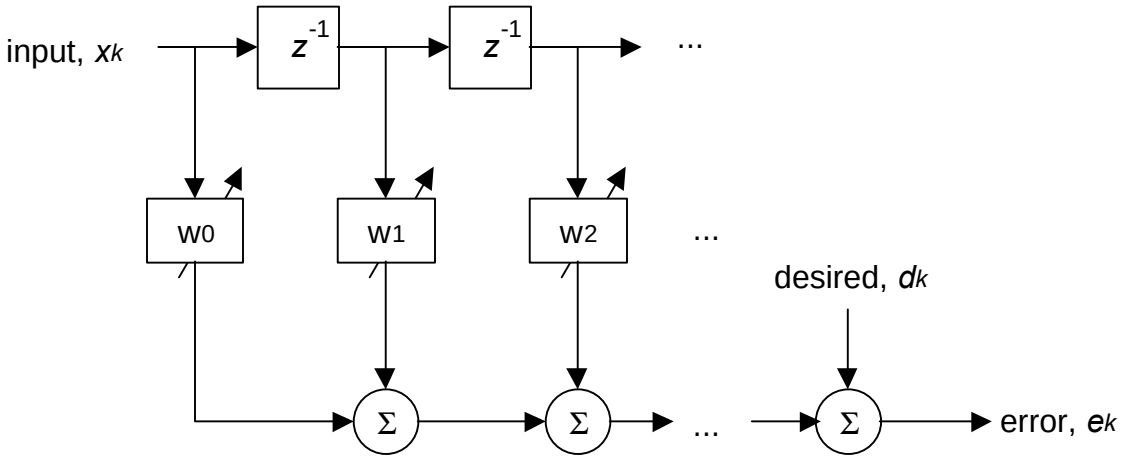

Figure 4.25 General LMS system

4.7.1. Filtered-X LMS

The two LMS methods implemented differ in how the reference, the input to the adaptive LMS filter, is obtained. The quality of the reference signal directly determines the quality of the resulting control. If the reference has a low signal-to-noise ratio, then the control will reflect that accordingly, resulting in poor control.

The filtered-X LMS algorithm used an electronic reference (Figure 4.26). The disturbance was the artificial player being driven with a single frequency tone. The tone generator signal fed directly to the reference input of the LMS algorithm, i.e. no acoustic path. With this system, the signal at the error microphone would be minimized only at the single tone frequency.

An approximation of the control to error transfer function, ***J***, was found through a system identification with white noise.

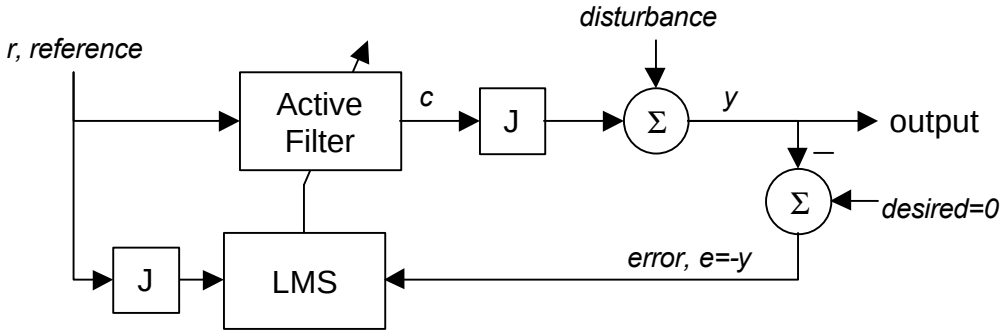

Figure 4.26 System diagram of adaptive filtered-X LMS algorithm

If the signal at the error microphone is minimized, then the farfield sound pressure level is also reduced. The error microphone sound pressure level is shown Figure 4.27.

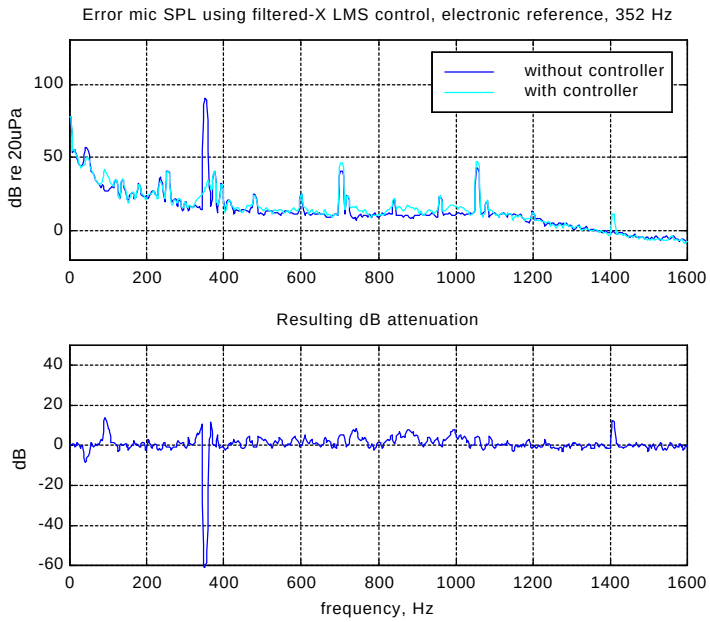

Figure 4.27 Error microphone SPL using filtered-X LMS control and an electronic reference

At the frequency of the electronic reference, f=352 Hz, tone there is a 60 dB reduction in the error microphone sound pressure level. At the farfield microphone there is a reduction of 29 dB as seen in Figure 4.28. No other frequency is affected other than the single frequency present in the reference signal. The slight amplification of a tone at 1408 Hz as seen in both the error and farfield microphone signals is due to the control driver beginning to distort while controlling the single tone. The fourth harmonic of the control driver is 1408 Hz.

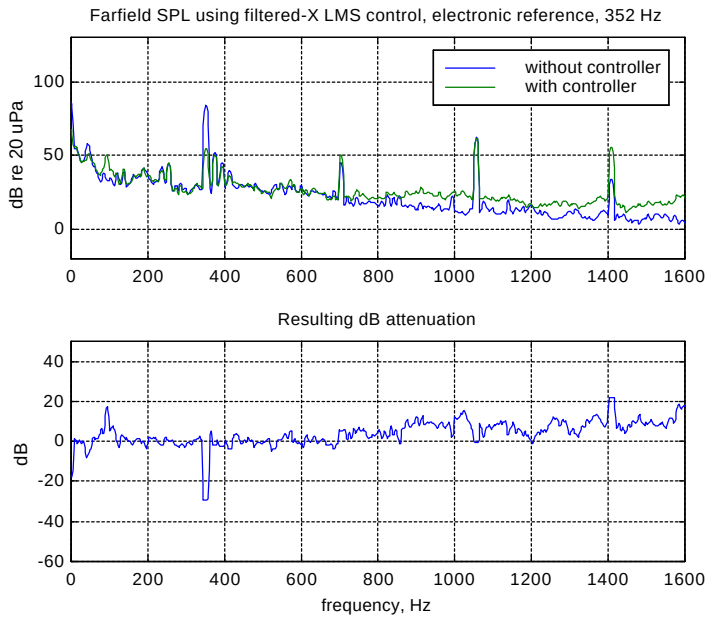

Figure 4.28 Farfield microphone SPL using filtered-X LMS control and an electronic reference

The other peaks found in Figure 4.27 and Figure 4.28 are due to the control player distorting while producing the single input tone. Since the reference input to the LMS algorithm contained only the original single tone, the LMS algorithm did not attempt to affect these tones whatsoever.

In reality, an electronic reference could not be used with the trumpet system since there is no originating electronic signal driving the trumpet system. Instead a microphone is used to detect the disturbance from the actual player of the trumpet. The microphone senses what disturbance the player is producing and inputs this signal as the reference to the LMS algorithm.

Since the control actuator is driving directly into the trumpet itself, the error microphone senses the resulting control pressure along with the disturbance. The reference to the LMS filtered-X algorithm is defined not to include the control signal. For this reason, another LMS algorithm was implemented which removes the control signal from the error microphone to obtain a reference for input into the LMS filter. This implementation is called filtered-E LMS.

4.7.2. Filtered-E LMS

This form of adaptive LMS control obtains the reference signal from the error microphone. With this implementation, only one sensor is needed in the entire system. Before the control system could be implemented, an approximation of the control to error transfer function, ***J***, needed to be obtained. The inverse of this transfer function was used to deconvolve the reference signal from the error microphone signal.

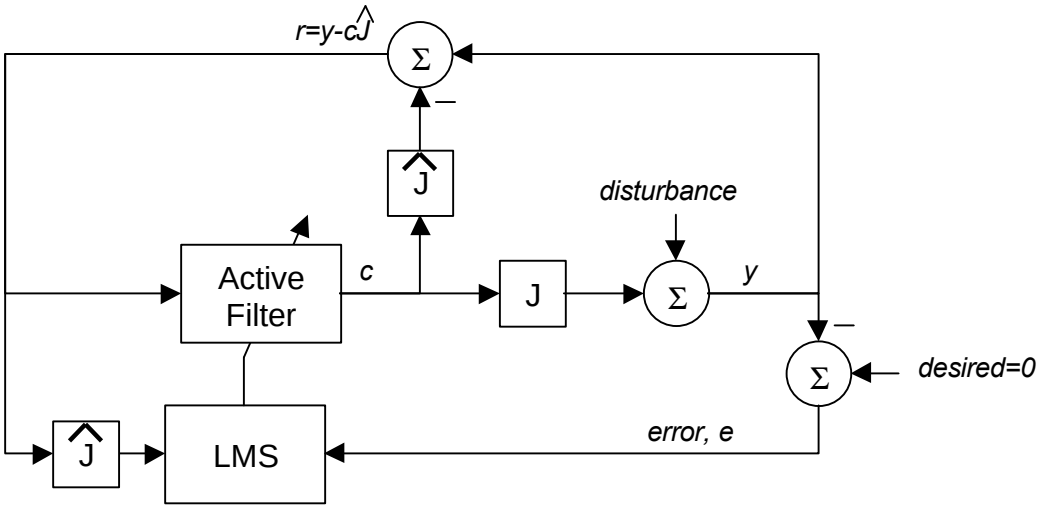

Figure 4.29 System diagram of adaptive filtered-E LMS algorithm

The artificial player reproduced a recorded trumpet buzz as described in *Section 4.5*. The resulting trumpet output with the artificial player producing the mouthpiece pressure sounded like a trumpet. Application of the filtered-E LMS algorithm to this disturbance resulted in attenuation of several peaks in the trumpet output spectrum. This algorithm strives to minimize the error signal at the microphone and so also reduces the farfield sound power level as seen in Figure 4.30 and Figure 4.31.

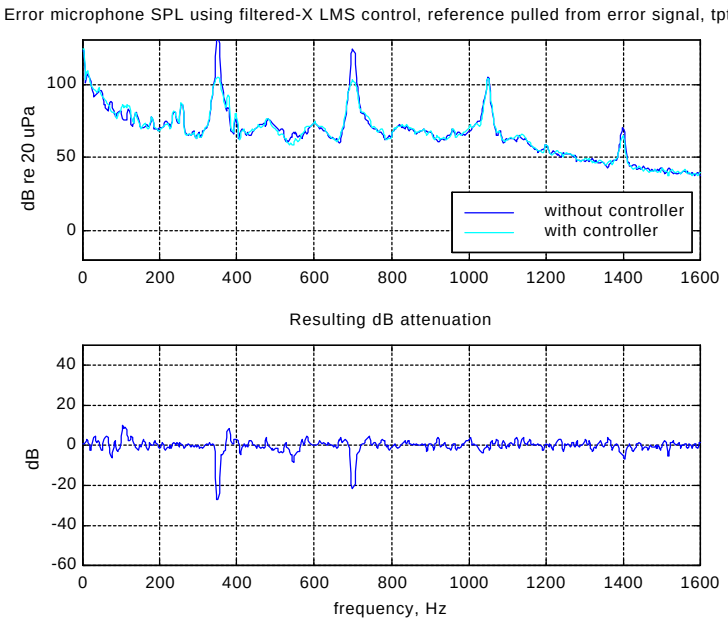

Figure 4.30 Error microphone SPL using filtered-E LMS control

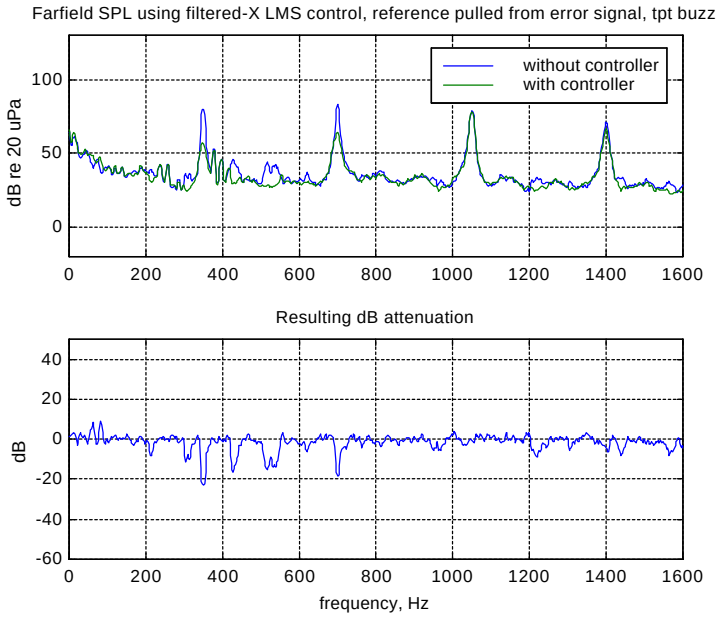

Generated from /4-8-98/results7.m

Figure 4.31 Farfield microphone SPL using filtered-E LMS control

Attenuation of the first two trumpet spectrum tonals, f=352 Hz and f=704 Hz, is obtained at the error and the farfield microphone locations. The attenuation of the first two trumpet

spectrum tonals is 28 dB and 22 dB at the error microphone location. Slightly less attenuation is obtained at the farfield microphone location, 22 dB and 18 dB. Attenuation is also apparent at other frequencies in the farfield spectrum, demonstrating the LMS Filtered-E algorithm's attempt to control more than just the trumpet tonal frequencies.

Since the control player tests proved successful, a real player was used to generate the disturbance. The initial tests conducted with the LMS adaptive control with low-level disturbances (80-100 dB (SPL)), but a real player produces much higher sound pressure levels on the order of 140-180 dB (SPL). Driving the system with these high levels causes the LMS algorithm to output high-level control signals so the control actuator will match levels with the disturbance levels. When a real player was used and the control actuator driven with the high-level control signals, the control actuator output was very distorted and caused the control driver to fail catastrophically. In order to obtain successful control with a real player, a much stronger driver needs to be implemented. The specifications for this driver are addressed in the next section.

Both LMS algorithms used for this testing were constructed and coded by Michael Vaudrey specifically for the trumpet application. The experimental procedures, data collection, and analysis were performed with some technical assistance from Vaudrey. For a further and more detailed discussion of many types of adaptive algorithms as well as new multiple input techniques that may be applicable to the trumpet noise control problem in future research efforts, please see [Widrow and Stearns, 1985] and [Vaudrey, 1996].

4.8. Control Actuator Model

Since the control actuator was found to be generating significant harmonic distortion while driven with the control signal, a linear, frequency domain model was derived to model the control actuator. From this model, an actuator was theorized that could successfully control this system without unnecessary stress on the driver, thus preventing distortion.

A simplified speaker/tube representation of the driver system was modeled and is shown in Figure 4.32.

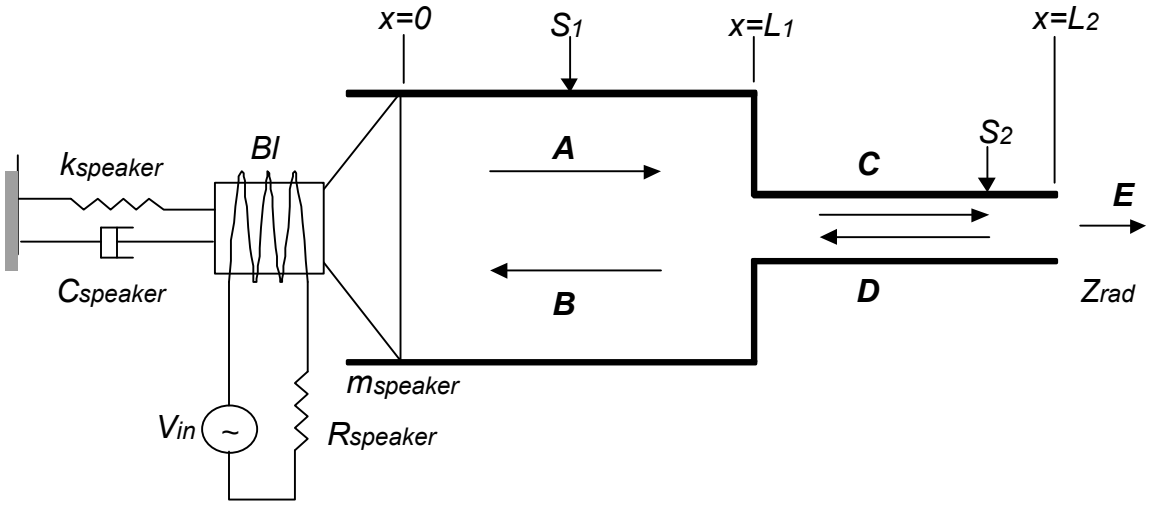

Figure 4.32 Simplified speaker/connecting tube system

The cross sectional areas of section 1 ($0 \le x \le L_1$) and section 2 ($L_1 \le x \le L_2$) are S_1 and S_2 respectively. Section 1 represents the chamber located directly above the speaker cone. Section 2 represents the connecting tube between the speaker and the trumpet.

Only plane waves are assumed to be present in the system. In each of the two model sections there is a forward and backward traveling plane wave, represented by their complex amplitudes: A, B, C, and D.

$$\begin{aligned} P_A &= Ae^{j(\omega t - k_1 x)} \\ P_B &= Be^{j(\omega t + k_1 x)} \\ P_C &= Ce^{j(\omega t - k_2 x)} \\ P_D &= De^{j(\omega t + k_2 x)} \end{aligned} \tag{4.3}$$

Included in this system are complex wave numbers, k_1 and k_2.

$$k_1 = \frac{\omega}{c} - j\alpha_1$$
$$k_2 = \frac{\omega}{c} - j\alpha_2 \tag{4.4}$$

The complex wave numbers account for wave propagation loss in each of the two cylindrical sections. This is especially significant in section 2 since the small tube has a high-impedance and incurs a high transmission loss causing $\alpha_2 >> \alpha_1$.

The pressure and particle velocities within each section are:

$$\begin{aligned}
p &= Ae^{j(\omega t - k_1 x)} + Be^{j(\omega t + k_1 x)} && 0 \le x \le L_1 \\
p &= Ce^{j(\omega t - k_2 x)} + De^{j(\omega t + k_2 x)} && L_1 \le x \le L_2 \\
U &= \frac{1}{\rho c}\left[Ae^{j(\omega t - k_1 x)} - Be^{j(\omega t + k_1 x)}\right] && 0 \le x \le L_1 \\
U &= \frac{1}{\rho c}\left[Ce^{j(\omega t - k_2 x)} - De^{j(\omega t + k_2 x)}\right] && L_1 \le x \le L_2
\end{aligned} \tag{4.5}$$

Performing a continuity of pressure and particle velocity at $x=L_1$ results in:

$$\begin{aligned}
cont.\,of\ \ pressure: &\quad Ae^{-jk\ L_1} + Be^{jk_1 L_1} = Ce^{-jk_2 L_1} + De^{jk_2 L_1} \\
cont.\,of\ \ velocity: &\quad Ae^{-jk_1 L_1} - Be^{jk_1 L_1} = \frac{S_2}{S_1}\left[Ce^{-jk_2 L_1} - De^{jk_2 L_1}\right]
\end{aligned} \tag{4.6}$$

Since the tube opens into the trumpet bore at $x=L_2$, the radiation impedance, Z_{rad}, is assumed to be that of a flanged pipe [Kinsler and Frey et al., 1982].

$$Z_{rad} = \rho c S_2\left(\frac{1}{2}(ka)^2 + j\frac{8}{3\pi}ka\right) \tag{4.7}$$

The radiation impedance at $x=L_2$ is related to the waves traveling in the second section by:

$$Z_{rad} = \rho c S_2 \left[\frac{Ce^{j(\omega t - k_2 x)} + De^{j(\omega t + k_2 x)}}{Ce^{j(\omega t - k_2 x)} - De^{j(\omega t + k_2 x)}} \right] \tag{4.8}$$

Also, at $x = L_2$,

$$Z_{rad} = \frac{p(L_2, t)}{u(L_2, t)} \tag{4.9}$$

Solving (4.8) for D results in:

$$D = C \left[\frac{Z_{rad} - \rho c S_2}{Z_{rad} + \rho c S_2} \right] e^{-2jk_2 L_2} \tag{4.10}$$

Substituting (4.10) into (4.6) and solving for A and B results in:

$$\begin{aligned} A &= -\frac{C}{2} \left[\left(1 + \frac{S_2}{S_1} \right) e^{j(-2k_2 L_1 + k_1 L_1)} + \left(1 - \frac{S_2}{S_1} \right) e^{j(-2k_2 L_2 + k_2 L_1 + k_1 L_1)} \right] \\ B &= \frac{C}{2} \left[\left(1 - \frac{S_2}{S_1} \right) e^{j(-2k_2 L_1 - k_1 L_1)} + \left(1 + \frac{S_2}{S_1} \right) e^{j(-2k_2 L_2 + k_2 L_1 - k_1 L_1)} \right] \end{aligned} \tag{4.11}$$

The ratio of the pressures at the exit, $p(L_2)$ and $p(0)$, is:

$$\frac{p(L_2)}{p(0)} = \frac{Ce^{-jk_2 L_2} + De^{jk_2 L_2}}{A + B} \tag{4.12}$$

Substituting (4.10) into (4.12) results in an expression for the ratio between $p(L_2)$ and $p(0)$:

$$\frac{p(L_2)}{p(0)} = \frac{(1+R)e^{-jk_2L_2}}{\left(1+\frac{S_2}{S_1}\right)\left(e^{jL_1k_1-jL_1k_2}+Re^{jk_2L_1-2jk_2L_2-jk_1L_1}\right)+ \left(1-\frac{S_2}{S_1}\right)\left(e^{-jL_1k_1-jL_1k_2}+Re^{jk_2L_1-2jk_2L_2+k_1L_1}\right)} \tag{4.13}$$

With R as:

$$R = \frac{Z_{rad} - \rho c S_2}{Z_{rad} + \rho c S_2} \tag{4.14}$$

At $x=0$, the input impedance of driver is:

$$Z_{md} = C_{speaker} + j\left(\omega m_{speaker} - \frac{k_{speaker}}{\omega}\right) \tag{4.15}$$

The input impedance of the first cylindrical section is:

$$Z_{m0} = S_1 \frac{p(0,t)}{u(0,t)} = S_1 \rho c \tag{4.16}$$

Therefore, the particle velocity at $x=0$ is related to the force applied by the driver by:

$$u(0,t) = \frac{force_{driver}}{Z_{m0} + Z_{md}} \tag{4.17}$$

The force applied by the driver is proportional to the voltage input by electromechanical coupling:

$$force_{driver} = Bl \cdot I_{in} = \frac{BlV_{in}}{R_{speaker}} \tag{4.18}$$

Where Bl is the electromechanical coupling constant.

Combining equations (4.9), (4.13), (4.16), and (4.17) gives:

$$\frac{p(L_2,t)}{p(0,t)} = \frac{u(L_2,t)Z_{rad}}{\frac{force_{driver}}{Z_{md}+Z_{m0}}\rho cS_1} \tag{4.19}$$

From (4.19), the particle velocity at the output of the system, $x=L_2$, is solved for in terms of the input voltage to the speaker, V_{in}:

$$u(L_2) = \frac{BlV_{in}}{R_{speaker}}\left[\frac{p(L_2)}{p(0)}\frac{S_1\rho c}{(Z_{md}+Z_{m0})Z_{rad}}\right] \tag{4.20}$$

From equation (4.9), the output pressure of the system is solved for.

$$p(L_2) = u(L_2)Z_{rad} \tag{4.21}$$

Expanding equation (4.21) gives the final pressure output relationship:

$$p(L_2) = \frac{p(L_2)}{p(0)}\frac{\rho c\frac{BLV_{in}}{R_{speaker}}}{(Z_{md}+Z_{m0})S_2}Z_{rad} \tag{4.22}$$

Also important to the quality of the speaker performance is the amount of speaker displacement. The displacement of the driver cone is of consequence in considering distortion effects. If the displacement becomes large, then the electromagnetic coil of the

driver travels outside of the linear force region of the magnetic field of the fixed magnet resulting in nonlinear force application.

The displacement of the speaker can be found by integrating equation (4.17) assuming a harmonic, linear response.

$$x_{speaker}(t) = \frac{u(0,t)}{j\omega} \tag{4.23}$$

4.8.1. Speaker Model Results

The current driver system was measured so that it could be compared to the model prediction in order to validate the model. A high-level microphone was attached to the end of the high-impedance connecting tube to measure the driver system output. The driver was excited with white noise and the transfer function between the driver input and the microphone output was measured. This transfer function was compared to equation (4.22) and is shown in Figure 4.33 along with the other modeled responses including the speaker displacement.

Speaker parameters such as the speaker cone mass, stiffness, damping, and the magnet constant were initially estimated. An interative process was then performed to match the model transfer function to the measured transfer function by varying the estimated model parameters. The parameters did not change significantly from the initial estimates and the resulting error between the model and the measured transfer functions was minimized (Figure 4.33).

Table 4.1 Resulting speaker parameters

Cone Mass, $m_{speaker}$	0.00307 kg
Cone Stiffness, $k_{speaker}$	12129.5 N/m
Cone Damping, $C_{speaker}$	9.06e-005 N/m^2

Cone Diameter	3.026 in
Tube Diameter	0.015 in
Bl	0.237 Tesla-m
$R_{speaker}$	7 Ω
L_1	4 In
L_2	3.15 in
a_1	1.0915
a_2	1.1086
V_{in}	0.5 volts peak

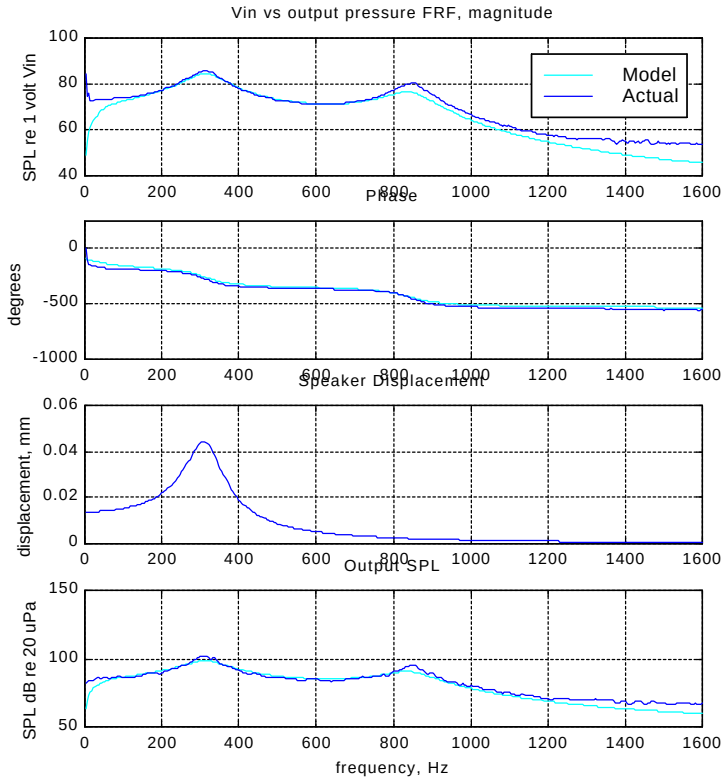

Figure 4.33 Comparison of speaker model FRF and measured speaker FRF

Since the model was shown to approximate the current actuator system, the parameters were then adjusted so the model predicted a 160 dB (SPL) output required by the ANC system. There are many combinations of speaker parameters that would result in a speaker capable

of producing 160 dB (SPL). If the current actuator system were simply driven with a higher voltage to obtain the higher sound pressure level, it would theoretically require 1000 volts resulting in the response shown in Figure 4.34.

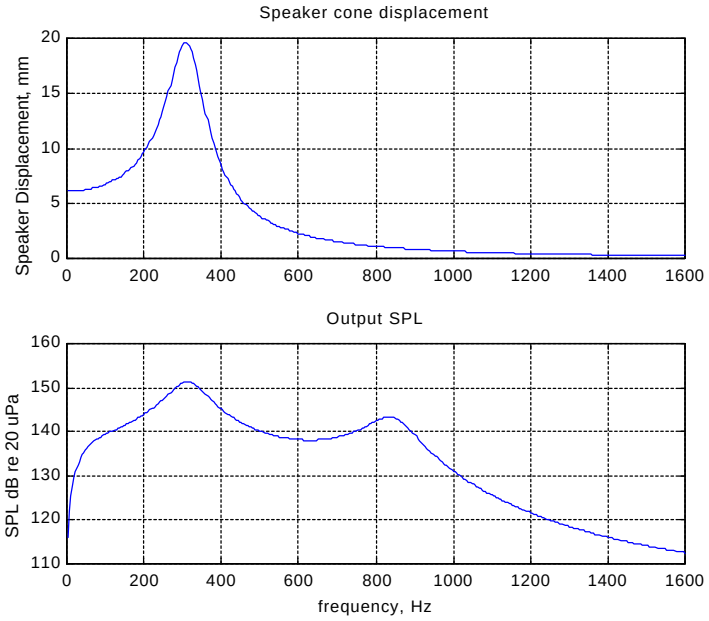

Figure 4.34 Original speaker model with higher driving voltage

The required SPL is almost obtained, but with an impossible speaker cone displacement, 40 mm. Obviously a different speaker is needed that can deliver the high sound pressure and do it with a reasonable speaker cone displacement. One possible solution was predicted using the following values:

Table 4.2 New speaker parameters (all other parameters remaining the same)

Cone Mass, $m_{speaker}$	0.0307 kg
Cone Stiffness, $k_{speaker}$	242580 N/m
Cone Diameter	18 in
Bl	230 Tesla-m
$R_{speaker}$	16 Ω
V_{in}	25 volts peak

A speaker with these parameters is predicted to perform as shown in Figure 4.35.

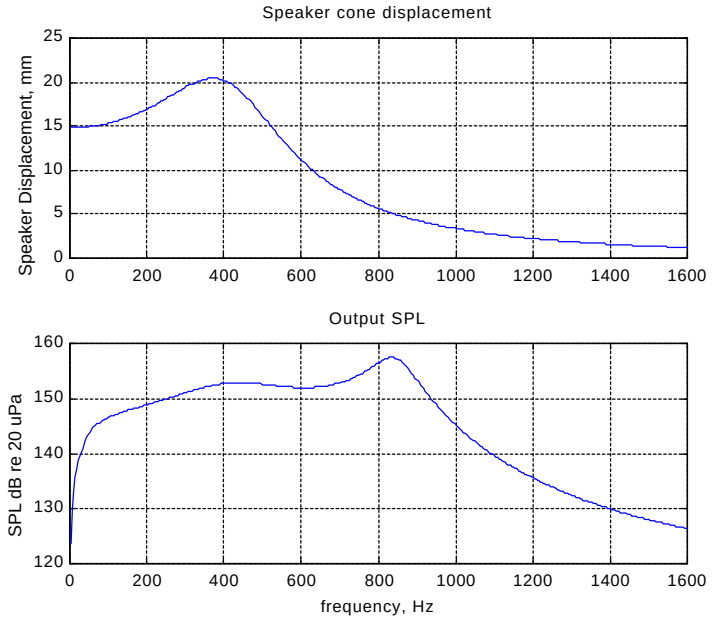

Figure 4.35 Predicted speaker output with new parameters

Unfortunately, these parameters are not found in a typical speaker. The magnet used on the new speaker is over 2000 times stronger and the cone diameter is much larger, 18 inches. An 18-inch diameter speaker does exist that can reach a 20 mm displacement, but without the extremely light cone mass and extremely high stiffness that is obtainable with a small speaker. A driver system capable of delivering 160 dB (SPL) was not found.

4.9. Effects of the Control System on the Player s Embouchure

With the current location of the control actuator, the control pressure not only propagates towards the output of the trumpet, but also back towards the player's embouchure. Therefore, there must exist a physical feeling difference to the player due to this extra pressure. To investigate this difference, a simple control actuator input was included in the analytical trumpet model developed in *Chapter 3* and the embouchure movement observed.

The single complex conjugate pole controller from *Section 4.6.3* was implemented in the trumpet model. The input to the controller was obtained from the pressure in the mouthpiece, p, as would be measured with the microphone. This pressure was converted to a microphone output voltage, m_{out}, with the microphone sensitivity*. The controller output voltage was input into the model of the actuator and high-impedance connecting tube. The output from the actuator-tube model was pressure. The pressure from the control actuator was applied directly to the pressure summation in the mouthpiece cup. The location that the pressure was applied in the trumpet model was not the location in the real system. The location of the control actuator input port in the actual system is shown in Figure 4.8. This difference contributed most of the error to the model mouthpiece pressure output waveforms as compared to the actual measured mouthpiece pressure as seen in Figure 4.36.

The gain of the feedback controller in the trumpet model was adjusted to maximize the amount of overall sound power reduction and not to become unstable.

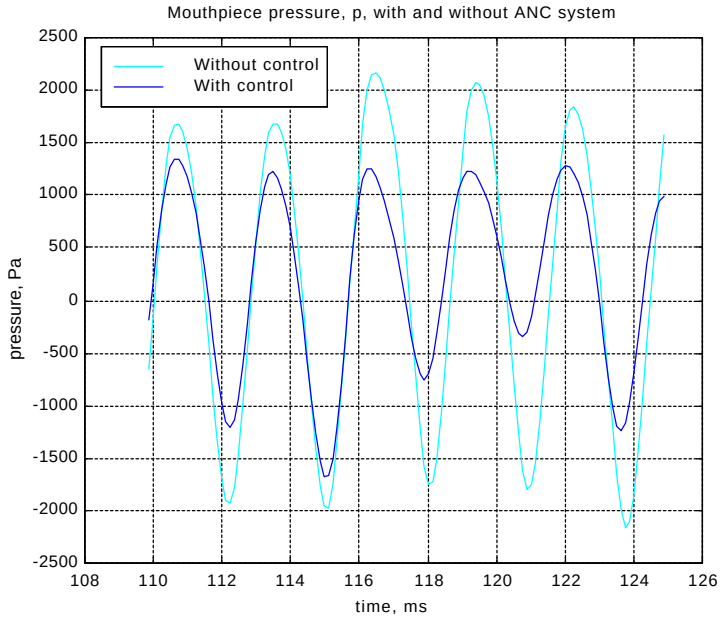

Figure 4.36 Mouthpiece pressure, p , with and without an analog single conjugate pole pair feedback filter, g, f_o=352 Hz

* *Ex. Sensitivity=1.967 mV/Pa for the B&K type 4136 ¼ microphone*

A slight frequency shift can be seen in Figure 4.36. This is due to the spillover that occurs with the feedback controller. The one tone is attenuated, but as seen by the closed-loop response (Figure 4.17), there is an amplification of a slightly lower frequency tone. The spillover frequencies are now apparent in the new mouthpiece pressure time response.

The player's embouchure is shown by the trumpet model to have reduced in motion amplitude (Figure 4.37). This translates to the overall trumpet system becoming less resonant. The initial inputs to the system, including the static player pressure, the player's embouchure equilibrium position and others, were kept the same with and without the controller activated. The embouchure's amplitude of motion was reduced.

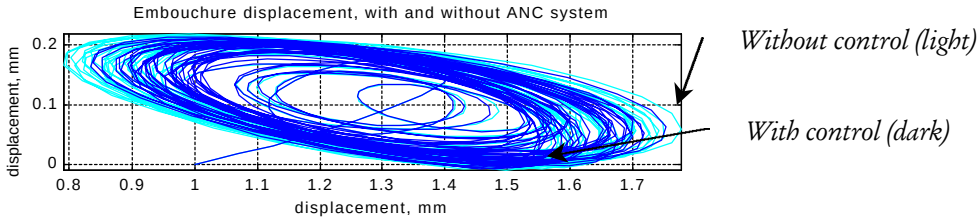

Figure 4.37 Embouchure movement, with and without an analog single conjugate pole pair feedback filter

To illustrate the effect of the control actuator at this location more obviously, the control algorithm in the model was extended to show the limiting case. By applying ideal control, the lip vibration will be reduced altogether. If the control system was to apply ideal control (Equation (4.24)), thus not including any controller or speaker system dynamics, then the mouthpiece pressure would be always be zero. This results in the embouchure just opening slightly to allow the static player pressure, p_o, to escape (Figure 4.38).

$$p_{control} = -p_{microphone} \tag{4.24}$$

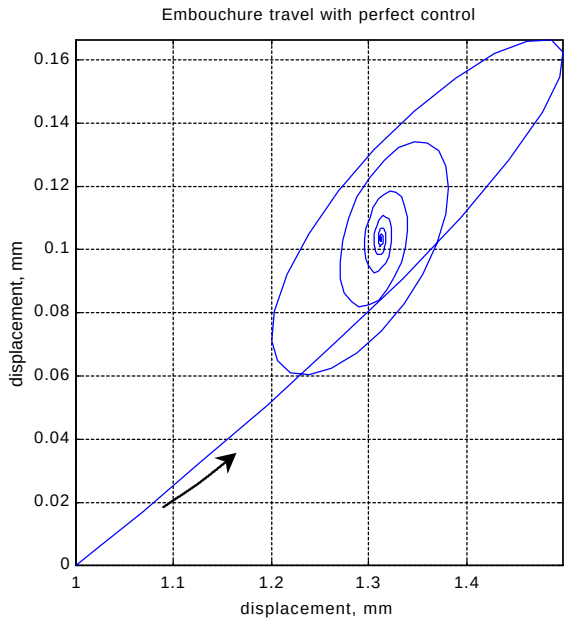

Figure 4.38 Embouchure movement with theoretical application of perfect control, $p_{control} = -p_{microphone}$

Since the ideal controller applies the best possible control to the system, it successfully reduces the output sound spectrum of the trumpet over all frequencies and also obtains this with excellent global control.

The ideal control example demonstrates that the controller along with successfully attenuating the farfield sound level, also reduces the amplitude of travel of the trumpet player's embouchure. If the controller applies to much control to the ANC/trumpet system, the player is believed to become uncomfortable since it would prevent the player's embouchure from vibrating with the normal amplitude. If the controller could effect a significant change in the farfield trumpet spectrum without affecting the player's embouchure substantially, then the system may be more acceptable.

4.10. Conclusion

Application of the ANC system to the trumpet system was successful in attenuating the farfield, listener perceived sound pressure level. With both the analog feedback and digital LMS controllers, the quality of sound in the farfield was changed from the full-bodied tone of the original trumpet to a thinner, weak sounding tone, similar to that of a straight mute. This effect was due to the successful attenuation of the first two tones in the trumpet spectrum. The successful spectrum modification illustrates that it is possible to actively and predictably change the listener perceived tonal spectrum of the trumpet.

Selection and placement of the control actuator and error sensor were performed after studying the effectiveness of each one with the system. The placement of the control actuator was found to affect the farfield spectrum as well as the travel of the player's embouchure.

In order to implement either of these ANC systems with a real trumpet player, a more powerful control actuator and a high-level microphone will need to be implemented. Without these components, the control system will not interface well with the trumpet resulting in poor, ineffective attenuation of the farfield spectrum. To illustrate the requirements for the more powerful control actuator, an analytical model was derived that predicted the required actuator parameters.

The feedback controller would not be as suitable of a solution as the LMS adaptive controller due to the fixed frequency attenuation bands of the feedback controller. Disadvantages of the feedback controller also include the inability to change based on the trumpet player's input. Since the player does vary his/her intonation and pitch, a digital adaptive filter would likely be preferred.

Chapter 5. Results and Conclusions

This thesis has demonstrated the preliminary success in application of two types of ANC systems to a musical instrument. Each type of controller met the stated objectives of attenuating selective tones in the trumpet output spectrum and maximizing the zone of control. The results of this research only begin to demonstrate the ANC system's potential effects; for example, the ANC system may be used to deliver special timbre effects.

5.1. Thesis Results

Both the analog feedback controllers and the digital LMS controllers successfully attenuated specific tones in the trumpet output spectrum. The best analog feedback controller attenuated the first two tones of the trumpet output spectrum by 10 dB and 13 dB respectively. The best digital LMS controller attenuated the same two tones by 22 dB and 18 dB respectively. With the implementation of either type of controller, the listener perceived-sound changed from the original, full trumpet sound to a thinner, weaker sound due to the attenuation of the first two trumpet spectrum tonals.

An analytical model was derived and implemented to observe the player and trumpet interaction with and without the controller activated. With the analog feedback controller activated, it was found that the player's amount of embouchure travel was reduced. Whether or not this effect is actually significant or whether it would be acceptable by a real trumpet player is still left to answer.

The initial choice of the control actuator was determined to be inadequate for producing the required SPL for the control of the instrument during normal use. Sound pressure levels of 160 dB (SPL) were required to obtain control with a real player. The driver initially implemented was a small horn compression driver capable of producing 100 dB (SPL) with minimal distortion. An analytical model was derived to predict the parameters of a driver capable of producing 160 dB (SPL). The proposed driver was not obtainable.

The type and location of the error sensor was determined. Due to the high sound pressure levels of 160 dB (SPL) in the trumpet bore, a conventional condenser microphone could not be used with a real trumpet player. For this study, low level tests and measurements were successfully conducted using a condenser microphone. The microphone was located on a pressure tap on the mouthpiece. It was found that at this location, the microphone rejected the most amount of non-trumpet sound.

5.2. Future Work

Despite the optimistic results, there are several qualitative and quantitative issues still to be addressed in order for this ANC system to be successfully applied with a real trumpet player. The first of these issues concerns how the player feels while playing the trumpet/controller system. Secondly, a control actuator capable of producing the high SPL required for maximizing the trumpet output attenuation needs to be obtained.

5.2.1. Qualitative Player Opinion

A disadvantage to the proposed ANC system is the occurrence of a player-perceived feeling difference. The player may only want the listener to perceive a change in the farfield spectrum and the player to not feel any difference in his/her embouchure. From the control experiments and model results, one must rethink the placement of the control actuator. The control actuator impinges pressure on the player's embouchure, disrupting normal movement, which is believed to be undesirable. It follows from this observation that the control actuator should be placed outside of the resonant trumpet system. This ties in to the discussion in *Section 4.2 Placement of the Control Actuator*. Placing the control actuator at the bell reduced the amount of global control that was achieved with the internally placed control actuator. However, it prevented the control actuator pressure from coming in contact with the player's embouchure, thus affecting a change only perceived by the listener, not the player.

Since the control actuator and controller in this study are internal to the trumpet system, the trumpet system dynamics themselves are altered. This, at least, causes the player to feel as though they are playing a different trumpet which may or may not be desired by the player. With the control actuator located at the bell of the trumpet, the trumpet will still play the same as an uncontrolled trumpet, but the output sound spectrum will sound different, which is one of the objectives of this thesis. The desirability of feeling the control actuator pressure can only be answered by the trumpet player and the testing conducted in this research was not sufficient to determine how significant this issue will actually be. Future research will be needed to determine the significance.

5.2.2. Control Actuator Selection

The weakest link in the controller/trumpet system is the control actuator. The actuator needs the capability to exert force equal to the disturbance force as shown earlier. This translates to a sound pressure level output of approximately 160-180 dB (SPL). From the predictions of the speaker model, an actuator capable of producing this sound pressure level would need a very large magnet and a large (18 inch diameter), light (0.03 kg), and very stiff cone suspension (121900 N/m). These qualities are difficult to find together in one actuator since typically a large speaker has a very heavy cone along with a compliant suspension.

5.2.3. Controller Choice and Implementation

In this thesis, only preliminary work was conducted with the digital LMS adaptive controllers. This type of controller is better suited than the fixed-gain analog feedback controller for this application due to its ability to change and adapt to the trumpet system. With an improved LMS controller, more effects could be realized with the controller-trumpet system other than simple tonal reductions.

An issue not addressed in this thesis was the relative speed of which the controller could adapt to the system while being played by a real trumpet player. During a musical passage of rapidly successive notes, could the control adapt quickly enough to continue the perceived listener effect? With an analog feedback filter, the time to affect the output sound is relatively quick due to the low-order dynamics in the feedback controller. With the LMS adaptive controller, a maximum time is set for the LMS algorithm to find the optimal weights to effect the sound as desired. In the case of a rapid trill as illustrated in Figure 5.1, there are 120 beats per minute, thus, each note in the trill lasts $^{1}/_{16}$ of a second.

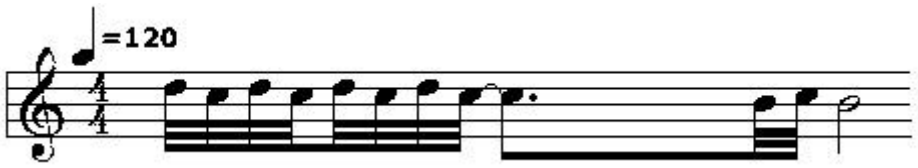

Figure 5.1 Trill example

The maximum time the LMS algorithm could take should be less than $^{1}/_{16}$ of a second so the ANC system has a chance to converge and to change the sound while it is still being produced.

5.3. Final Vision

The results of the controlled trumpet trials suggest that extending the present control system could result in an infinite range of adjustment in the trumpet output sound. Since the trumpet system dynamics can be predictably modified with the addition of the control system, any type of instrument dynamics could be implemented. As a result, the player would possibly be given an infinite amount of control over the feel and sound quality of his/her trumpet.

Extending this idea further by adapting the system for any brass or woodwind instrument could give the same tonal shaping ability to those instruments as well. All of these musical

instruments are acoustic resonant devices. Thus, these instruments could also be controlled with a system similar to the one proposed in this thesis.

Having the ability to transform the sound produced by a trumpet into any imaginable sound is a very intriguing and fascinating dream. With a system capable of this action, a trumpet player would have infinite control over his/her output sound and would be capable of changing it at will. In this thesis, a very basic form of this dream system has been developed. Extending this research by studying each element more closely will lead to a system capable of realizing an infinitely variable, real-time tonal modification system. With a trumpet capable of sounding like any instrument, the future symphony orchestra may consist of all trumpets with the E-Mute attachment.

Appendix A: Matlab Code Listings

A.1. Trumpet Simulation

The following Matlab code implements the time domain simulation of the trumpet/player system as developed in *Chapter 3*. This code also includes one of the feedback controllers in the trumpet/player system as discussed in *Chapter 4*.

```
% Trumpet/Player Interaction Model
% Peter Pickett
% pickett@vt.edu
% Virginia Tech
% Blacksburg, VA

% this version uses a single complex conjugate pole controller

disp('Setting up windows...');
anim=0;  % animation switch, (1=perform animation graphics, 0=no graphics(faster)).

% set up initial figure window positions
%close all;
figure(1);set(1,'position',[48      47     375     295],'menubar','none','name','Animation
       Graphics(if on)','numbertitle','off');  % animation graphics(if on)
figure(2);set(2,'position',[9       56      513     920],'menubar','none','name','Waveform
       Output','numbertitle','off');   % waveform outputs
figure(3);set(3,'position',[576     751     705     223],'menubar','none','name','Simulation
       Step Times','numbertitle','off');   % simulation time step times
figure(4);set(4,'position',[579      92     705     290],'menubar','none','name','Reflection
       Function','numbertitle','off');   % reflection function
figure(5);set(5,'position',[577     438     705     290],'menubar','none','name','Frequency
       Analysis  of  Output','numbertitle','off');     %  frequency  analysis  of  pressure
       waveform

disp('Initializing static and global variables...');

% make several variables available to all functions:
global dt rho c Zc po d Scup Ulip Uacoust i Slip p r U st

% fixed parameters to set for single run

flip=241;                   % lip eigen frequency, Hz, (frequency player wants to play)
po=3000;                    % player blowing pressure(Pa)

t0 = clock;                  % start real time timer to see how long this takes
now=t0;
simutime=1000/8000;          % how long to run simulation (s)
dt=1/8000;                   % timestep size size (s)
c=340;                       % speed of sound in air (m/s)
rho=1.21;                    % air density (kg/m^3)
Scup=2.3E-4;                 % area of mouthpiece cup (m^2)
b=7E-3;                      % width of lips (m)
d=2.0E-3;                    % thickness of lips (m)
zjoint=[0 4E-3];             % location of rotation joint of lips (m)
 zequi=[1E-3 (0)*10^(-3)];   % lip rest positions (m)

% implement  feedback  controller  for  active  pressure  control  (does  not  include  gain),
       voltage->voltage
disp('Calculating controller and speaker difference equations...');
```

```
% single complex conjugate pole pair
analog_controller_num=[0 0 1  471.4902 1.7798e+007 4.0057e+009 7.2178e+013];

analog_controller_den=[1     398.9823     3.0782e+007  7.5738e+009  2.9286e+014  3.0094e+016
       8.0705e+020]./2./pi;

bodegain=1.4;  % gain used on analog controller

analog_controller_num=analog_controller_num*bodegain*(analog_controller_den(length(analog
       _controller_den))/analog_controller_num(length(analog_controller_num)));    %  adds
       gain in numerator

% convert to digital representation, discrete time format (bb=numerator, aa=denominator)
[bb,aa]=c2dm(analog_controller_num, analog_controller_den,dt,'zoh');

% model speaker/high impedance tube system to get speaker transfer function
load spek4     % real-world, measured transfer function (speaker input voltage to BK mic
       output voltage (o2i1)
f=0:4:3200;    % frequency vector for that data file
[B,A]=invfreqs(o2i1,f*2*pi,8,8);       % model the system in analog domain
[speknum,spekden]=c2dm(B,A,dt,'zoh');  % convert model to discrete domain
speknum=speknum(3:length(speknum));    % remove leading zeros

% put controller and speaker systems together, convolution of the two systems
[sysnum,sysden]=series(bb,aa,speknum,spekden);


% initialize rest of variables.
% since this is a second order system and the controller/speaker system relies on the
% last 13-15 steps (depending on the order of the controller difference equation),
% the first several time steps were assumed (=0) so the simulation could be started.
% i.e. the system is at rest for several time steps.

disp('Initializing all other variables...');
p_steps=15;                    % the number of steps to assume system at rest.
z=[zequi' zequi' zequi' zequi' zequi' zequi' zequi' zequi' zequi' zequi' zequi' zequi'
       zequi' zequi' zequi' ];      % first two initial time step of lip position
p=[zeros(1,p_steps)];          % initial pressure output
Uacoust=[zeros(1,p_steps)];    % initial acoustic volume velocity
Ulip=[zeros(1,p_steps)];       % initial lip volume velocity
U=[zeros(1,p_steps)];          % initial total volume velocity
plip=[zeros(1,p_steps)];       % initial plip pressures
reflection=[zeros(1,p_steps)]; % initial integral values
yy=[];                         % initial integral values
Slip=[zeros(1,p_steps)];       % initial lip opening area values
Frestore=[zeros(1,p_steps)];   % keep track of lip restoring force
Fdp=[zeros(1,p_steps)];        % keep track of delta P force
Fbernoulli=[zeros(1,p_steps)]; % keep track of bernoulli lip force
steptime=[zeros(1,p_steps)];   % keep track of how long each time step takes to compute

cont_press=[zeros(1,p_steps)]; % keep track of applied control pressure

% calculate lips parameters based on above:
Qopen=3;                   % damping factor for open lips
Qclosed=0.5;               % damping factor for closed lips
m=1.5/( (2*pi)^2*flip);    % mass of lips (kg)
k=1.5.*flip;               % stiffness of lips (N/m)
Q=Qopen;                   % initial lip quality factor
closedforce=0;             % initial extra force present if lips touching (N)

denom=m/(2*dt^2);            % denominator of both zetax and zetay terms, doesn't change
       during simulation

Zc=rho*c/Scup;             % player impedance, modeled as infinitly long tube

% now compute reflection function using Adachi's method
disp('Calculating reflection function...');

cd ..
cd trum1
findref3;     % script that calculates reflection function, returns 'r'
```

```
cd ..
cd trmpmodl

% plot reflection function
figure(4);
time=0:dt:length(r)*dt-dt;
plot(time*1E3,r,'b-');
axis([0 50 -600 200]);
grid;
title('Reflection function, r(t)');
xlabel('time, ms');

disp('Drawing static graphics...');
% Draw unchanging and initial parts of graphics
figure(1);                          % open animation window
clf;                                % clear window if already open
axis([-.007 .007 -.007 .007]);
axis('image');
axis('off')

% draw bone structure(non-moving lip graphics...)
line([zjoint(1)-d,zjoint(1)],[zjoint(2),zjoint(2)]);
line([zjoint(1)-d,zjoint(1)],[-zjoint(2),-zjoint(2)]);
line([zjoint(1),zjoint(1)],[zjoint(2),zjoint(2)+.004]);
line([zjoint(1),zjoint(1)],[-zjoint(2),-zjoint(2)-.004]);
line([zjoint(1)-d,zjoint(1)-d-.002],[zjoint(2),zjoint(2)+.004]);
line([zjoint(1)-d,zjoint(1)-d-.002],[-zjoint(2),-zjoint(2)-.004]);

% write parameters to figure and title
text(-0.0093,0.0015,['Po=' num2str(po) ' Pa']);
text(-0.0093,0.0005,['Stops at ' num2str(simutime/dt) ' steps']);
text(-0.0058,0.0075,'Graphic Trumpet Simulation Model');
drawnow;

% run simluation
disp('Simulation starting...');
tic                     % start simulation timer to time each step
for i=15:simutime/dt;    % run simulation
  steptime(i)=toc;       % keep track of how long it takes to do each step
  tic;

  C=(1/2)*sqrt(m*k)/Q;   % calculate damping term

  % calculate forces on lips
  Frestore(1:2,i)=-(1/2)*k.*(z(1:2,i)-zequi(1:2)');   % spring restoring force(x,y)
  Fdp(1,i)=b*(po-p(i))*( -z(2,i)+zjoint(2)  );        % pressure force(x)
  Fdp(2,i)=b*(po-p(i))*( z(1,i)-zjoint(1)  );         % pressure force(y)
  FBernoulli(i)=b*d*plip(i);                          % Bernoulli force(y direction)

  % calculate new x component of lip position
    z(1,i+1)=(      (m/dt^2)*z(1,i)-(m/(2*dt^2))*z(1,i-1)   -   C*(z(1,i)-z(1,i-1))/dt   +
       Frestore(1,i) + Fdp(1,i)) / denom;
  % calculate new y component of lip position
    z(2,i+1)=(      (m/dt^2)*z(2,i)-(m/(2*dt^2))*z(2,i-1)   -   C*(z(2,i)-z(2,i-1))/dt   +
       Frestore(2,i) + Fdp(2,i) + FBernoulli(i) + closedforce) / denom;

  % calculate new lip opening area

    Slip(i+1)=max([2*b*z(2,i+1) 1E-10]);   % if y<=0 then set Slip=0(lips are closed),
       otherwise Slip=2*b*z(2,i+1)

  % find new volume swept by lips

    Ulip(i+1)=b*(  (z(1,i+1)-zjoint(1))*(  (z(2,i+1)-z(2,i))/dt  )-(z(2,i+1)-zjoint(2))*(
       (z(1,i+1)-z(1,i))/dt ));

  % non-linear vibration condition when lips are closed:

    if z(2,i+1)>0,
       closedforce=0;             % set closedforce and Q on open lips
       Q=Qopen;
```

```
  else                          % set closedforce and Q on closed lips
     closedforce=-3*k*z(2,i+1);
     Q=Qclosed;
  end;

% solve for the new Uacoust and p interatively using FMIN

% first do one time pre-integration calculations
 % build integrand data

 if i<length(r),     % decide how far to go back in time to run integral
   st=i+1;           % we can't go back in time farther than we know.
 else
   st=length(r);     % ok, now only go back as long as the impulse function is
 end;

 % solve for p(i+1), pressure in mouthpiece at time (i+1)*dt
  p(i+1)=fmin('integral',p(i)-500,p(i)+500,[0,1e-2]);

 % calculate control source influence here in this difference equation

  % input is pressure (Pa), need to convert to voltage through microphone sensitivity
     to pressure, positive feedback
 % mic_voltage(i+1)=p(i+1)*.035;  % 1.963 mV/Pa, negative feedback

  % calculate control voltage to speaker, with resulting pressure output

    cont_press(i+1)=-p(i+1);

    % add control pressure to pressure in mouthpiece, ie. the speaker feed into
      mouthpiece cup

    p(i+1)=p(i+1)+cont_press(i+1);  % add control

% and now solve directly for the new plip
  plip(i+1)=p(i+1)-rho*Uacoust(i+1)^2*(1/(Scup*Slip(i+1))-1/(Scup^2));      % find new
     lip flow pressure

% draw lips and data (if animation switch is on):
 if anim==1,
  toplip=patch([zjoint(1),z(1,i),z(1,i)-d,zjoint(1)-
     d],[zjoint(2),z(2,i),z(2,i),zjoint(2) ],'red');
  botlip=patch([zjoint(1),z(1,i),z(1,i)-d,zjoint(1)-d],[-zjoint(2),-z(2,i),-z(2,i),-
     zjoint(2) ],'red');

  frest=text(0.0021,0.0037,['Frestore=('       num2str(Frestore(1,i))       ',       '
     num2str(Frestore(2,i)) ') N']);
  fdpp=text(0.0021,0.0047,['Fdp=(' num2str(Fdp(1,i)) ', ' num2str(Fdp(2,i)) ') N']);
  fb=text(0.0021,0.0057,['FBernoulli=' num2str(FBernoulli(i)) ' N']);

  ti=text(-0.0093,-0.0010,['time=' num2str(i*dt,3) ' s']);
  zx=text(0.0041,-0.0047,['zx=' num2str(z(1,i)*1000,3) ' mm']);
  zy=text(0.0041,-0.0057,['zy=' num2str(z(2,i)*1000,3) ' mm']);
  zxx=text(0.0041,-0.0067,['zx(i+1)=' num2str(z(1,i+1)*1000,3) ' mm']);
  zyy=text(0.0041,-0.0077,['zy(i+1)=' num2str(z(2,i+1)*1000,3) ' mm']);

  Ua=text(0.0041,-0.0037,['U=' num2str(U(i),3) ' m3/s']);
  plipt=text(0.0041,-0.0027,['plip=' num2str(plip(i),3) ' Pa']);
  bigQ=text(0.0041,-0.0017,['Q=' num2str(Q,1)]);
  stiffx=text(0.0041,-0.0007,['k=' num2str(k,3) ' N/m']);
  slipsize=text(0.0041,0.0003,['Slip=' num2str(Slip(i)*1000*1000,3) ' mm2']);
  hornp=text(0.0041,0.0017,['p=' num2str(p(i),4) ' Pa']);
  stepnum=text(-0.0093,0.0025,['i=' num2str(i) ' step']);

  x1=line([zequi(1),zequi(1)],[zequi(2),zequi(2)]);
  x2=line([zequi(1),zequi(1)],[-zequi(2),-zequi(2)]);
  drawnow;         % output everything now to screen and update

% erase everything for next time
  delete(frest);
  delete(fdpp);
```

```
    delete(fb);

    delete(toplip);
    delete(botlip);
    delete(ti);
    delete(zx);
    delete(zy);
    delete(zxx);
    delete(zyy);
    delete(Ua);
    delete(plipt);
    delete(bigQ);
    delete(stiffx);
    delete(stepnum);
    delete(slipsize);
    delete(hornp);

    delete(x1);
    delete(x2);
   else

  % if no animation, just display the current time step:

     disp(['Step #' num2str(i) ' of ' num2str(simutime/dt)]);  % direct to matlab window

   end;  % animation subroutine
end;     % end of simulation loop


% show actual time it took to complete the entire simulation

  disp(['Simulation  End,  it  took  '  num2str(floor(etime(clock,t0)/60),6)  '  min,  '
       num2str(rem(etime(clock,t0),60),3) ' seconds to run the simulation'])

   time=0:dt:length(p)*dt-dt;   % create time vector corresponding to simulation length

% now save data
disp('Saving Data File..... please wait.... ');
filenumber=[num2str(now(2)) num2str(now(3)) num2str(now(4)) num2str(now(5))];

filename=['S' num2str(filenumber) '.mat'];

eval(['save ' filename ' time dt p Slip z U Uacoust Ulip cont_press bodegain flip zequi
       po ']);

% now plot resulting waveforms and outputs
disp('Plotting Data now....');

% calculate and plot out frequency content of output
figure(5);
clf;
maxfreq=1000;  %plot upto what frequency
number_of_points=length(p);
pfft=fft(p,number_of_points);
fundamental=((2*pi)/(length(pfft)*dt))/(2*pi);
xscale=[(1:length(pfft))*fundamental];
plot(xscale,20*log10(abs(pfft)*2/number_of_points/20E-6));
axis([0 maxfreq 0 160]);
xlabel('frequency, Hz');

hold on;
% plot finer grid lines every 25 Hz
for kl=0:100:maxfreq-100,
  for jk=kl+25:25:kl+100-25,
    plot([jk jk],[0 max(20*log10(abs(pfft)*2/number_of_points/20E-6)+10)],'g:');
  end;
end;

grid;
hold off;
% calculate overall power
```

```
summ=0;
for   i=1:floor(length(pfft)/2),summ=summ+10^(2*log10(abs(pfft(i))*2/number_of_points/20E-
       6));end;
overall_SPL=10*log10(summ);
disp(['Overall SPL= ' num2str(overall_SPL) ' dB']);
title(['Frequency content of pressure waveform, Overall SPL= ' num2str(overall_SPL) ' dB,
       ' filename]);
 xlabel(['frequency,  Hz,...  Performed:  '  num2str(now(2))  '/'  num2str(now(3))  '/'
       num2str(now(1))    '       '    num2str(now(4))    ':'    num2str(now(5),2)    ':'
       num2str(floor(now(6))) ]);

 figure(2); % summary figure

 % plot lip displacement
 subplot(711);plot(z(1,:)*1000,z(2,:)*1000);
 xlabel('mm');
 ylabel('mm');
 title(['po=' num2str(po) ' Pa, flip=' num2str(flip) ' Hz, zequiy=' num2str(zequi(2),3)
       ', #steps=' num2str(i) ]);
 axis([0 2.5 0 2]);
 axis('image');
 grid;

 % plot cup pressure
 subplot(712);plot(time*1000,p,time*1000,cont_press);
 ylabel('Pressue, Pa');
 title(['Pressure(sound) output, simulation time:' num2str(floor(etime(clock,t0)/60),6) '
       min,     '     num2str(rem(etime(clock,t0),60),3)     '     seconds,     bodegain='
       num2str(bodegain)]);
 axis([0 simutime*1000 -2500 2500]);
 grid;

 % plot volume velocity
 subplot(713);plot(time*1000,U/1E-4);
 ylabel('U,m^3/s x 1E-4');
 title('Acoustic Volume Velocity, U, output');
 axis([0 simutime*1000 0 2]);
 grid;

 % plot lip opening, Slip
 time=0:dt:length(Slip)*dt-dt;
 subplot(714),plot(time*1000,Slip*1000^2);
 grid;
 ylabel('mm^2');
 title('Slip, lip opening area');
 axis([0 simutime*1000 0 7])

 % now zoom in to a portion or the simulation results

 % plot cup pressure
 subplot(715);plot(time*1000,p);
 ylabel('Pressue, Pa');
 title(['Pressure(sound) output, zoomed in']);
 axis([110 130 -2500 2500]);
 grid;

 % plot volume velocity
 subplot(716);plot(time*1000,U/1E-4);
 ylabel('U,m^3/s x 1E-4');
 title('Acoustic Volume Velocity, U, output, zoomed in');
 axis([110 130 0 2]);
 grid;

 % plot lip opening, Slip
 time=0:dt:length(Slip)*dt-dt;
 subplot(717),plot(time*1000,Slip*1000^2);
 grid;
 xlabel(['time, ms, ' filename ', Performed: ' num2str(now(2)) '/' num2str(now(3)) '/'
       num2str(now(1))    '       '    num2str(now(4))    ':'    num2str(now(5),2)    ':'
       num2str(floor(now(6))) ]);
```

```
 ylabel('mm^2');
 title('Slip, lip opening area, zoomed in');
 axis([110 130 0 6])

% plot how long each simulation step took
figure(3);
plot(steptime);
axis([0 length(p)-1 0 2]);
title('Individual Step Times');
xlabel('step number');
ylabel('seconds');

disp('Printing figures...');

% now print out figures

% time waveforms
figure(2)
orient tall
print

% DFT of pressure waveform
figure(5)
orient landscape
print
```

A.2. Iterative Integral Solution

This function was used by the trumpet simulation in *Section A.1* to iteratively solve for $p(t+\Delta t)$ and $U_{acoust}(t+\Delta t)$.

```
function minthis=integral(pnow,st);

% use of this routine by FMIN results in the solution to the simulatenous equations
% involving Uacoust(i+1) and p(i+1)
%
% note:  the variable pnow is only p(i+1), the variable we're solving for.

global dt rho Zc po d Scup Ulip Uacoust i Slip p r U st

% calculate Uacoust guess with p(t+dt) in it:

Uacoust(i+1)=sqrt(     (po-pnow-((rho*d)/Slip(i+1))*(Uacoust(i)-Uacoust(i-1))/dt  )    /  (
        rho/(2*Slip(i+1)^2)-rho/(Scup*Slip(i+1))+rho/Scup^2)         );  ;     %  new  way
        (quadratic)

% add the p(i+1) guess on to the complete p() vector for the integration

   p(i+1)=pnow;

% combine volume velocities

    U(i+1)=Uacoust(i+1)+Ulip(i+1);

% build actual numerical integrand
% by cycling through time

  integrand=[];
    for w=1:st,
     integrand(w)=r(w)*(Zc*U(i+(2-w))+p(i+(2-w)));
    end;
```

```
% perform integration over all of the elements

    reflection(i+1)=trapz(integrand)*dt;

% calculate function to minimize

    minthis=abs(-pnow+Zc*U(i+1)+reflection(i+1));  % this will solve for pnow.
```

A.3. Reflection Function

The following Matlab code determines the reflection (impulse response) function, *r(t)*, based on the trumpet input impedance.

```
% From Zin, we calculate r^c(t)  August 1, 1997

global rho c Zc

load('zin.mat')             % load input impedance data from my trumpet
Zin=za1;
load('zout.mat');           % load piston(output) impedance
Zout=za2;

zr=Zin/Zc;

rorg_f = zeros([8000 1]);
rorg_f(1:8000) = (zr-1)./(zr+1);    % Zin/Z_c = z

f = 1:8000;, f = f';
filterfreq=4000;
flt = 1./(1 + exp((f-filterfreq)./33.33));   % low pass filter
rwdw_f = flt.*rorg_f;
rwdw_f(4001:8000) = conj(rwdw_f(4000:-1:1)); % reality assurance
rwdw =flipud(real(fft(rwdw_f)));
rhilmod = zeros([8000 1]);, rhilmod(1:700) = rwdw(1:700);
rhilmod(2:102) = rhilmod(2:102) + rwdw(8000:-1:7900);    % lapping over
rhilmod(1) = rhilmod(1)*2;                               % lapping over for t = 0 data
rhilmodsft = zeros([8000 1]);
rhilmodsft(1:700)   =   rhilmod(1:700)   +   (8000   -   sum(rhilmod)+0.5*rhilmod(1))/700;   %
       renormalization

howlong=400;
r=rhilmodsft(1:howlong);
```

A.4. Trumpet Input Impedance

The following Matlab code calculates the trumpet input impedance based on dimensional measurements of any arbitrary instrument shape.

```
% compute arbitrary horn throat impedance approximation from cone sections
```

```
% Peter Pickett

clear all;

% load horn shape data file
filename=input('what data file(no *.dat ext)-=> ');
tic
load([filename '.dat']);
data1=eval(filename);

f=1:5:3000;    % choose frequencies to look at, Hz (max valid freq is ~30kHz)

disp(['Frequency Range: ' num2str(min(f)) '-' num2str(max(f)) ' Hz']);

S2=((data1(1,2)*.0254)/2)^2*pi; % mouth area of trumpet

za2=piston2(f,sqrt(S2/pi));     % calculate the mouth impendance

disp('finished calculating piston impedance')


% dx and S are in inches!

% load trumpet size data
% fix metal thickness problem:
% data1(2:28,2)=data1(2:28,2)-.004;

data1=flipud(data1);
dx=data1(:,1);
sum(dx)

diameters=data1(:,2);  % cross diameters
radiuses=diameters/2;  % cross radiuses
S=pi*radiuses.^2;      % calculate cross sectional area
dx=dx*.0254;           % convert to meters
S=S*.0254^2;           % convert to meters squared

figure(1);
clf;
hold on;
%axis([0 sum(dx) -sqrt(S2/pi) sqrt(S2/pi) ])

mouthz=za2;  % mouth impendance is in "acoustic ohms"

for t=length(S)-1:-1:1,
   disp(num2str(t))
   mouthz=cone(f,S(t),S(t+1),dx(t),mouthz); %calculate the impedance back one section
   %all impedance's are acoustic ohms

 % graphically plot cross sectional view

  offset(t)=sum(dx(1:t-1));
  r1(t)=sqrt(S(t)/pi);
  r2(t)=sqrt(S(t+1)/pi);

  line([offset(t),offset(t)+dx(t)],[r1(t),r2(t)]);
  line([offset(t),offset(t)+dx(t)],[-r1(t),-r2(t)]);
  plot(offset(t),r1(t),'x');
  plot(offset(t),-r1(t),'x');
  hold on;

end;

title('Trumpet discetization shape');
xlabel('distance from mouthpiece, meters');
ylabel('radius, meters');

za1=mouthz;

rho=1.21;
c=343;
```

```
S1=S(1);
L=sum(dx);
zc=(rho*c)/S(1);    % impedance of input...(acoustic ohms)
figure(2);
clf;
subplot(211);semilogy(f,abs(za1)/zc)
grid
title('Trumpet input impedance from discrete model');
ylabel('Acoustic Impedance/Zc');
axis([0 3000 1E-2 1E4]);
subplot(212);plot(f,angle(za1)*180/pi)
ylabel('angle, degrees');
xlabel('frequency, Hz');
axis([0 3000 -100 100]);
grid;

% now find where frequencies are (using intune.m)

intune(f,za1,'r');


save ..\trmpmodl\Zin.mat za1
save ..\trmpmodl\Zout.mat za2
save Zin.mat za1
save Zout.mat za2

toc


c=340;               % speed of sound (m/s)
rho=1.21;            % air density (kg/m^3)
Scup=2.3E-4;         % area of mouthpiece cup (m^2)

Zc=(rho*c)/Scup;        % equivalent input impendance

r=(za1-Zc)./(za1+Zc);   % calculate reflection function

figure;
subplot(211),plot(f,abs(r))
subplot(212),plot(f,imag(r))
title(['1-' num2str(max(f)) 'Hz'])

figure;
rifft=ifft(r);
plot(real(rifft));
```

A.5. Conical Horn Impedance

The following Matlab code calculates the throat (input) impedance, z_{a1}, of a finite conical horn section based on given horn dimensions and mouth impedance, z_{a2}.

```
% this M file calculates the theoretical throat impedance of a cone horn section

function za1=cone(f,S1,S2,L,za2);

c=343;      % speed of sound(meters/sec);
rho=1.21;   % density of air (kg/meter^3)

w=2*pi*f;   % frequency conversion, rad/sec
```

```
k=w/c;      % wave number (rad/sec / meters/sec  = 1/meters)

% now solve for conical horn throat impedance

r1=sqrt(S1/pi);      % radius of throat (meters)
r2=sqrt(S2/pi);      % radius of mouth (meters)
x2=(-r2*L)/(r1-r2);  % distance from apex to mouth (meters)
x1=x2-L;             % distance from apex to throat (meters)
t1=atan(k.*x1)./k;
t2=atan(k.*x2)./k;


za1=(rho*c/S1).*(i.*za2.*(sin(k.*(L-t2))./sin(k.*t2))+(rho*c/S2).*sin(k.*L)             );
       %numerator
za1=za1./(za2.*sin(k.*(L+t1-t2))./(sin(k.*t1).*sin(k.*t2))-
       (i.*rho.*c/S2).*sin(k.*(L+t1))./sin(k.*t1) );  % denomintor
```

A.6. Speaker Model

The following Matlab code implements the frequency domain speaker/tube model developed in *Chapter 4*.

```
% Speaker model with complex wave propagation of trumpet actuator system

function out=speaker(parameter);
M=abs(parameter(1));
K=abs(parameter(2));
damp=abs(parameter(3));
alpha1=abs(parameter(4));
alpha2=abs(parameter(5));
Bl=abs(parameter(6));
L1=abs(parameter(7));
L2=abs(parameter(8));
S1dia=abs(parameter(9));
S2dia=abs(parameter(10));
Vin=abs(parameter(11));

c=343;    % speed of sound, (m/s)
rho=1.21; % density of medium, air, (kg/m3)

f=4:4:1600;  % frequency to calculate over (Hz)
w=f*2*pi;    % convert to rad/sec

k1=w./c-i*(alpha1);   % complex wavenumber for section 1
k2=w./c-i*(alpha2);   % complex wavenumber for section 2
k3=w/c;             % wave number, for radiating system into free space

%S1dia=4;      % diameter of section one (speaker) (inches)
%L1=1.5;       % length of section one (inches)
%S2dia=0.016;  % diameter of section two (tube)  (inches)
%L2=3;         % length of section two (inches)

% convert above numbers to metric
S1dia=S1dia*0.0254;   % convert inches into meters
S2dia=S2dia*0.0254;   % convert inches into meters
S1=(pi/4)*(S1dia)^2;  % cross sectional area of section 1 (m^2)
S2=(pi/4)*(S2dia)^2;  % cross sectional area of section 2 (m^2)
L1=L1*0.0254;  % convert inches into meters
L2=L2*0.0254;  % convert inches into meters

a=S2dia/2;
```

```
% define the radiation impedance with pipe/flange combination
Zrad=((1/2).*(k3.*a).^2+i.*(8/3/pi).*k3.*a)*rho*c*S2;  % kinsler/frey


% speaker parameters
%M=0.002;  % mass of speaker cone (kg)
%K=30000;  % stiffness of speaker (N/m)
%C=0.1;  % damping of speaker (N/m^2)
Resistance=16; % resistance of speaker (ohms)
%B=5;    % speaker magnet strength (Teslas)
l=6;    % length of wire on coil (m)
induct=125e-6;  % speaker coil inductance

speaker_wn=sqrt(K/M)/2/pi;  % resonance of speaker itself
cc=2*M*speaker_wn;  % critical damping
zeta=damp/cc;  % damping ratio
speaker_wd=sqrt(1-zeta^2)*speaker_wn; % damped natural frequency

% define the mechanical impedance for the speaker
Zmd=damp+i*(w.*M-K./w);

% input impedance to section 1, plane waves (Zm0=p/u=rho*c*S1, Fannin)
Zm0=rho*c*S1*ones(1,length(f));

R=(Zrad-rho*c*S2)./(Zrad+rho*c*S2);     % symbolic simplification
C=1;  % this doesn't matter because it cancels out in the PL2_over_P0 expression;

AA=(C/2).*(                     (1+S2/S1).*exp(j*(-k2.*L1+k1.*L1))+(1-S2/S1).*R.*exp(j.*(-
       2.*k2.*L2+k2.*L1+k1.*L1)));
BB=(C/2).*(    (1-S2/S1).*exp(j*(-k2.*L1-k1.*L1))+(1+S2/S1).*R.*exp(j.*(-2.*k2.*L2+k2.*L1-
       k1.*L1)));

PL2_over_P0=(2.*C.*(1+R).*exp(-j.*k2.*L2) )./(AA+BB);     % solving pressure & velocity
       conservation

PL2_over_Vin=(PL2_over_P0).*rho.*c.*(Bl/Resistance)./(Zmd+Zm0).*S2./Zrad;

UL2_over_Volt=PL2_over_Vin.*(S2./Zrad);

speaker_voltage=Vin;  % speaker input voltage (volts)

PL2=PL2_over_Vin.*speaker_voltage;   % calculate output pressure!

U0_over_Vin=(Bl/Resistance)./(Zmd+Zm0);

% calculate speaker displacement
U0=U0_over_Vin.*speaker_voltage;

% calculate pressure at speaker diaphgram
P0=U0.*rho.*c;

speaker_displacement=U0./j./w;

load spek13;
transfunct=o2i1(2:401);

load spek12
outputps=c2(2:401);

f2=4:4:1600;


figure(1);
subplot(411);plot(f,20*log10(abs(PL2_over_Vin)/20E-
       6),'c',f2,20*log10((abs(transfunct))/20E-6));
ylabel('SPL re 1 volt Vin');
title('Vin vs output pressure FRF, magnitude');
axis([0 1600 40 100]);
grid;
legend('Model','Actual');
```

```
subplot(412);plot(f,unwrap(angle(PL2_over_Vin))*180/pi,'c',f2,unwrap(angle(transfunct))*1
       80/pi);
ylabel('degrees');
axis([0 1600 -1000 250]);
grid;
title('Phase');

%figure(2);
subplot(413);plot(f,abs(speaker_displacement)*1E3);
ylabel('displacement, mm');
grid;
title('Speaker Displacement');

subplot(414);plot(f,20*log10(abs(PL2)/20E-6),'c',f2,20*log10(abs(outputps)/4.1E-8));
xlabel('frequency, Hz');
ylabel('SPL dB re 20 uPa');
grid;
title('Output SPL');

% show another plot with displacement and SPL output
figure(2)
subplot(211);plot(f,abs(speaker_displacement)*1E3);
ylabel('Speaker Displacement, mm');
grid;
title('Speaker cone displacement');

subplot(212);plot(f,20*log10(abs(PL2)/20E-6));
xlabel('frequency, Hz');
ylabel('SPL dB re 20 uPa');
grid;
title('Output SPL');

drawnow;
out=abs(20*log10(abs(PL2_over_Vin))-(20*log10(abs(transfunct'))));                    %
       +.2*abs(unwrap(angle(PL2_over_Vin))*180/pi-unwrap(angle(transfunct'))*180/pi+360);

out=sum(out(2:length(out)))^2;

disp(' ');
disp(['Speaker undamped natural frequency: ' num2str(speaker_wn) ' Hz']);
disp(['Speaker damped natural frequency:   ' num2str(speaker_wd) ' Hz']);
disp(['alpha1: ' num2str(alpha1)]);
disp(['alpha2: ' num2str(alpha2)]);
disp(['Mass:      ' num2str(M) ' kg']);
disp(['Stiffness: ' num2str(K) ' N/m']);
disp(['Damping:   ' num2str(damp) ' N/m^2']);
disp(['Mag Cnst, Bl: ' num2str(Bl) ' Teslas']);
disp(['Speaker Dia: ' num2str(S1dia/.0254) ' in']);
disp(['Tube Dia:    ' num2str(S2dia/.0254) ' in']);
disp(['Speaker L1:  ' num2str(L1/.0254) ' in']);
disp(['Tube L2:     ' num2str(L2/.0254) ' in']);
disp(' ');

disp(['---minimization variable: ' num2str(out)]);
```

Appendix B: The Struve Function

The Struve Function (H) and its derivatives satisfy the equation:

$$H_{n-1}(z) - H_{n+1}(z) = 2H_n'(z) - \frac{\left(\frac{1}{2}z\right)^n}{\sqrt{p}\,\Gamma\left(n+\frac{3}{2}\right)} \tag{B.1}$$

Several numerical formulas exist to solve for the Struve Function values. Abramowitz and Stegun defined the Struve Function of order n of the argument z as an infinite series:

$$H_n(z) = \left(\frac{1}{2}z\right)^{n+1} \sum_{k=0}^{\infty} \frac{(-1)^k \left(\frac{1}{2}z\right)^{2k}}{\Gamma\left(k+\frac{3}{2}\right)\Gamma\left(k+n+\frac{3}{2}\right)} \tag{B.2}$$

The Struve Function of order n of the argument z as defined by Watson, p. 338 is:

$$H_n(z) = \frac{2\left(\frac{1}{2}z\right)^n}{\Gamma\left(n+\frac{1}{2}\right)\Gamma\left(\frac{1}{2}\right)} \int_0^1 \left(1-t^2\right)^{n-\frac{1}{2}} \sin(zt)\,dt \tag{B.3}$$

Use of Watson's equation was used for the calculation of the baffled piston impedance. Trapezoidal integration was used to evaluate the integral.

```
% M file to calculate the Struve function (order 1) using
% Watson's technique(integral)

function H=Struve1(x);

term1=(2*(.5*x)^1)./(gamma(1+1/2)*gamma(1/2));

N=25;    % number of integration terms between 0 and 1;

for io=0:N,
  integrand(io+1)=(1-(io/N)^2)^(1-1/2)*sin(x*io/N);
end;

integrand=trapz(integrand)*1/N;

H=term1*integrand;
```

Appendix C: Dynaco Mark III Amplifier Performance Data

The Dynaco Mark III Amplifier is a 60 watt pure Class A push-pull tube based amplifier. The frequency response is shown in Figure C.1. The magnitude of the amplifier response was flat (±0.5 dB) within the required frequency range (>200 Hz) and the phase did not roll off significantly, thus, it did not affect the feedback controller design. Frequency response was tested with a constant, pure resistive load of 8 ohms. From previous experience, it has been found that the Dynaco Mark III is extremely insensitive to changes in output load.

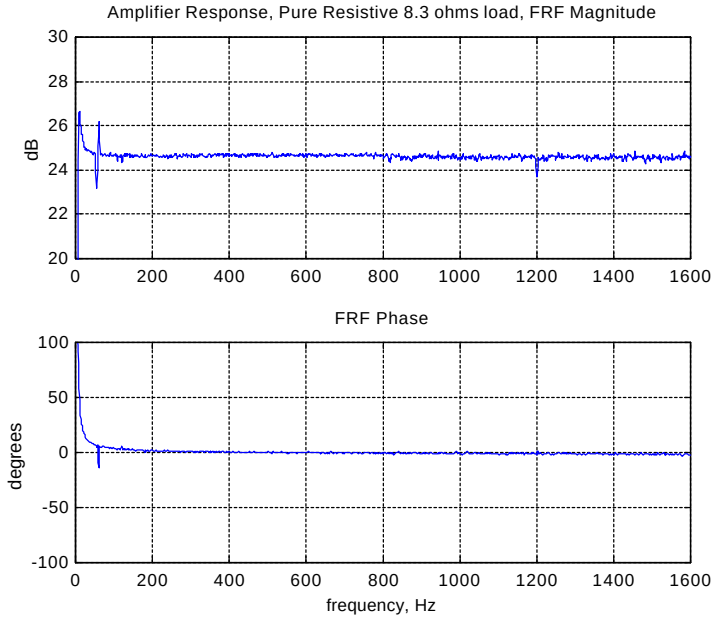

Figure C.1 Dynaco Mark III amplifier frequency response

Appendix D: Filter Implementation Schematics

The filters used in the feedback controller in *Chapter 4* were implemented using biquad configurations of operational amplifiers. Several configurations were implemented, depending on the desired controller transfer function. Each biquad circuit implements a second order transfer function. Higher order transfer functions are obtained by cascading two or more biquad circuits.

For a single complex conjugate pole pair (frequency = w, damping constant = z), the following biquad circuit was used:

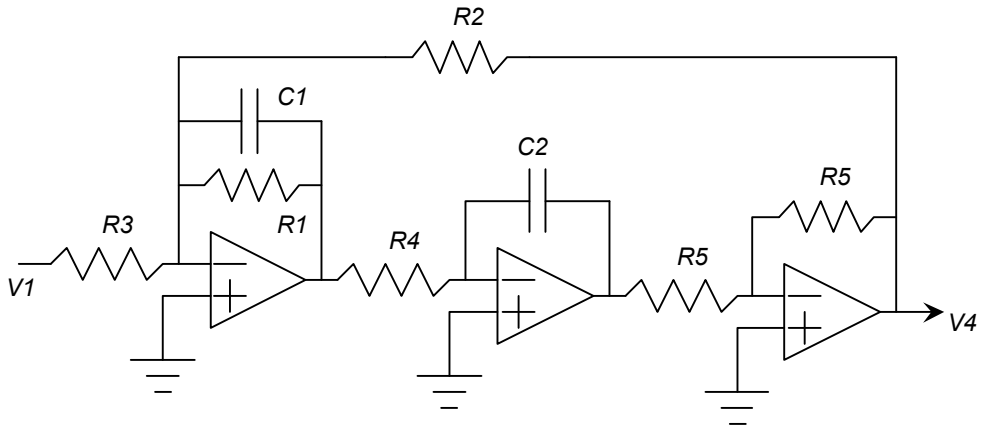

$$\omega_n = \sqrt{\frac{1}{R_2 R_4 C_1 C_2}} \qquad DC\ Gain = \frac{R_2}{R_3} \qquad \zeta = \frac{1}{2R_1 C_1 \omega_n}$$

$$\frac{V_4}{V_1} = \frac{\dfrac{1}{R_3 R_4 C_1 C_2}}{s^2 + \dfrac{1}{R_1 C_1} s + \dfrac{1}{R_2 R_4 C_1 C_2}}$$

Figure D.1 Single complex conjugate pole pair circuit transfer function implementation

If a complex conjugate zero pair was desired, a complex conjugate pole pair must be implemented in conjunction with it. A conjugate zero pair by itself is an improper transfer function and can not be realized.

For a combined complex conjugate pole pair and complex conjugate zero pair system, one of four possible biquad circuits is selected depending on the natural frequency and damping ratio of the complex conjugate pole and complex conjugate zero pair. The four possible biquad circuit implementations are listed below with their respective conditions.

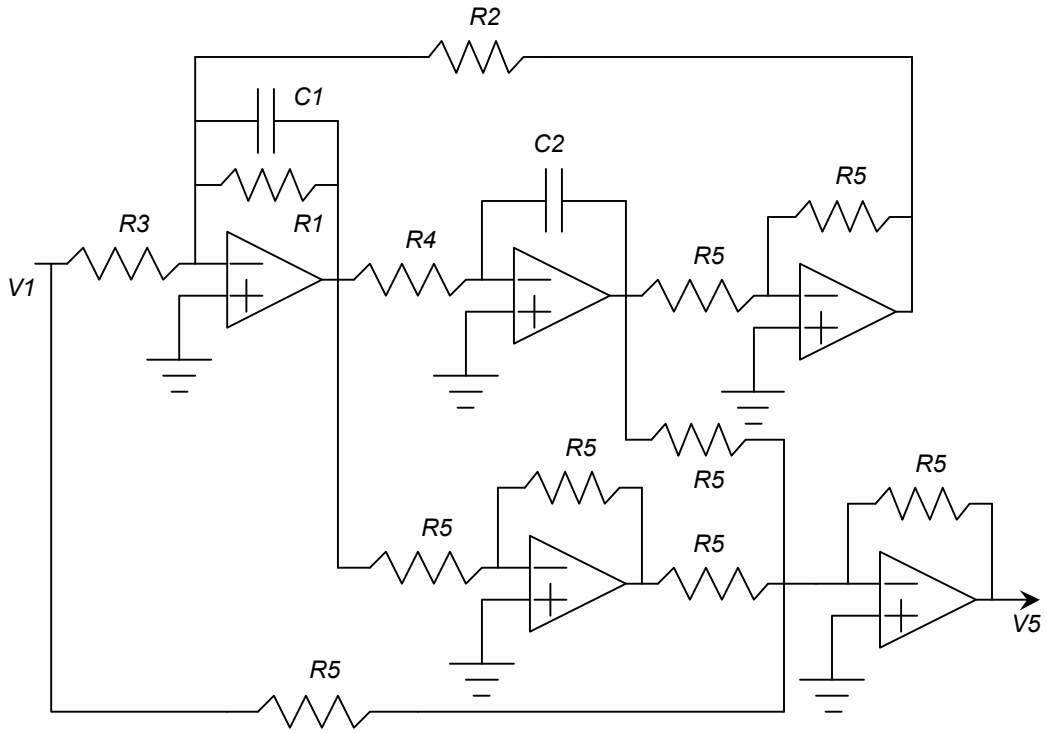

$$\omega_{nz} > \omega_{np} \qquad \zeta_z > \zeta_p \qquad \frac{\zeta_z}{\zeta_p}\frac{\omega_{nz}}{\omega_{np}} > 1$$

$$\omega_{np}^2 = \frac{1}{R_2 R_4 C_1 C_2} \qquad \omega_{nz}^2 = \frac{R_3 + R_2}{R_2 R_3 R_4 C_1 C_2} \qquad 2\zeta_p \omega_{np} = \frac{1}{R_1 C_1} \qquad 2\zeta_z \omega_{nz} = \frac{1}{R_1 C_1} + \frac{1}{R_3 C_1}$$

$$\frac{V_5}{V_1} = -\frac{s^2 + \left(\frac{1}{R_1 C_1} + \frac{1}{R_3 C_1}\right)s + \left(\frac{R_3 + R_2}{R_2 R_3 R_4 C_1 C_2}\right)}{s^2 + \left(\frac{1}{R_1 C_1}\right)s + \left(\frac{1}{R_2 R_4 C_1 C_2}\right)}$$

Figure D.2 Complex conjugate pole and conjugate zero pair transfer function implementation, case 1

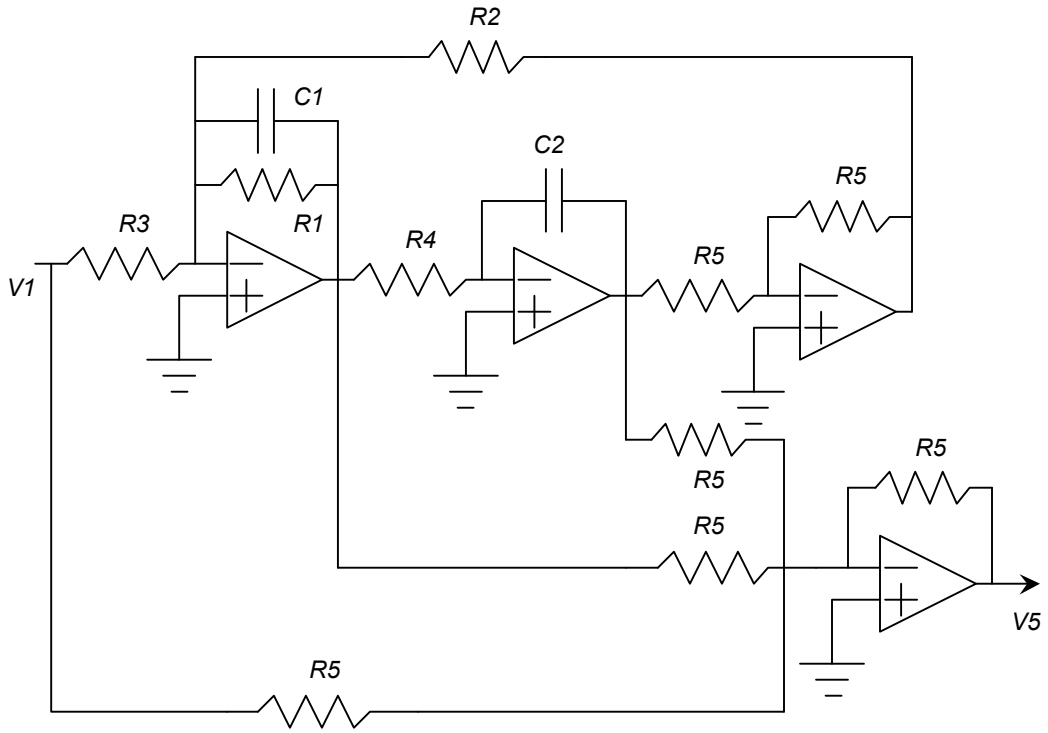

$$\omega_{nz} > \omega_{np} \qquad \rho_p > \rho_z \qquad \frac{\rho_p}{\rho_z}\frac{\omega_{np}}{\omega_{nz}} > 1$$

$$\omega_{np}^2 = \frac{1}{R_2 R_4 C_1 C_2} \qquad \omega_{nz}^2 = \frac{R_3 + R_2}{R_2 R_3 R_4 C_1 C_2} \qquad 2\rho_p \omega_{np} = \frac{1}{R_1 C_1} \qquad 2\rho_z \omega_{nz} = \frac{1}{R_1 C_1} - \frac{1}{R_3 C_1}$$

$$\frac{V_5}{V_1} = -\frac{s^2 + \left(\frac{1}{R_1 C_1} - \frac{1}{R_3 C_1}\right)s + \left(\frac{R_3 + R_2}{R_2 R_3 R_4 C_1 C_2}\right)}{s^2 + \left(\frac{1}{R_1 C_1}\right)s + \left(\frac{1}{R_2 R_4 C_1 C_2}\right)}$$

Figure D.3 Complex conjugate pole and conjugate zero pair transfer function implementation, case 2

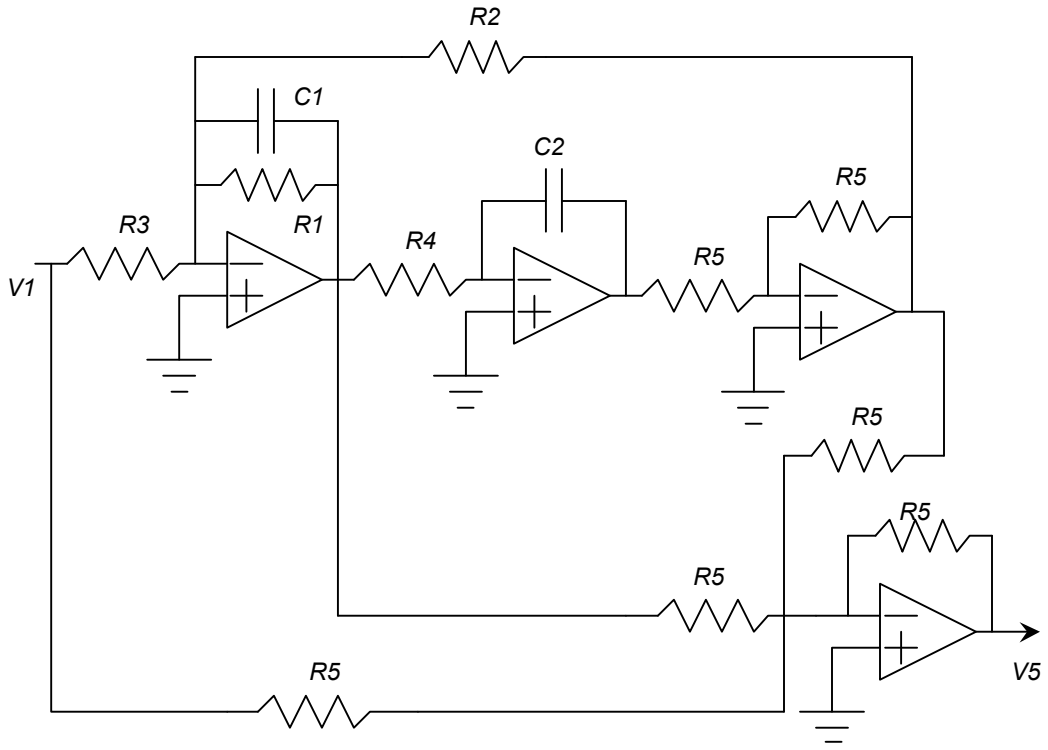

$$\omega_{np} > \omega_{nz} \qquad \rho_p > \rho_z \qquad \frac{\rho_p}{\rho_z}\frac{\omega_{np}}{\omega_{nz}} > 1$$

$$\omega_{np}^2 = \frac{1}{R_2 R_4 C_1 C_2} \qquad \omega_{nz}^2 = \frac{R_3 - R_2}{R_2 R_3 R_4 C_1 C_2} \qquad 2\rho_p \omega_{np} = \frac{1}{R_1 C_1}$$

$$2\rho_z \omega_{nz} = \frac{1}{R_1 C_1} - \frac{1}{R_3 C_1} = 2\rho_p \omega_{np} - \frac{1}{R_3 C_1}$$

$$\frac{V_5}{V_1} = -\frac{s^2 + \left(\frac{1}{R_1 C_1} - \frac{1}{R_3 C_1}\right)s + \left(\frac{R_3 - R_2}{R_2 R_3 R_4 C_1 C_2}\right)}{s^2 + \left(\frac{1}{R_1 C_1}\right)s + \left(\frac{1}{R_2 R_4 C_1 C_2}\right)}$$

Figure D.4 Complex conjugate pole and conjugate zero pair transfer function implementation, case 3

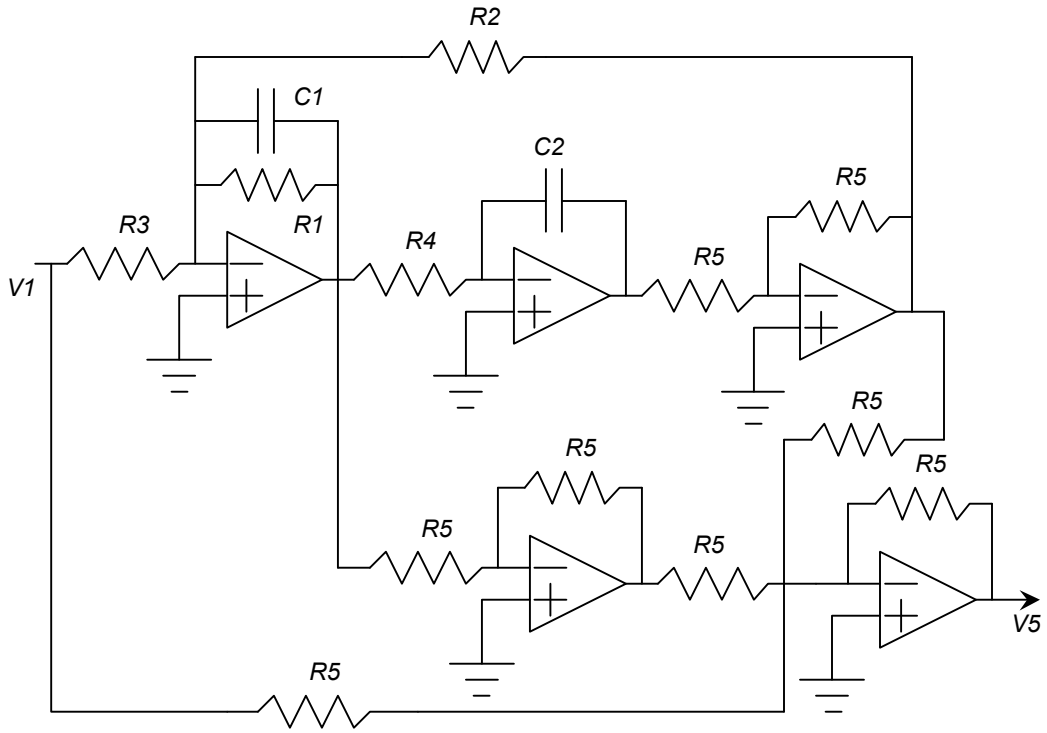

$$\omega_{np} > \omega_{nz} \qquad \rho_z > \rho_p \qquad \frac{\rho_z}{\rho_p}\frac{\omega_{nz}}{\omega_{np}} > 1$$

$$\omega_{np}^2 = \frac{1}{R_2 R_4 C_1 C_2} \quad \omega_{nz}^2 = \frac{R_3 - R_2}{R_2 R_3 R_4 C_1 C_2} \quad 2\rho_p \omega_{np} = \frac{1}{R_1 C_1}$$

$$2\rho_z \omega_{nz} = \frac{1}{R_1 C_1} + \frac{1}{R_3 C_1} = 2\rho_p \omega_{np} + \frac{1}{R_3 C_1}$$

$$\frac{V_5}{V_1} = -\frac{s^2 + \left(\frac{1}{R_1 C_1} + \frac{1}{R_3 C_1}\right)s + \left(\frac{R_3 - R_2}{R_2 R_3 R_4 C_1 C_2}\right)}{s^2 + \left(\frac{1}{R_1 C_1}\right)s + \left(\frac{1}{R_2 R_4 C_1 C_2}\right)}$$

Figure D.5 Complex conjugate pole and conjugate zero pair transfer function implementation, case 4

For more information concerning the biquad circuit and their operational theory, refer to [Clatterbuck, 1998].

References

Abramowitz, M. and Stegun, C. A. (Eds.), 1972. "Struve Function, $H_v(x)$." §12.1 in *Handbook of Mathematical Functions with Formulas, Graphs, and Mathematical Tables, 9th printing.* New York: Dover Publications, pp. 496-498.

Adachi, Seiji, 1995. "Time-Domain simulation of sound production in the brass instrument," J. Acoust. Soc. Am. Vol. 97, June, pp. 3850-3861.

Agullo, Joaquim and Ana Barhau, Jordi Martinez, 1988. "Alternatives to the impulse response, h(t), to describe the acoustical behavior of conical ducts," J. Acost. Soc. Am., Vol. 84, No. 5, November, pp. 1606-1612.

Ayers, R. Dean, 1996. "Impulse responses for feedback to the driver of a musical wind instrument," J. Acost. Soc. Am., Vol. 100, No. 2, Pt. 1, August, pp. 1190-1198.

Ayers, R. Dean, 1995. "Two complex effective lengths of musical wind instruments," J. Acoust. Soc. Am. Vol. 98, July, pp. 81-87.

Backus, John and T. C. Hundley, 1971. "Harmonic generation in the trumpet," J. Acost. Soc. Am. Vol. 49, February, pp. 509-519.

Backus, John, 1976. "Input impedance curves for the brass instruments," J. Acost. Soc. Am. Vol. 60, No. 2, August, pp. 470-480.

Backus, John, 1974. "Input impedance curves for the reed instruments," J. Acost. Soc. Am. Vol. 56, No. 4, October, pp. 1266-1279.

Bachelder, Allen, 1974. "The Trumpet in Transition: 1750-1850." Eastman School of Music.

Bachelder, Allen, 1973. "The Acoustics of the Trumpet." Eastman School of Music.

Bate, Philip, 1978. *The Trumpet and Trombone.* London: Ernest Benn Limited.

Benade, Arthur H, 1976. *Fundamentals of Musical Acoustics*. New York, NY: Oxford University Press.

Bowsher, J.M., 1975. *The Physics of Music*. Westport, Connecticut: Greenwood Press Publishers.

Carse, Adam, 1971. *Musical Wind Instruments*. New York: Da Capo Press.

Causse, Rene, 1984. "Input impedance of brass musical instruments - Comparison between experiment and numerical models," J. Acost. Soc. Am., Vol. 75, No. 1, January, pp. 241-254.

Clatterbuck, Daniel, 1998. *An Investigation of Performance Limitations in Active Noise Reduction Headsets.* Masters Thesis, Virginia Tech.

Crandall, Irving B, 1926. *Theory of Vibrating Systems and Sound*. New York: D. Van Nostrand Company, Inc.

Darlington, Paul and Anthony Simpson, 1992. "Cooling rates of the Bb trumpet," Applied Acoustics, Vol. 36, pp. 145-157.

Dent, E.J., 1905. *Alessandro Scarlatti*. London: Edward Arnold.

Elliott, S.J. and J. M. Bowsher, 1982. "Regeneration in brass wind instruments," J. Sound and Vibration, Vol. 83, No. 2, pp. 181-217.

Elliott, S.J. and J. M. Bowsher, 1982. "Input and transfer response of brass wind instruments," J. Sound and Vibration, Vol. 72, No. 6, December, pp. 1747-1760.

Fletcher, N. H., 1979. "Excitation mechanisms in woodwind and brass instruments," Acustica, Vol. 43, pp. 63-72.

Galphin, F. W., 1937. *A Textbook of European Musical Instruments*. London: Williams and Norgate.

Helmholtz, Hermann L. F., 1954. *On the Sensations of Tone*. New York, NY: Dover Publications.

Jansson, E. V. and A. H. Benade, 1974. "On plane and spherical waves in horns with non-uniform flare, prediction and measurements of resonance frequencies and radiation losses," Acustica, Vol. 31, No. 4, pp. 185-202.

Kinsler, Lawrence E. and Austin R. Frey, Alan B. Coppens, James V. Saunders, 1982. *Fundamentals of Acoustics*. New York: John Wiley & Sons.

Knauss, H.P. and W. J. Yeager, 1941. "Vibration of the walls of a cornet," J. Acost. Soc. Am., Vol. 13, October, pp. 160-162.

Martin, Daniel W., 1942. "Directivity and the acoustic spectra of brass wind instruments," J. Acoust. Soc. Am., Vol. 13, January, pp. 309-313.

Martin, Daniel W., 1942. "Lip vibrations in a cornet mouthpiece," J. Acost. Soc. Am., Vol. 13, January, pp. 305-308.

McIntyre, M. E. and J. Woodhouse, 1979. "On the fundamentals of bowed-string dynamics," Acustica, Vol. 43, No. 2, pp. 93-108.

Meyer, Erwin and Ernest-Georg Neumann, 1972. *Physical and Applied Acoustics*. New York, NY: Academic Press.

Naylor, Tom L, 1979. *The Trumpet & Trombone in Graphic Arts, 1500-1800*. Tennessee: The Brass Press.

Olson, Harry F, 1967. *Music, Physics and Engineering*. New York, NY: Dover Publications.

Olson, Harry F, 1940. *Elements of Acoustical Engineering*. New York, NY: D. Van Nostrand Company, Inc.

Saneyoshi, J., 1987. "Feedback oscillations in reed woodwind and brasswind instruments," Acustica, Vol. 62, pp. 194-210.

Schumacher, R.T, 1981. "Ab initio calculations of the oscillations of a clarinet." Acustica, Vol. 48, No. 2, pp. 71-85.

Schumacher, R.T, 1979. "Self-Sustained oscillations of the bowed string." Acustica, Vol. 43, pp. 109-120.

Schumacher, R. T. 1978. "Self-sustained oscillations of the clarinet: An integral equation approach," Acustica, Vol. 40, pp. 298-308.

Smithers, Don L., 1988. *The Music and History of the Baroque Trumpet before 1721*. Carbondale: Southern Illinois University Press.

Sommerfeldt, Scott D. and William J. Strong, 1988. "Simulation of a player-clarinet system." J. Acost. Soc. Am., Vol. 83, No. 5, May, pp. 1908-1918.

Strawn, John, 1987. "Analysis and synthesis of musical transitions using the discrete short-time fourier transform." J. Audio Eng. Soc, Vol. 35, No. 1/2, January/February, pp. 3-14.

Vaudrey, Michael A, 1996. "A novel approach to multiple reference frequency domain adaptive control," Master's Thesis, Virginia Tech, December.

Watkinson, P. S. and J. M. Bowsher, 1982. "Vibration characteristics of brass instrument bells," J. Sound and Vibration, Vol. 85, No. 1, pp. 1-17.

Watson, G. N., 1966. *A Treatise on the Theory of Bessel Functions, 2nd ed.* Cambridge, England: University Press.

Widrow, Bernard, Samuel D. Stearns, 1985. *Adaptive Signal Processing*. New Jersey, Prentice-Hall, Inc.

Woodward, J.G., 1941. "Resonance characteristics of a cornet," J. Acoust. Soc. Am. Vol. 13, October, pp. 156-159.

Yoshikawa, Shigeru, 1995. "Acoustical behavior of brass player's lips," J. Acost. Soc. Am. Vol. 97, No. 3, March, pp. 1929-1939.

Vita

Peter Pickett was born August 8, 1973 in Charlottesville, Virginia. After spending 18 years in Charlottesville, he graduated from Charlottesville High School in June 1991 and started his undergraduate work the following fall in Mechanical Engineering at Virginia Tech. During his undergraduate program, Peter interned at the Crutchfield Corporation in Charlottesville, Virginia. He worked in the installation kit design and manufacturing department for three summers. Along with his undergraduate studies, Peter also worked as a research assistant during the summer. He received his Bachelors of Science in Mechanical Engineering in May 1995. Along with his Engineering studies, Peter also studied trumpet performance extensively, performing with numerous area groups and ensembles. He completed a Bachelors of Arts the following year in Trumpet Performance. He started his Master's Degree in the fall of 1996 in Trumpet Acoustics and Active Noise Control under Dr. Will Saunders. Peter was a GTA for the department for two semesters for two undergraduate senior level labs.